

# **The regulation of calcitonin genes upon bacterial infection and sepsis in human adipocytes**

## **Inauguraldissertation**

zur

Erlangung der Würde eines Doktors der Philosophie

vorgelegt der

Philosophisch-Naturwissenschaftlichen Fakultät  
der Universität Basel

von

Tanja Marianna Radimerski

aus

Zürich (ZH)

Basel, 2010

Genehmigt von der Philosophisch-Naturwissenschaftlichen Fakultät  
auf Antrag von

Prof. Dr. Beat Müller

Prof. Dr. Alex N. Eberle

Prof. Dr. Karl Hofbauer

Basel, 22.06.2010

Prof. Dr. Eberhard Parlow

---

**Table of content**

<b>1. Abbreviations .....</b>	<b>4</b>
<b>2. Summary.....</b>	<b>5</b>
<b>3. Introduction.....</b>	<b>7</b>
3.1 The Calcitonin Gene Family .....	7
3.1.1 The CALC-I gene product .....	8
3.1.1.1 <i>CT</i> .....	8
3.1.1.2 <i>CGRP-I</i> .....	9
3.1.2 The CALC-II gene product.....	10
3.1.3 The CALC-IV gene product .....	10
3.1.4 The CALC-V gene product.....	10
3.2 CT peptides and sepsis.....	11
3.2.1 Sepsis .....	11
3.2.2 The hormokine concept.....	11
3.2.3 Increased levels of CT precursor peptides in bacterial infection and sepsis .....	12
3.2.3.1 <i>ProCT as a toxic factor in bacterial infection and sepsis</i> .....	13
3.2.3.2 <i>Improved survival after ProCT immunoneutralisation</i> .....	13
3.2.3.3 <i>Mode of action of CT peptides</i> .....	14
3.2.4 Increased levels of CGRP and ADM in bacterial infection and sepsis.....	14
3.2.5 Extrathyroidal expression of CALC gene mRNA and CT precursor peptides in bacterial infection and sepsis.....	15
3.3 Infection and sepsis-related expression of CT peptides in adipose tissue .....	16
3.3.1 Human adipose tissue .....	16
3.3.2 Inflammatory signaling in adipocytes.....	17
3.3.3 Adipocytes and CT peptides .....	18
3.4. CALC genes and calcium .....	19
3.4.1 Hypocalcemia in sepsis.....	19
3.4.2 Calcium .....	19
3.4.3 Calcium and CALC genes .....	22
3.4.3.1 <i>Calcium and CT</i> .....	22
3.4.3.2 <i>Molecular mechanism of CT expression</i> .....	22
3.4.3.3 <i>Calcium and CGRP</i> .....	24
3.4.3.4 <i>Calcium and ADM</i> .....	24
3.5 CALC genes and cAMP.....	25
3.5.1 cAMP .....	25
3.5.2 cAMP and calcium.....	25
3.5.3 cAMP and DREAM.....	27
3.5.4 cAMP and CALC genes.....	28
3.6 Aim of the thesis .....	29
<b>4. Materials and Methods.....</b>	<b>30</b>
4.1 Cell culture.....	30
4.1.1 Primary human adipocyte cell culture model .....	30
4.1.2 HEK293T and TT cells.....	31
4.1.3 Splitting, freezing and thawing of cells .....	31
4.1.3.1 <i>Splitting</i> .....	31
4.1.3.2 <i>Freezing</i> .....	31
4.1.3.3 <i>Thawing</i> .....	31

---

4.2 RNA and DNA applications .....	32
4.2.1 RNA isolation .....	32
4.2.2 cDNA synthesis .....	33
4.2.3 Real-time polymerase chain reaction (RT-PCR) .....	33
4.3 Bacterial transformation.....	34
4.3.1 Vector information.....	34
4.3.2 Competent cells.....	34
4.3.3 Plasmid transformation into bacteria .....	34
4.3.4 Plasmid amplification and purification .....	34
4.3.4.1 <i>Small scale purification miniprep (Mini-Prep)</i> .....	34
4.3.4.2 <i>Large scale purification (Maxi-Prep)</i> .....	35
4.3.5 DNA digestion .....	35
4.3.6 Agarose gel eletrophoresis.....	35
4.4 Cytosolic Ca <sup>2+</sup> measurements by confocal microscopy.....	35
4.5 Flow cytometry .....	36
4.5.1 Quantification of differentiation capacity .....	36
4.5.2 Assessment of cell viability .....	37
4.5.3 Transfection efficiency .....	37
4.6 Cell transfections .....	37
4.6.1 Generation of recombinant lentiviruses .....	37
4.6.2 Infection of cells .....	38
4.6.3 Microscopy .....	38
4.6.4 Luciferase assays .....	38
4.7 Protein measurements .....	38
4.7.1 Immunoluminometric Assay (ILMA).....	38
4.7.2 Radioimmuno Assay (RIA) .....	39
4.7.3 Enzyme-linked immunoassay (ELISA) .....	39
4.8 cAMP concentration measurement .....	39
4.9 Adipocyte lysates .....	39
4.10 Western blot analysis .....	40
4.11 Statistical analysis .....	40
<b>5. Results .....</b>	<b>41</b>
5.1 Differentiation efficiency of preadipocyte-derived adipocytes in our human cell culture model .....	41
5.2 Effects of bacterial infection and inflammation on preadipocyte-derived adipocytes .....	43
5.2.1 Different doses of LPS do not affect cell viability .....	43
5.2.2 Variations in LPS-induced CALC-I gene expression.....	44
5.2.3 LPS induces IL-6 and CALC-I gene mRNA expression in human adipocytes .....	46
5.2.4 LPS-induced CALC-I gene expression is independent from NFκB pathway .....	47
5.2.5 IL-1β and CALC-I gene expression.....	48
5.2.6 Effect of IL-1RA on LPS-induced CALC-I gene expression.....	49
5.3 Effects of ionomycin and LPS on intracellular calcium concentration in human preadipocyte-derived adipocytes .....	51
5.3.1 Effect of ionomycin on cell viability .....	51
5.3.2 Effect of ionomycin on intracellular calcium concentration changes.....	53
5.3.3 Effect of LPS on intracellular calcium concentration.....	54

5.4 Role of calcium in lipopolysaccharide-induced CALC gene expression in human adipocytes.....	58
5.4.1 Effect on LPS-induced CALC-I gene mRNA expression by inhibiting LPS-induced intracellular calcium increase.....	58
5.4.2 Effects of intracellular calcium increase on LPS-induced CALC-I gene and IL-6 expression .....	60
5.4.3 Effects of altering calcium concentration on CT peptide and IL-6 secretion .....	62
5.4.4 Effects of intracellular calcium concentration changes on LPS-induced CALC-V gene expression .....	63
5.5 CALC-I gene promoter activity upon increased Ca <sup>2+</sup> .....	65
5.5.1 Stable transfection of CALC-I gene promoter deletion constructs.....	65
5.5.2. Increased luciferase activity upon ionomycin.....	68
5.6 Expression of DREAM in human preadipocytes and adipocytes .....	69
5.7 Effects of cAMP on LPS-induced CALC-gene expression in preadipocyte-derived adipocytes .....	70
5.7.1 Increase in CALC-I gene mRNA expression with forskolin .....	70
5.7.2 Effects of LPS and IL-1 $\beta$ on cAMP levels in adipocytes .....	71
<b>6. Discussion.....</b>	<b>73</b>
<b>7. References .....</b>	<b>81</b>
<b>8. Acknowledgments .....</b>	<b>91</b>
<b>9. Curriculum vitae.....</b>	<b>93</b>
<b>10. Appendix.....</b>	<b>95</b>

## 1. Abbreviations

AC:	adenylate cyclase
ADM:	adrenomedullin
AMP:	adenosine monophosphate
ATP:	adenosine triphosphate
Ca <sup>2+</sup> :	calcium, ionic calcium
[Ca <sup>2+</sup> ] <sub>i</sub> :	intracellular calcium concentration
[Ca <sup>2+</sup> ] <sub>e</sub> :	extracellular calcium concentration
CALC:	calcitonin (genes)
cAMP:	cyclic adenosine monophosphate
CASR:	calcium-sensing receptor
CCP-I:	calcitonin carboxypeptide-I, katalcalcin
CGRP:	calcitonin gene related peptide
CRE:	cAMP-response element
CREB:	CRE binding protein
CREM:	CRE modulator
CRP:	C-reactive protein
CT:	calcitonin
DRE:	downstream regulatory element
DREAM:	downstream regulatory element antagonist modulator
IL-1:	interleukin-1
IL-6:	interleukin-6
IL-8:	interleukin-8
INF:	interferon
IP <sub>3</sub> :	inositol-1,4,5-trisphosphate
IP <sub>3</sub> R:	inositol-1,4,5-trisphosphate receptor
LPS:	lipopolysaccharide
MCP 1:	monocyte chemoattractant protein 1
MMCP:	mitochondrial membrane calcium pump
MNCX:	mitochondrial sodium/calcium exchanger
MPT:	mitochondrial permeability transition
MR-ProADM:	midregional fragment of pro-adrenomedullin
MSC:	mesenchymal stem cells
MTC:	medullary thyroid carcinoma
MyD88:	Myeloid differentiation primary response gene (88)
NCX:	sodium/calcium exchanger
NFκB:	nuclear factor kappa B
N-ProCT:	aminoprocalcitonin
PAM:	peptidylglycine-amidating monooxygenase
PAMP:	pathogen-associated molecular patterns
PK:	protein kinase
PMCA:	plasma membrane calcium pump
ProADM:	proadrenomedullin
ProCT:	procalcitonin
PTH:	parathyroid hormone
RyR:	ryanodine receptor
SERCA:	sarco-endoplasmic reticulum Ca <sup>2+</sup> ATPase
SIRS:	systemic inflammatory response syndrome
SVF:	stromal vascular cell fraction
TIR:	Toll/interleukin-1-receptor
TIRAP:	(TIR)-domain-containing-adaptor protein
TLR:	toll-like receptor
TNF-α:	tumor necrosis factor alpha

## 2. Summary

Systemic bacterial infections induce an ubiquitous expression of calcitonin (CALC) genes with sustained release of calcitonin (CT) peptides, namely procalcitonin (ProCT), calcitonin-gene related peptide (CGRP) and adrenomedullin (ADM). ProCT is a marker to follow the course of sepsis and to guide antibiotic therapy and a dose-dependent toxic mediator. Persistently and markedly elevated levels of ProCT and even more of ProADM during bacterial infection and sepsis indicate a bad prognosis. The molecular mechanisms as to how extrathyroidal CALC gene expression and protein secretion is regulated in sepsis are unknown.

Since the neuro-endocrine CT expression in the parafollicular C-cells of the thyroid is calcium dependent, we hypothesized that calcium might also be involved in the non-neuro-endocrine expression and secretion of CT peptides. We therefore monitored preadipocyte-derived adipocytes for changes in intracellular calcium concentrations upon treatment with lipopolysaccharide (LPS) with confocal microscopy. LPS-stimulated cells were treated with substances which provoke or block an increase in intracellular calcium concentrations or increase levels of cAMP and changes in CALC-I gene (i.e. CT and CGRP-I) and CALC-V gene (i.e. ADM) mRNA expression were assessed by real-time PCR. Protein secretions in supernatants were measured by specific assays. In addition to the CALC genes, changes of IL-6 mRNA and protein were measured.

Administration of LPS on human adipocytes led to a slow and sustained increase in the intracellular calcium concentration without apparent cytotoxic effect on the cells. LPS-induced CALC-I mRNA expression was potentiated with increasing intracellular calcium concentrations through addition of the calcium ionophore ionomycin or depletion of intracellular stores with thapsigargin. When diminishing intracellular calcium concentrations in LPS-treated adipocytes by verapamil or 2-aminoethoxydiphenyl borate, the CALC-I gene expression was reduced. This was confirmed at the protein level for ProCT and CGRP-I.

Interestingly, we observed an inverse effect of intracellular calcium on the expression of the CALC-I and the CALC-V gene. Elevations of intracellular calcium in an inflammatory background caused by LPS potentiated the activity of the CALC-I genes CT and CGRP-I but reduced the expression of the CALC-V gene ADM, both at the mRNA and the protein level. IL-6 mRNA expression levels was also altered upon

increased and decreased levels of intracellular calcium concentrations, but to a much lower extent as compared to that of the CALC-I gene. LPS-induced expression of CT and CGRP-I mRNA was independent from nuclear factor kappa B (NF $\kappa$ B), in contrast to IL-6-expression.

In conclusion, the expression of CT and CGRP-I in human preadipocyte-derived adipocytes upon stimulation with LPS is mediated by changes in intracellular calcium concentrations and by cAMP and is independent of NF $\kappa$ B. The distinct and inverse effect of calcium on CALC-I and CALC-V gene expression might at least in part explain the different clinical characteristics of ProCT as diagnostic and ProADM as prognostic marker.



### 3. Introduction

#### 3.1 The Calcitonin Gene Family

The calcitonin (CALC) gene family of peptides consists of calcitonin (CT), calcitonin gene related peptides-I and -II (CGRP-I, CGRP-II), amylin (AMY) and adrenomedullin (ADM). These calcitonin peptides (CT peptides) are translated from the CALC genes CALC-I, CALC-II, CALC-IV and CALC-V (Fig. 1), which were derived from gene duplication during evolution. The CALC III gene is a non-transcribed pseudo gene.

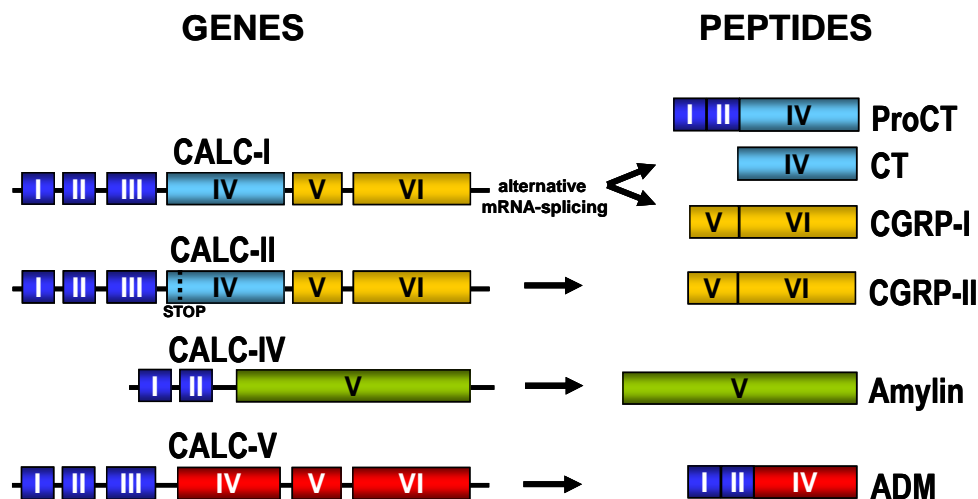


**Figure 1: CALC genes and the CT peptides.** CALC-I gene products include CT, its precursor peptide ProCT and through alternative splicing CGRP-I. CALC-II gene encodes CGRP-II. ProCT and CT can not be expressed from the CALC-II gene due to a stop codon in exon 4. CALC-III (not shown) is a non-translated pseudogene. CALC-IV encodes the peptide amylin. CALC-V gene encodes ADM (adapted from Becker et al. 2001 (1)).

Human CT, CGRP-I, CGRP-II, amylin and ADM have in common a N terminal 6-7 amino acid ring structure, required for biological activity (2), and amidated C-termini (Fig. 2). Additional amino acids in the middle and C-terminal regions are identical in several peptides. Unique among this family of peptides, human ADM has a linear N-terminal extension of the ring structure of 15 amino acids (3).



Thyroid C-cells contain secretory granules which are stored as a pre-made pool of stable granules. Like most peptide hormones, mature CT is initially biosynthesized as a large molecular weight precursor hormone, i.e. preprocalcitonin, which then is subsequently processed into smaller peptides, including CT, ProCT, free calcitonin carboxypeptide-I (CCP-I), conjoined CT:CCP-I and free aminoprocaltitonin (N-ProCT) (Figure 3).

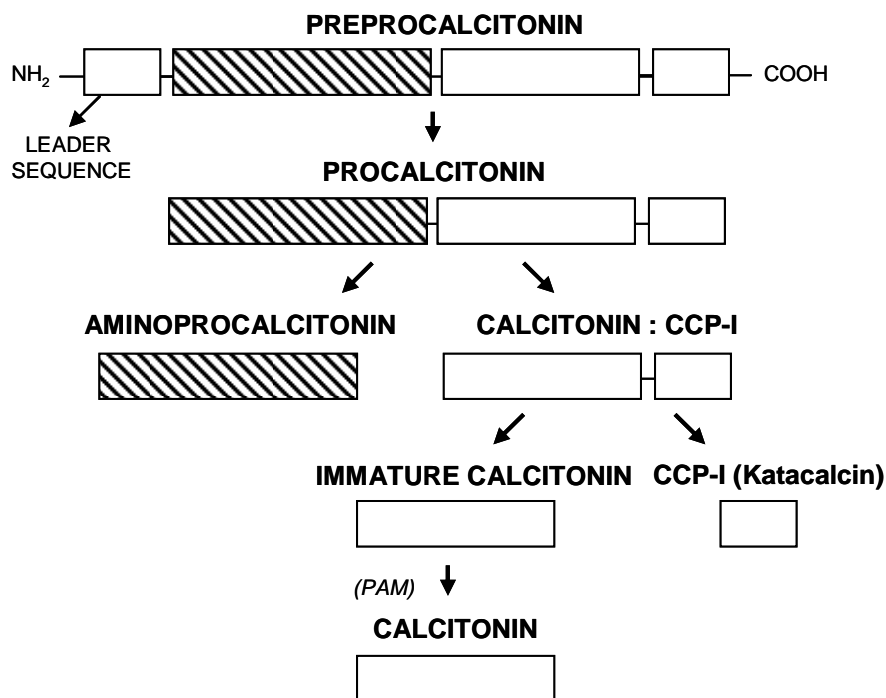


**Figure 3: Schematic diagram of the human calcitonin precursors.** Mainly in thyroidal C-cells, immature calcitonin is amidated into mature calcitonin by the enzyme peptidylglycine-amidating monooxygenase (PAM). CCP-I = calcitonin carboxypeptide-I (Müller et al. 2000 (13)).

All of these component peptides are found in the sera of healthy persons (14).

### 3.1.1.2 CGRP-I

CGRP-I was identified in 1981 by Rosenfeld et al. (15) as an alternative splicing variant of the CALC-I gene. CGRP-I mRNA is the predominant transcription product of the CALC-I gene in neural tissues, but it is also present in the pituitary and C-cells of normal thyroid glands and in medullary thyroid carcinoma. CGRP-I is released from nerve terminals by voltage-dependent calcium uptake, among other mechanisms.

As a result, CGRP-I acts mainly locally without reaching the general circulation. It is the most potent vasodilator known so far. ProCGRP and ProCT share an identical aminoterminal precursor fragment. Nothing is known on the bioactivity of its carboxy-terminal precursor peptides.

### **3.1.2 The CALC-II gene product**

No preproCT-II mRNA is detected due to a mutated STOP codon in exon IV. The CALC-II gene is transcribed to preproCGRP-II mRNA and translated into CGRP-II protein and its precursor peptides. Mature CGRP-I and-II only differ in three from 37 amino acids. CGRP-II is a less potent vasodilator but a more potent inhibitor of gastric acid as compared to CGRP-I (16).

### **3.1.3 The CALC-IV gene product**

The peptide Amylin is generated from the CALC-IV gene and shares over 40% amino acid sequence homology with CGRP and 20% with human CT. Amylin is predominantly located in the beta cells of the islets of the pancreas and is co-secreted with insulin. It is involved in the pathogenesis of type II diabetes by deposition as amyloid within the pancreas, leading to “amyloidosis” and beta cell destruction (17), hence its initial name as “islet amyloid polypeptide” (IAPP).

### **3.1.4 The CALC-V gene product**

The vasoactive peptide ADM was discovered in 1993 in the adrenal medulla and is translated from the CALC-V gene. It shares 24% homology with CGRP and also has a biological activity profile similar to that of CGRP. Together with CGRP ADM belongs to the most potent vasodilators known so far (18). Due to its high expression in endothelial cells it has come to be regarded as a secretory product of the vascular endothelium. The ADM gene is expressed in a wide range of tissues and has additional immune modulating, metabolic properties. ADM also has bactericidal activity, which is further enhanced by modulation of complement activity and regulation (19, 20).

## **3.2 CT peptides and sepsis**

### **3.2.1 Sepsis**

Sepsis is a major challenge in the intensive care unit, where it's one of the leading causes of death. It arises unpredictably and can progress rapidly (21, 22). Sepsis is the systemic response to the infection and is manifested by two or more of the following criteria of the systemic inflammatory response syndrome (SIRS), which is a clinical expression of nonspecific inflammation. SIRS is characterized by varying combinations of fever or hypothermia, tachypnea, tachycardia, and polymorphonucleocytosis or leucopenia. The infection causing sepsis can originate anywhere in the body. Many different types of microbes such as bacteria, fungi and viruses can cause sepsis, but bacteria are the most common initiators. In sepsis, the patient is harmed because of the initial injury or infection but also because of the humoral and / or cellular overreaction of the host. This triggers a widespread inflammation, which leads to blood clots and leaky vessels and organ dysfunctions. An impaired blood flow damages metabolically activated inflamed organs by depriving them of nutrients and oxygen. In severe cases, one or more organs fail. Ultimately, blood pressure drops and the patient dies from multiorgan failure.

### **3.2.2 The hormokine concept**

Hormones are produced by endocrine and neuro-endocrine cells and are secreted into the circulatory system from where they are disseminated throughout the body in order to regulate the function of peripheral tissues and, thus, maintaining feedback-regulated homeostasis. Cytokines are produced by multiple cell types of different embryonic origin and mediate mainly local and immunomodulating effects. Importantly upon systemic infection and inflammatory stimulation, allegedly hormonal CALC genes become transcribed and translated. As a result, hormonal precursor peptides of the CALC genes are ubiquitously released by non-endocrine, parenchymal cells throughout the body in a cytokine-like behavior. To encompass this plasticity of hormones, the term "hormokine" was coined. The concept was based on the finding of a ubiquitous expression of the CT peptides during sepsis in a hamster model (23, 24), subsequently verified for pigs (25, 26) and primates (26), including humans (27, 28). The ubiquitous inflammatory release is induced either directly, via microbial toxins such as the endotoxin lipopolysaccharide (LPS), or indirectly, by

mediators of the humoral or cell mediated host response (e.g. interleukin (IL)-1 $\beta$ , tumour necrosis factor (TNF) -  $\alpha$  and IL-6) (28). Parenchymal cells such as liver, kidney, muscle cells and adipocytes provide the largest tissue mass in the body and the principle source of circulating hormones in sepsis. The induction in mRNA and the release of peptides from parenchymal cells is much greater compared to that of circulating blood cells in sepsis, where only a transient release can be found (29). This indicates for hormones a tissue based rather than leukocyte based form of host defense. As such, hormones are thought to adapt metabolism and vascular tone to acute needs in inflammation and to combat invading microbes during exogenous infections.

### **3.2.3 Increased levels of CT precursor peptides in bacterial infection and sepsis**

In the healthy state, circulating levels of CT precursors, including ProCT, are very low (< 0.05 ng/ml). In patients with severe inflammation and especially in systemic bacterial infection (“sepsis”) up to septic shock circulating levels of several CT precursor peptides increase to levels up to 1000 ng/ml. This increase correlates with the severity of the illness and with mortality (30). Within 2-3 hours after induction of an infection (e.g. by endotoxin), ProCT levels increase, rising rapidly to reach a plateau within 6-12 hours. ProCT concentrations remain high for up to 48 hours and then, upon resolution of the infection, fall back to their baseline values with a half-life of 20 to 24 hours (30, 31).

ProCT has a superior diagnostic accuracy for the diagnosis of sepsis as compared to other markers of inflammation (e.g. IL-6), C-reactive protein (CRP) or lactate (6, 30, 32, 33) (Figure 5). Presently a variety of biomarkers with distinct diagnostic spectrum for sepsis is available. Some markers primarily indicate the severity of inflammation (e.g. IL-6), others respond to infection, but do not indicate the host response well (endotoxin, lipoprotein binding protein, triggering receptor on myeloid cells). In comparison, ProCT is a well-established biomarker of sepsis that fulfills several criteria of clinical needs: it responds both to infection and to the severity of inflammation and thus has an impact on therapy. Highly sensitive ProCT measurements, embedded in diagnosis-specific clinical algorithms, have been shown to markedly reduce the overuse of antibiotic therapy without increasing risk to patients in 11 randomized controlled trials including over 3500 patients from different European countries (34).

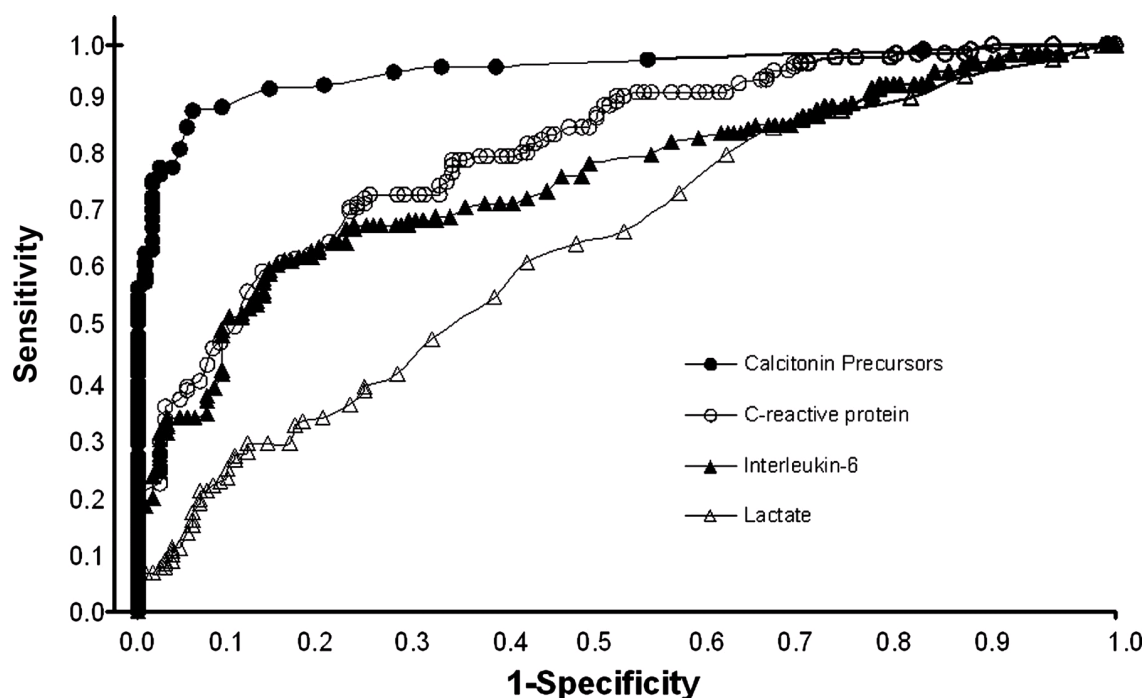


**Figure 5: ProCT versus CRP, IL-6 and Lactate.** The receiver-operating characteristics of the daily values of several markers for the severity of sepsis in 101 patients in the intensive care unit. In this study, calcitonin precursors (i.e. ProCT) showed near- optimal sensitivity and specificity, whereas the lactate level showed a near-random correlation. (adapted from Müller et al. 2000 (30)).

### 3.2.3.1 ProCT as a toxic factor in bacterial infection and sepsis

Circulating ProCT levels correlate with severity of the bacterial insult and with mortality in humans, hamsters and pigs. In septic hamsters, the levels of serum CT precursor peptides such as ProCT, CT:CCP-I, and N-ProCT increased markedly and peaked 12 h after induction of sepsis (35, 36). ProCT levels increased dose-dependently with increased quantity of bacteria administered. Exogenous human ProCT increased mortality of septic hamsters but not in non-infected control animals. Mortality remained unchanged when mature CT was administered to septic animals (36-38).

### 3.2.3.2 Improved survival after ProCT immunoneutralisation

Treatment with ProCT reactive antiserum was leading to an increased survival rate in a hamster sepsis model of monomicrobial *e. coli* peritonitis and in a polymicrobial sepsis model puncturing a ligated coecum into pigs. Importantly, in pigs the

immunoneuralisation of ProCT remained effective even when the antiserum was administered after the pigs became moribund (35, 38). These characteristics of ProCT, improving the clinical diagnosis and antibiotic stewardship in sepsis and bacterial respiratory tract infections and a treatable sepsis mediator in several animal models of mono- and polymicrobial sepsis both early and late during the course of the disease are unmatched by any other molecule.

### ***3.2.3.3 Mode of action of CT peptides***

A recent paper by Sexton et al. shed light on the molecular mechanism on the action of ProCT on the receptor level (39).

Based on their structural homologies, calcitonin peptides have overlapping bioactivities, which they exert by binding to the same family of receptors (40). There are two subgroups of these G protein coupled receptors with seven transmembrane domains: calcitonin receptors (CR) and calcitonin receptor-like receptor (CLR). Three accessory proteins, receptor activity-modifying proteins (RAMPs 1–3), bind on these receptors and alter their specific responsiveness and ligand affinity (12). The presence, the concentration, and the timing of the three RAMPs determine the specific cellular phenotype of the receptor that is biologically active on the cell surface. Depending on which of the different RAMPs is associated with the receptor, different CT peptides bind with distinct affinities. It is tempting to speculate that the extraordinary increase of circulating ProCT in sepsis prevents CGRP and ADM from exerting their actions, and thus acts as an antagonist with or without its own agonistic (i.e., intrinsic) activity. ProCT was found to be a potent agonist of the CGRP1 receptor, a weak agonist at the amylin (AMY1) receptor of medicine, and virtually inert at the calcitonin (CTa) and adrenomedullin (AM1, AM2) receptors, respectively, as assessed by cAMP production. In addition, ProCT inhibited the response to endogenous agonist peptides at their respective receptors, especially CGRP (CGRP1), and to a lesser extent also calcitonin (CTa) and amylin (AMY1) (Christ-Crain M, Müller B., Editorial, Crit Care Med 2008 Vol 36, No.5 ).

### **3.2.4 Increased levels of CGRP and ADM in bacterial infection and sepsis**

In addition to ProCT, levels of circulating CGRP (41) and ADM (42) are elevated in human patients with sepsis (for CGRP from 2.0 +/- 0.3 pg/ml in control patients up to 14.9 +/- 3.2 pg/ml in sepsis and for ADM from 7.9 +/- 3 fmol/ml in normal up to 107



+/- 139 fmol/ml in sepsis) but in a much lower extent than ProCT. Unfortunately, the measurement of ADM for diagnostic or prognostic purposes is technically challenging (43). Due to their potent bioactivity as vasodilators, the circulating levels of CGRP and ADM are much more tightly regulated as compared to levels of the less active ProCT. The measurement of the mature hormones, however, is cumbersome due to the short half-life of only few minutes. Reliable measurement is almost impossible because ADM is rapidly cleared from the circulation and masked by the binding protein complement factor H, making it inaccessible for immunometric analysis (20, 44). Recently, the more stable midregional fragment of pro-adrenomedullin (MR-ProADM) was identified in plasma of patients with septic shock and shown to be a useful prognostic marker (43). In this context, elevated levels of MR-ProADM have been shown to be helpful for individual risk assessment and outcome prediction in sepsis (43, 45, 46).

### **3.2.5 Extrathyroidal expression of CALC gene mRNA and CT precursor peptides in bacterial infection and sepsis**

Muller et al. (23) identified a uniform and ubiquitous expression of CT-mRNA in tissue of septic hamsters. The expression pattern of CT-mRNA is more specifically increased in sepsis compared to that of other established pro-inflammatory mediators of systemic infection such as TNF- $\alpha$  and IL-6, meaning that high levels of TNF- $\alpha$  and IL-6 mRNA expression are already present in several tissues of the non-septic, apparently healthy control animals (Figure 6). This ubiquitous sepsis-induced expression pattern characteristic for hormokines is also present in other species, namely pigs (25) and primates (26) including humans (28, 47).

Similar as for CT, mRNA of the second CALC-I gene splicing product CGRP-I is present in several tissues of septic hamsters compared to healthy control animals and here as well, CGRP mRNA is more specifically up-regulated than the mRNA of TNF- $\alpha$  and IL-6 (24). In septic humans, serum levels of CGRP also increase (41), but the levels are considerably lower as compared to the level of the CT precursor peptides.

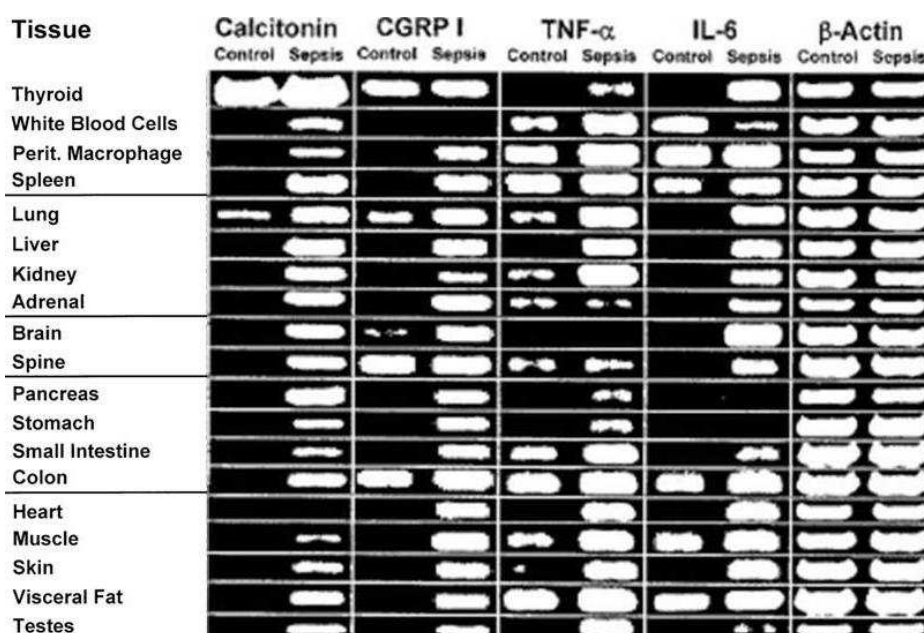


**Figure 6: CT- , CGRP-I and cytokine mRNA expression in septic and control hamsters.**

Total RNA was extracted from the different control and septic tissue. For all different PCR-products, the specificity was verified by direct sequencing of DNA from four randomly chosen tissues with a positive signal. To facilitate comparison, the control and septic tissues were aligned for each PCR- product. (Suarez Domenech et al. 2001(24)).

### 3.3 Infection and sepsis-related expression of CT peptides in adipose tissue

#### 3.3.1 Human adipose tissue

The composition of adipose tissue is complex. Heterogenous and many different cell types including adipocytes, preadipocytes, pericytes, monocytes, macrophages and cells of the endothelium such as endothelial and vascular smooth muscle cells form adipose tissue. Adipocytes are the most predominant cells and the additional cells are collectively referred as the stromal vascular cell fraction (SVF).

Adipose tissue is known to act as an endocrine organ actively participating in the regulation of a variety of physiologic and pathologic processes, including immunity and inflammation. Adipose tissue contributes to the immune response through direct effects caused by several cell types of the SFV, among which are cells of the immune system. On the other hand, preadipocytes and adipocytes themselves are important

contributors to some aspects of the immune system. Like macrophages, they are sensitive to infectious disease agents and cytokine-mediated inflammatory signals (48). Preadipocytes and adipocytes express a broad spectrum of Toll-like receptors (TLRs) and preadipocytes can convert into macrophage-like cells (49, 50). Adipose tissue produces and releases a variety of pro-inflammatory and anti-inflammatory factors, including the adipokines leptin, adiponectin, resistin, and visfatin, which regulate monocyte and macrophage function, as well as cytokines and chemokines, such as TNF- $\alpha$ , IL-1 $\beta$ , IL-6, IL-8, monocyte chemoattractant protein 1 (MCP-1), and others (51, 52).

### **3.3.2 Inflammatory signaling in adipocytes**

TLRs are a class of proteins which play a key role in innate immunity. They belong to a family of transmembrane proteins characterized by an extracellular domain composed of leucine-rich repeats and a Toll-IL-1R domain in their cytoplasmic region. Each of them is specialized in the recognition of a particular subset of pathogen-associated molecular patterns (PAMPs). Their activation by various ligands triggers a signaling cascade leading to cytokine production and initiation of an adaptive immune response (53). The description of the TLRs, including their role, has mainly been determined in immune cells (54), but these receptors are also expressed by several other cell types, such as epithelial cells (55) keratinocytes (56) and adipocytes (57), whereby in adipocytes the two receptors TLR2 and TLR4 have been shown to be present.

TLR4 is the receptor for the bacterial endotoxin LPS and plays a critical role in the nuclear factor kappa B (NF $\kappa$ B) and MAP kinase signaling pathways. Stimulation of TLR4 by LPS activates pro-inflammatory pathways, whereby one is activated by the adaptors TIRAP (Toll/interleulin-1-receptor (TIR)-domain-containing-adaptor protein) and MyD88, which induces the expression of cytokines such as IL-6, IL-1 $\beta$  and TNF- $\alpha$ . TLR4 activation also leads to the induction of type I interferons (INF) such as INF- $\beta$  (58) (Figure 4).

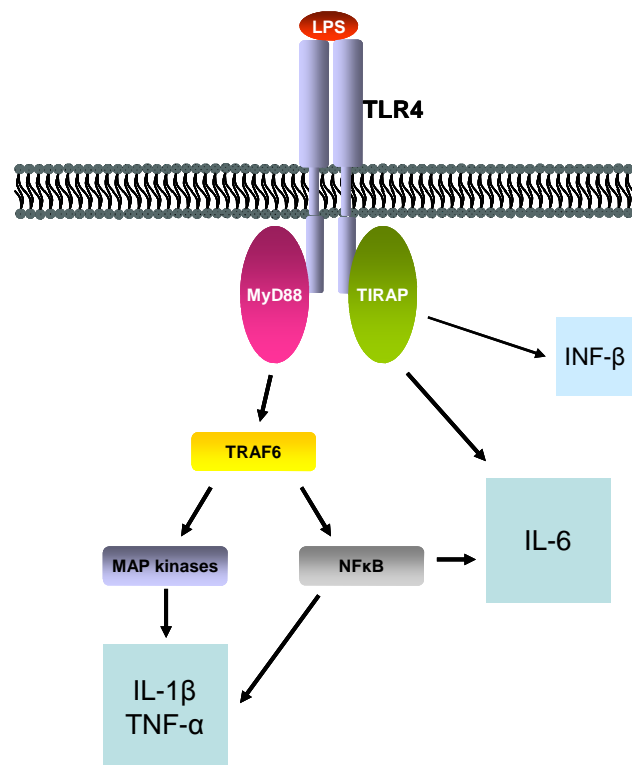


**Figure 4: TLR4 signaling.** Binding of LPS on TLR4 induces expression of pro-inflammatory cytokines such as IL-1 $\beta$ , TNF- $\alpha$  and IL-6 and of INF- $\beta$ . TLR proteins utilize the adapter protein MyD88 to activate a signaling pathway leading to the activation of the transcription factor NF- $\kappa$ B and MAP kinases in a TRAF-6-dependent manner. These signaling events culminate in expression of the pro-inflammatory cytokines IL-1 $\beta$  and TNF- $\alpha$ . TLR4 uses an additional adapter molecule, called TIRAP, to induce the expression of IL-6 and INF- $\beta$  (adapted from Armant and Fenton 2002 (58)).

Most of the TNF- $\alpha$  mRNA in adipose tissue is found within adipocytes (59, 60) and Hoch et al. (61) demonstrated in adipose tissue explants an increased secretion of the cytokines IL-6, IL-8, IL-10 and TNF- $\alpha$  upon LPS and in preadipocyte- or MSC-derived adipocytes a dose dependent release of IL-6 and IL-8 induced by LPS.

### 3.3.3 Adipocytes and CT peptides

Adipose tissue is an important extrathyroidal source of CT peptides during bacterial infection and inflammation. The increase in ProCT occurs both in subcutaneous and

omental fat depots. Linscheid et al. (47) measured increased CALC-I gene expression in adipose tissue samples from infected compared to noninfected patients with different levels of serum ProCT. Adipocyte selecting ceiling-cultures confirmed that the source of CALC gene products is from adipocytes directly and not from non-adipose cells potentially present in their tissue and cell-culture model such as macrophages or endothelial cells (47). Upon inflammatory stimuli such as bacterial LPS and of LPS, IL-1 $\beta$  and TNF- $\alpha$  in combination, MSC-derived adipocytes were shown to express mRNA and secrete protein of CT, CGRP (-I and -II) and the CALC-V gene ADM *in vitro* (28).

### **3.4. CALC genes and calcium**

#### **3.4.1 Hypocalcemia in sepsis**

In critically ill patients, especially in those with sepsis and major burn injuries hypocalcemia is a common phenomenon and indicates an adverse outcome (62-64) . Several factors may be involved, including resistance to parathyroid hormone (PTH) action in the kidney and bones, an impaired vitamin D metabolism and function or the chelation of calcium by lactate. Additionally, CT precursors which are increased in the circulation of critically ill patients with sepsis are suspected to contribute to hypocalcemia (64).

While sepsis is accompanied by a decrease in extracellular Ca<sup>2+</sup> concentration levels ([Ca<sup>2+</sup>]<sub>e</sub>) , increased intracellular calcium concentrations ([Ca<sup>2+</sup>]<sub>i</sub>) have been observed in parallel. In the aortic smooth muscles of septic rats, [Ca<sup>2+</sup>]<sub>i</sub> is increased more than 2-fold during sepsis (65). The increase in the activity of calcium-activated enzymes in tissues of septic animals such as the calcium-activated protease calpain (66) and glycogen phosphorylase b kinase (67) also explains the elevated [Ca<sup>2+</sup>]<sub>i</sub> in sepsis. Not only in animal models but also in human cells an increase in [Ca<sup>2+</sup>]<sub>i</sub> can be observed in septic patients compared with healthy control patients or cardiac surgical and head-injured patients (68).

#### **3.4.2 Calcium**

Calcium is one of the major elements of the body and plays an essential role in the mineral hydroxyapatite which gives rigidity to the skeleton. The skeleton can be

denoted as a valuable mineral reservoir, since a vast majority of the total body calcium is stored in bones whereby 99% is tied up in the mineral phase and the remaining 1% is in a pool that can rapidly exchange with extracellular calcium. However, besides the skeleton, there are two not less important pools of calcium in the body, namely the calcium in the blood and extracellular fluid and the intracellular calcium. Ionized calcium ( $\text{Ca}^{2+}$ ) plays a crucial role in many physiological and cellular processes which include neuromuscular excitability, membrane permeability, muscle contraction, blood clotting, enzymatic activation and regulation of gene expression. There are three forms of circulating calcium in the blood; roughly 50% of the calcium in blood is bound to proteins, 10% in a diffusible but non-ionized chelated fraction and 40% in an ionized fraction. The concentration of ionized calcium is constant at approximately 1 mM, or 10,000 times the basal concentration of free calcium within cells. In contrast,  $[\text{Ca}^{2+}]_i$  fluctuate greatly, from around 100 nM to greater than 1  $\mu\text{M}$ , due to release from cellular stores or influx from extracellular fluid (64, 69). A large majority of intracellular calcium is sequestered in the endoplasmic reticulum and in mitochondria. The cytoplasmic calcium level is low in resting cells and maintained at 100 nM by extrusion via plasma membrane calcium pumps (PMCA) and sarco-endoplasmic reticulum  $\text{Ca}^{2+}$  ATPases (SERCA). Additionally, the sodium/calcium exchanger (NCX) is a major secondary regulator of  $[\text{Ca}^{2+}]_i$  and is exchanging three Na ions for one  $\text{Ca}^{2+}$ . Calcium-binding proteins in the cytoplasm and in the endoplasmic reticulum (ER) offer additional  $\text{Ca}^{2+}$  buffering capacity.  $[\text{Ca}^{2+}]_i$  can increase through release from ER stores through the ryanodine (RyR) and inositol-1,4,5-trisphosphate receptors ( $\text{IP}_3\text{R}$ ) and through calcium influx from extracellular pools through various channels (voltage-, receptor- or store-operated channels) and, under extreme circumstances, through the NCX. Additionally, increased  $[\text{Ca}^{2+}]_i$  drives  $\text{Ca}^{2+}$  overload in mitochondria through mitochondrial membrane calcium pump (MMCA), and relaxed specificity channels (uniporter). In turn, calcium overload triggers secondary release of  $\text{Ca}^{2+}$  from mitochondrial stores, through the mitochondrial NCX (MNCX) and mitochondrial pores opened during mitochondrial permeability transition (MPT) (Figure 5) (70).

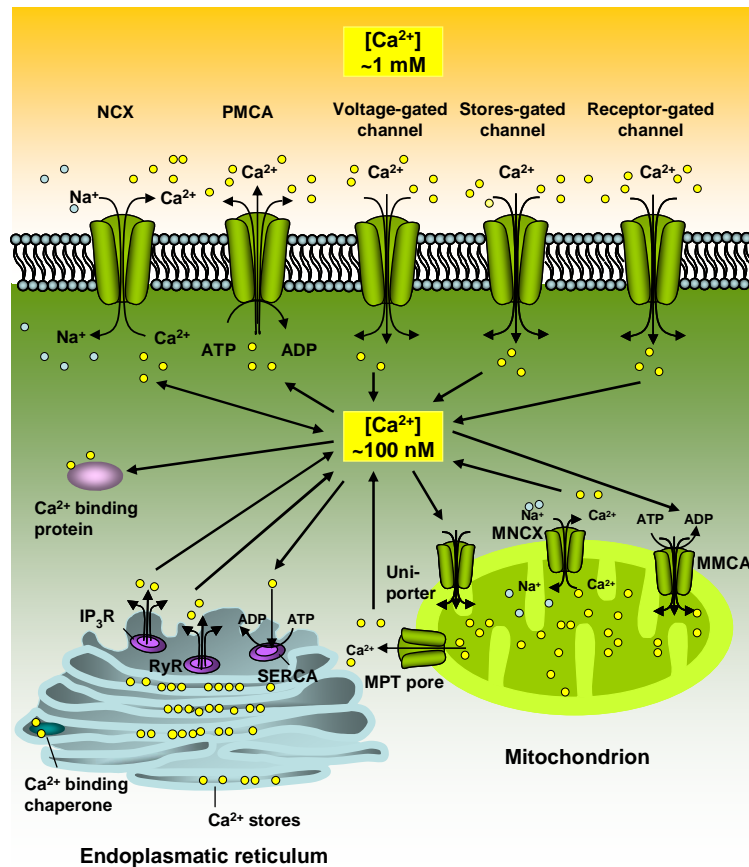


**Figure 5: Mechanisms of calcium homeostasis.**  $[Ca^{2+}]_i$  increase through ryanodine receptor (RyR), and inositol-1,4,5-trisphosphate receptors (IP<sub>3</sub>R) in the endoplasmic reticulum, through influx through voltage-, receptor- or store-gated channels and through the sodium/calcium exchanger (NCX).  $Ca^{2+}$  enters mitochondria through mitochondrial membrane calcium pump (MMCA) and relaxed specificity channels (Uniporter) and triggers secondary release of  $Ca^{2+}$  from mitochondrial stores, through the mitochondrial NCX (MNCX) and mitochondrial pores opened during mitochondrial permeability transition (MPT). The plasma membrane calcium pump (PMCA), NCX and sarco-endoplasmic reticulum  $Ca^{2+}$  ATPase (SERCA) restore normal calcium levels. Calcium-binding proteins in the cytoplasm and in the endoplasmic reticulum act as calcium buffers (adapted from Syntichaki P. et al. 2003 (70)).

### **3.4.3 Calcium and CALC genes**

#### ***3.4.3.1 Calcium and CT***

The calcium-sensing receptor (CASR) is expressed in CT-producing C-cells, in parathyroid hormone (PTH) -producing cells of the parathyroid gland, and in the cells lining the kidney tubule. The CASR is a plasma membrane G protein-coupled receptor which senses small changes in circulating calcium concentration and stimulates CT secretion and suppresses PTH secretion. The CT release occurs within minutes of the elevation of plasma calcium and CT acts promptly to suppress calcium release from bones and inhibits tubular reabsorption in the kidney (71-73). Conversely, increased expression of the CASR leads to a decrease in the extracellular calcium set-point, thereby reducing PTH secretion and renal calcium reabsorption and increasing CT secretion (74, 75). Conversely, decreased calcium binding on the extracellular side induces a conformational change of the receptor, which, on the intracellular side, initiates the phospholipase C pathway (76), ultimately increasing  $[Ca^{2+}]_i$ , triggering vesicle fusion and exocytosis of PTH.

In contrast to the persistent hypercalcaemic effects of PTH and 1,25-dihydroxyvitamin D3 the calcium-lowering hormone CT is only mild and transient. Basically, the true function of CT in humans remains enigmatic (77). In patients with MTC, which is a malignancy of the C-cells, large amounts of CT are secreted, but surprisingly no hypocalcemia occurs (78). Similarly, decreased levels of CT after thyroidectomy are not accompanied by elevations in serum calcium concentration (79). In the blood of MTC patients, the 116-amino-acid CT precursor peptide ProCT is universally present. High ProCT to CT ratios were prognostic and correlated with a high risk for progressive disease and a shorter progression-free survival (80, 81).

#### ***3.4.3.2 Molecular mechanism of CT expression***

The molecular entity through which C-cells detect changes in  $[Ca^{2+}]_e$  and modulate hormone secretion is unknown. Additionally, the molecular mechanism underlying the CT gene expression dependent on  $Ca^{2+}$  has not yet been clarified.

DREAM (downstream regulatory element antagonist modulator) was first identified as a  $Ca^{2+}$ -dependent transcriptional repressor of the prodynorphin gene. DREAM has a mass of 29 kDa, four EF hand motifs, and is the first known  $Ca^{2+}$ -binding protein to function as a DNA binding transcriptional regulator (82). The prodynorphin gene



contains a consensus DNA sequence called downstream regulatory element (DRE), and its transcription requires direct association with DREAM. The  $\text{Ca}^{2+}$ -unbound DREAM binds to the DRE site as a tetramer and represses the transcription of target genes (Figure 6, left panel). An increase in the  $[\text{Ca}^{2+}]_i$  causes the dissociation of the  $\text{Ca}^{2+}$ -bound DREAM from the DRE site and results in transcriptional derepression (Figure 6, right panel).

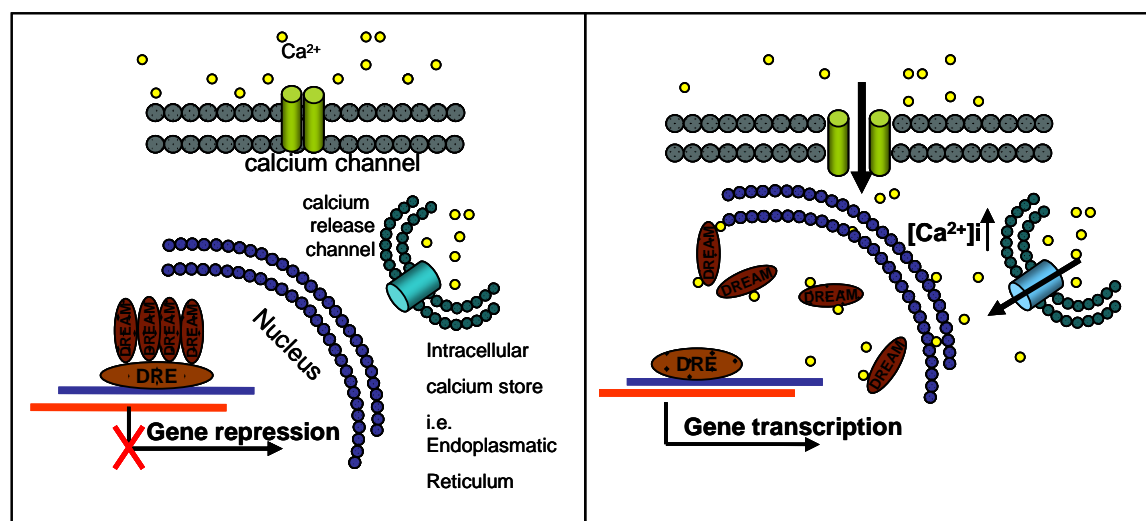


**Figure 6: Repression-derepression mechanism driven by DREAM on a potential target gene.** Under basal conditions, DREAM is bound to the promoter DRE as a tetramer and gene transcription is repressed (left panel).  $[\text{Ca}^{2+}]_i$  increase abolishes DREAM-DNA binding, resulting in derepression of gene transcription (right panel).

DREAM is highly expressed not only in the brain but also in the thyroid glands in human tissues (82) including TT cells (83). This human thyroid carcinoma cell line lacks the extracellular calcium-sensing function but secretes constitutively large amounts of CT and its precursors. Two DRE core sequences are present in the 5'-flanking region of the CALC-I gene. Thus, DREAM might play a role in human CT gene expression in TT cells. Furthermore it has been shown that DREAM binding to DRE sites is not only regulated by  $\text{Ca}^{2+}$  but also by specific protein-protein interactions with nuclear factor effectors of the cyclic AMP (cAMP) pathway and these interactions are independent of nuclear  $\text{Ca}^{2+}$  (84). Cellular stimulation by hormones or activation of membrane receptors is often followed by an elevation of

both second messengers  $\text{Ca}^{2+}$  and cAMP, indicating that both mechanisms can cooperatively derepress DRE-dependent transcription.

#### **3.4.3.3 Calcium and CGRP**

Although most of the body CGRP is of neural origin, the CALC-I gene in the thyroid C-cells is also generating mRNA encoding for CGRP-I and the CGRP peptide is also stored within secretory vesicles of the C-cells. Normally, administration of  $\text{Ca}^{2+}$  does not induce increases in the plasma CGRP concentrations, which was shown in several *in vivo* studies in rats (85, 86). But in humans with low blood pressure, an increase in CGRP has been observed upon elevated  $\text{Ca}^{2+}$  (87). *In vitro* studies in mice, neonatal rats and dogs demonstrated that  $\text{Ca}^{2+}$  stimulates the secretion of CGRP from thyroid glands (88-90).

Conversely, CGRP has been shown to trigger transient increases in  $[\text{Ca}^{2+}]_i$  in astrocytes and glia cells (91).

#### **3.4.3.4 Calcium and ADM**

In adrenal chromaffin cells ADM is stored in the secretory vesicles to be co-secreted with catecholamines. Catecholamine secretion and activation of catecholamine biosynthesis has been shown to result from an increase in the  $[\text{Ca}^{2+}]_i$  and ADM has been shown to stimulate  $\text{Ca}^{2+}$  efflux from adrenal chromaffin cells, probably through acceleration of  $\text{Na}^+/\text{Ca}^{2+}$  exchange (92). Additionally, ADM has been shown to induce a  $[\text{Ca}^{2+}]_i$  increase in bovine aortic endothelial cells in a dose-dependent manner (93). The same increasing effect of ADM on  $[\text{Ca}^{2+}]_i$  has been described in a human oligodendroglial cell line (94). In contrast, in hippocampal neurons (95) and retinal pigment epithelial cells (96), ADM has been shown to have an effect on  $[\text{Ca}^{2+}]_i$  the opposite way around, namely to reduce  $[\text{Ca}^{2+}]_i$  and to inhibit  $\text{Ca}^{2+}$  release from intracellular stores. Although numerous studies exist on the effect of ADM on  $[\text{Ca}^{2+}]_i$ , even with conflictive conclusions, little or nothing is known on the effect of  $[\text{Ca}^{2+}]_i$  on ADM.

## 3.5 CALC genes and cAMP

### 3.5.1 cAMP

Similar to  $\text{Ca}^{2+}$ , cAMP is an archetypic second messenger. It impacts on every aspect of the life of the cell, from differentiation and development through to cell death. cAMP is derived from adenosine triphosphate (ATP) and produced by enzymes of the adenylat cyclase (AC) family. In turn, the phosphodiester bond in cAMP gets degraded by enzymes called phosphodiesterases (PDE) which thereby regulate the localization, duration, and amplitude of cyclic nucleotide signaling within subcellular domains. cAMP is involved in the activation of several protein kinases (PK) (i.e. PKA and PKC), regulates the effects of different hormones such as adrenalin and glucagon and regulates the passage of  $\text{Ca}^{2+}$  through ion channels. To date, different isoforms of ACs have been described, namely 9 membrane-bound (AC1-9) and one soluble form. ACs are regulated by a range of signaling molecules and hormones in a stimulatory or inhibitory manner through the mediation of stimulatory and inhibitory G-proteins (97).

### 3.5.2 cAMP and calcium

Among the membrane-bound ACs, many of them have been found to be regulated by  $[\text{Ca}^{2+}]_i$ , whereby some are stimulated and others are inhibited by  $\text{Ca}^{2+}$  (Table 1). AC2, AC4, AC5 and AC6 mRNAs are significantly transcribed in white adipose tissue from rats (98). AC2 mRNA amount decreases from the undifferentiated to the late differentiated state. Conversely, AC4, AC5 and AC6 mRNA are more expressed in late differentiated preadipocytes and mature adipocytes compared to undifferentiated preadipocytes. Apparently, the different AC isoforms described in adipose tissue are either inhibited by  $\text{Ca}^{2+}$  or they are  $\text{Ca}^{2+}$ -insensitive. In hamster adipocytes it has been described that increasing  $[\text{Ca}^{2+}]_i$  results in stimulation of PDE and a decrease in cAMP levels (99).

AC isoform	Major source of expression	Response to Ca <sup>2+</sup>
AC1	brain	Stimulation
AC2	lung, brain, preadipocytes	No effect
AC3	olfactory epithelium, pancreas	Stimulation or inhibition
AC4	Widespread, adipocytes	No effect
AC5	heart, striatum, adipocytes	Inhibition
AC6	heart, kidney, widespread, adipocytes	Inhibition
AC7	widespread	No effect
AC8	brain, pancreas	Stimulation
AC9	Testis, widespread	inhibition

**Table 1:** Major sources of expression of each of the nine membrane-bound AC isoforms (adapted from Willoughby and Cooper, 2006 (97)).

IP<sub>3</sub>-mediated Ca<sup>2+</sup> release from the ER has the potential to act as a weak regulator of Ca<sup>2+</sup>-sensitive ACs and in nonexcitable cells, only the Ca<sup>2+</sup> entry pathway occurring via store-operated Ca<sup>2+</sup> channels has been shown to regulate AC activity (Figure 7).

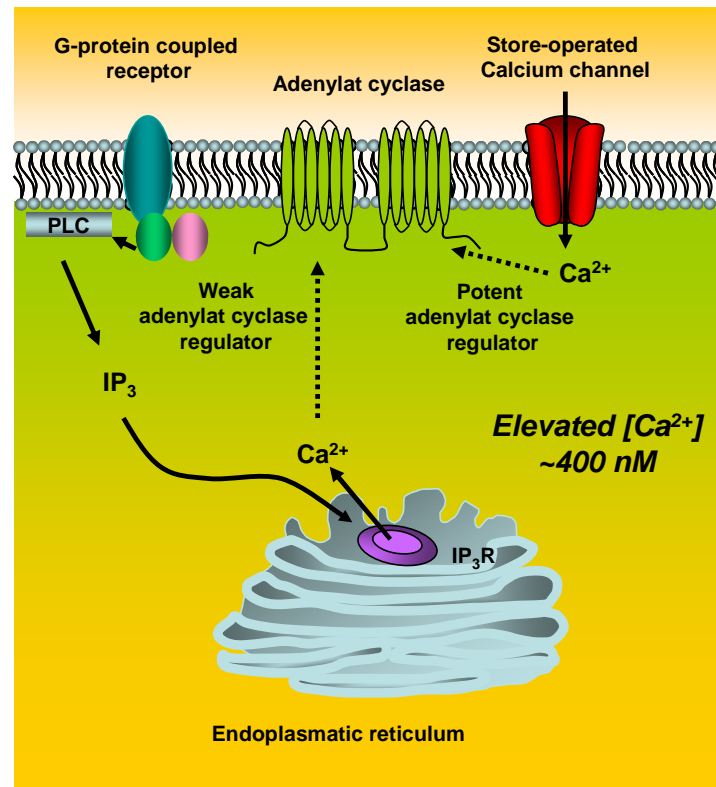


**Figure 7: Ca<sup>2+</sup> regulation in nonexcitable cells and effects on AC activity.** IP<sub>3</sub> –mediated Ca<sup>2+</sup> release from the endoplasmatic reticulum and Ca<sup>2+</sup> entry via store-operated calcium channels regulates the activity of Ca<sup>2+</sup> -sensitive ACs (adapted from Willoghby D. and Cooper D. 2007 (97)).

### 3.5.3 cAMP and DREAM

In addition to the DRE motif in the 5' flanking region of the CALC-I gene, cAMP responsive element (CRE) and CRE-like motifs have been identified in the same region and shown to be involved in transcriptional activation (100). cAMP-dependent gene expression is controlled at the transcriptional level by several leucine zipper transcription factors, including the cAMP responsive element binding protein (CREB) and cAMP responsive element modulator (CREM) which bind to CRE sites in target genes (101).

In human neuroblastoma cells, PKA activation by cAMP has been shown to result in loss of DREAM binding to the DRE motif and derepression of the target gene prodynorphin (102), both Ca<sup>2+</sup>-dependent (103) and independent (84).

### **3.5.4 cAMP and CALC genes**

Binding of CT to the CT receptor initiates cAMP responses in kidney cells, bone cells and in a human lymphoid cell line (104-106). In the lymphoid cell line, the formation of cAMP was suppressed by increased  $[Ca^{2+}]_i$ . CGRP binding to its receptor results in increased cAMP levels in different cell types (107, 108) and CGRP dose dependently elevates cAMP levels in kidney cells (109). In several cell types, the CALC-V gene product ADM stimulates the formation of cAMP, up to 10 fold stronger as compared to CGRP (110-113).

Conversly, cAMP, similar to  $Ca^{2+}$ , has an impact on CALC gene expression. cAMP enhances transcription of CT and CGRP mRNA in TT cells (100, 114) and CREB is a possible candidate to mediate cAMP induced transcriptional activation of the CALC-I gene.

### 3.6 Aim of the thesis

In human adipose tissue of septic patients and in a model of human preadipocyte- or MSC-derived adipocytes CALC gene expression and CT protein content increase upon stimulation with bacterial endotoxin and pro-inflammatory cytokines. The molecular mechanisms as to how bacterial infection stimulates this extrathyroidal CALC-gene expression are unknown so far. Thus, the aim of this thesis was to gain a better understanding of the regulation of CT peptides during bacterial infection and inflammation in our well established human adipocytes model.

- The main focus of this work was to study the effect of the bacterial endotoxin LPS as a model for bacterial infection on intracellular calcium concentration changes in our adipocyte cell cultures in respect to alterations in CALC-I and CALC-V gene expression
- Additionally we wanted to explore the effect of cAMP on CALC gene expression and the effect of LPS on cAMP levels in human adipocytes.

Minor aims of this thesis were the following:

- to evaluate the differentiation capacity of preadipocytes in our cell culture model
- to exclude cytotoxic effects of LPS on adipocytes
- to evaluate involvement of the NF $\kappa$ B pathway in LPS-induced CALC-I gene expression
- to examine whether the LPS-mediated effect on CALC-I gene expression is due to IL-1 $\beta$

## 4. Materials and Methods

### 4.1 Cell culture

#### 4.1.1 Primary human adipocyte cell culture model

The stromal-vascular cell fraction (SVF) containing preadipocytes was isolated from fat tissue from lean and from obese donors during elective abdominal surgery indicated for various non-malignant conditions (27). The study was approved by the local ethics committee and informed consent has been obtained from the patients. Bone marrow aspirates (20-40 ml) were obtained from healthy donors (18-63 years) during routine orthopedic surgical procedures, in accordance with the local ethics committee (University Hospital Basel, Switzerland) and after informed consent. Nucleated cells were isolated from the aspirate by Ficoll density gradient centrifugation (Histopaque1, Sigma, Buchs, Switzerland). Human mesenchymal stem cells (MSC) were selected within the nucleated cells in culture by adhesion and proliferation on the plastic substrate.

The SVF or the MSC cells were expanded *in vitro* in DMEM (Lonza, Verviers, Belgium) supplemented with 10% fetal bovine serum (FBS) and 5 ng/mL  $\beta$ -FGF (Lubio Science, Luzern, Switzerland). For experiments, cells from different donors between passages 3 and 8 were seeded into 6-well or 12-well plates. Differentiation into adipocytes was induced by incubating confluent cells in DMEM/F12 (Lonza) containing 3% FBS and supplements as follows: 30 mM HEPES (Lubio Science), 250  $\mu$ M 3-isobutyl-1-methylxanthine (IBMX), 1  $\mu$ M dexamethasone, 0.2 nM 3,3,5-triiodo-L-thyronine, 5  $\mu$ M transferrin, 8  $\mu$ g/ml biotin, 15 mM D-pantothenat (all from Sigma-Aldrich, Buchs, Switzerland), 100 nM insulin (Novo Nordisk, Künsnacht, Switzerland), 1  $\mu$ M rosiglitazone (GlaxoSmithKline, Worthing, UK). After 10–14 days, supplements were removed by washing two times with warm phosphate buffered saline (PBS) and DMEM/F12 containing 3% FBS was then added. Experiments were started 3 days after completing differentiation.



#### **4.1.2 HEK293T and TT cells**

Cells of the human embryonic kidney (HEK) cell line HEK293T (ATCC; SD3515) were cultured in DMEM medium supplemented with 10% FBS in 100 mm petridishes.

Human medullary thyroid carcinoma cells (TT cells line, kindly provided by Prof. A. Russo, Iowa City, Iowa, USA) were cultured in RPMI 1640 medium (Lucerna AG) supplemented with 10% FBS.

#### **4.1.3 Splitting, freezing and thawing of cells**

##### ***4.1.3.1 Splitting***

At 80 % confluence, cell layers were rinsed twice with pre-warmed PBS and trypsinised with a solution consisting of a mixture of trypsin/EDTA/PBS to disrupt cell-cell and cell-substratum interactions. The trypsin was inactivated by the addition of DMEM.

##### ***4.1.3.2 Freezing***

Cells were treated as above, and collected by centrifugation (200 rpm for 5 min). The pellet was resuspended in cold freezing media (normal medium supplemented with FCS and 10% DMSO). Cells were then transferred into cryo-tubes (Nunc), placed in a Styrofoam box and slowly frozen at -80°C. For long-term storage, cryo-tubes were transferred to liquid nitrogen.

##### ***4.1.3.3 Thawing***

Cells were thawed at room temperature and quickly transferred to a Falcon tube containing 5 ml of pre-warmed DMEM + 10% FCS. After centrifugation, the supernatant was removed and the cell pellet was resuspended in DMEM +10%FCS. Cells were seeded into cell culture dishes and grown in an incubator at 37°C + 5% CO<sub>2</sub>.

## 4.2 RNA and DNA applications

### 4.2.1 RNA isolation

Total RNA was extracted from 6-well or 12-well cell culture plates using the following protocol:

#### Homogenization:

First, the cell culture medium was removed. The cells were then lysed by adding 1 ml TRI<sup>®</sup> Reagent (Sigma-Aldrich, St. Louis, MO, USA) directly into the well. The cell lysate was passed several times through a pipette, transferred to a 2 ml Eppendorf<sup>®</sup> tube and homogenized by douncing it through a RNase-free 23-gauge needle using a syringe.

#### Phase Separation:

The homogenate was stored for several hours at -80°C to permit complete freezing of the samples. Next, the homogenate was unfrozen, supplemented with 0.1 ml 1-Bromo-3-Chloro-Propane per 1 ml of TRI Reagent, covered tightly and shaken vigorously for 15 sec. The resulting mixture was stored at room temperature for 2-15 min and then centrifuged at 14000 g for 15 min at 4°C in an Eppendorf centrifuge 5417R. Following centrifugation, the mixture separates into a lower red phenol-chloroform phase, interphase and the colorless upper aqueous phase. RNA remains exclusively in the aqueous phase whereas DNA and proteins are in the interphase and organic phase.

#### RNA Precipitation:

The aqueous phase was transferred to a Biosphere Safeseal Micro tube. RNA from the aqueous phase was precipitated by mixing with 0.5 ml of isopropanol. Samples were stored at -20°C for 20 min and then centrifuged at 14000 g for 15 min at 4°C

#### RNA Wash:

The supernatant was removed and the RNA pellet washed with 1ml of 75% ethanol and then centrifuged at 14000 g for 5 min at 4°C.

#### RNA elution:

Ethanol was removed and the RNA pellet was air dried for 5 min and briefly at 65°C.

The RNA was dissolved in RNase-free water and incubated for 10 min at 65° C and then directly put on ice.

RNA concentration and purity was measured using the NanoDrop ND-1000 Spectrophotometer.

#### **4.2.2 cDNA synthesis**

Specific PCR thin wall tubes with flat caps (Sarsteadt) were used.

1 µg of total RNA was reverse transcribed using the High Capacity cDNA RT Kit from Applied Biosystems. The RNA was mixed with 2 µl 10x RT buffer, 0.8 µl 25x dNTP mix (100mM), 2 µl 10x RT Random Primers and 0.5 µl RNase inhibitor (10000 U) and 3.7 µl nuclease-free H<sub>2</sub>O up to a final volume of 20 µl. The mix was incubated for 10 min at 25°C, followed by incubation for 120 min at 37°C. To inactivate the enzyme reaction, the samples were heated at 85°C for 5 sec and the stored at -20°C.

#### **4.2.3 Real-time polymerase chain reaction (RT-PCR)**

For quantitative PCR, optimal sets of primers were designed for each studied gene using the “ProbeFinder” (Roche Applied Bioscience) website interface (<http://qpcr2.probefinder.com>) and synthesized by Microsynth. 2 µl cDNA, 1 µl SYBR Fwd primer (from 10 µM stock), 1 µl SYBR Rev primer (from 10 µM stock), and 12.5 µl of Power SYBR Green PCR Master Mix from Applied Biosystems were mixed and adjusted to a final volume of 20 µl with H<sub>2</sub>O. The reaction was performed following the manufacturer’s instructions on a 7500 Fast Real Time PCR system Thermal Cycler from Applied Biosystems and the 7500 Fast System SDS analysis software.

The primers used were the following:

CT sense primer, 5'-GTGCAGATGAAGGCCAGTGA- 3'

CT antisense primer 5'-TCAGATTACCACACCGCTTAGATC- 3'

CGRP-I sense primer, 5'-CCCAGAAGAGAGCCTGTGACA- 3'

CGRP-I antisense primer: 5'-CTTCACCACACCCCCTGATC- 3'

ADM sense-primer, 5'-ACTTGGCAGATCACTCTCTTAGCA- 3'

ADM antisense primer 5'-ATCAGGGCGACGGAAACC- 3'

IL-6 sense primer 5'-TCTTCAGAACGAATTGACAAACAAA- 3'

IL-6 antisense primer 5'-GCTGCTTTCACACATGTTACTCTTG- 3'

IL-1 $\beta$  sense primer 5'-AGCTGATGGCCCTAAACAGA-3'

IL-1 $\beta$  antisense primer 5'-TCG GAG ATT CGT AGC TGG AT-3'

HPRT sense primer, 5'-TCAGGCAGTATAATCCAAAGATGGT-3'

HPRT antisense primer, 5'-AGTCTGGCTTATATCCAACACTTC-3'

### **4.3 Bacterial transformation**

#### **4.3.1 Vector information**

53RPA-PGK-GFPas: (6.93 kb) was provided by Prof. Patrick Salmon, University of Geneva, Switzerland. This vector contained an ampicillin resistance gene sequence and different CALC-I gene promoter deletion constructs cloned into the XhoI restriction site by Dalma Seboek and Kathrin Boelsterli.

#### **4.3.2 Competent cells**

*Escherichia coli* HB101 were ordered from Promega (Promega Corporation, Madison, WI, USA) and stored at -70°C.

#### **4.3.3 Plasmid transformation into bacteria**

The competent cells were thawed on ice for about 5 min, gently mixed by flicking the tube and 100  $\mu$ l were transferred into chilled culture tubes. 1-50 ng of plasmid DNA was added and incubated on ice for 10 min before heat shocking at 42°C for 45-50 sec. The mix was put back on ice for 2 additional min, then re-suspended in 900  $\mu$ l of chilled antibiotic-free LB medium and incubated for 60 min at 37°C with shaking. The cells were plated on LB-plates containing the appropriate antibiotics and incubated overnight at 37°C.

#### **4.3.4 Plasmid amplification and purification**

##### **4.3.4.1 Small scale purification miniprep (Mini-Prep)**

Bacterial colonies were picked from the agar plates with a sterile toothpick and transferred into sterile polypropylene culture tubes (Becton Dickinson Labware, Le Pont De Claix, France) containing 3 ml LB medium containing the plasmid-related antibiotic ampicillin. The mix was incubated overnight at 37°C on a shaker (200 rpm).

Plasmids were purified from this culture using the NucleoSpin<sup>®</sup> plasmid purification kit (Machery-Nagel, Düren, Germany) according to the manufacturer's protocol. Inserts were then checked by DNA digestion.

#### **4.3.4.2 Large scale purification (Maxi-Prep)**

Large scale DNA extraction was performed using the commercial kit NucleoBond<sup>®</sup> PC 500 from Machery-Nagel according to the manufacturer's instructions. Maxi-preps were done with the overnight culture grown in 100 ml LB medium containing ampicillin.

#### **4.3.5 DNA digestion**

Plasmid DNA products were digested in a buffer containing the adequate restriction enzyme(s), double-distilled water and BSA, if required. Incubation time and temperature varied according to the enzyme(s) used.

#### **4.3.6 Agarose gel electrophoresis**

Samples were analyzed by running an aliquot of the digestion products in an agarose gel containing 0.5 µg/ml of ethidiumbromide. 1% agarose gels were prepared by weighing agarose (Agarose LE, Analytical Grade, Promega) in TBE buffer and boiling the mixture in a microwave oven. Before casting the gel, ethidiumbromide (Biorad, Reinach, Switzerland) was added to the mixture. Loading-buffer was added to the samples and gels were run at 80 V for approximately one hour. To visualize the DNA, an UV transilluminator was used.

### **4.4 Cytosolic Ca<sup>2+</sup> measurements by confocal microscopy**

[Ca<sup>2+</sup>]<sub>i</sub> in human preadipocyte-derived adipocytes was measured using a dual-excitation fluorescence imaging system with a cell permeant acetoxymethyl ester of the coumarin benzothiazole-based Ca<sup>2+</sup> indicator (BTC AM, Lubio Science, Luzern, Switzerland). Alternatively, the cells were loaded with Fluo-3 AM or Fura-2 AM (both from Lubio Science). Preadipocytes were plated into 2- well or 4-well glass chamber slides (NC-155380K, Nunc, Rochester, NY, USA) and differentiated into adipocytes as described before. Fully differentiated adipocytes were washed twice with a modified Krebs-Ringer buffer (MgSO<sub>4</sub> 1,2 mM, KCl 4,8 mM, KH<sub>2</sub>PO<sub>4</sub> 1,2

mM, NaHCO<sub>3</sub> 20 mM, NaCl 118 mM, CaCl<sub>2</sub> 2,5 mM and D-Glucose 1.8 g/l, pH 7.4). Cells were loaded alternatively with BTC AM, Fluo-3 AM or Fura-2 AM (all at 3 μM) in the same buffer for 30 min at 37°C in a dark incubator with 5% CO<sub>2</sub>. To remove extracellular dye, cells were rinsed twice with pre-warmed modified Krebs-Ringer buffer and then post-incubated at 37°C in a dark incubator with 5% CO<sub>2</sub> for a minimum of 30 min before ionomycin or LPS infection for complete hydrolysis of cytoplasmic BTC AM, Fura-2 AM or Fluo-3 AM, respectively.

The chamber slide was mounted in an incubation chamber on a 40x oil-immersion objective, and the chamber was thermostatically regulated at 37°C with 5% CO<sub>2</sub>. Images were acquired using the live cell imaging mode of a confocal laser scanning microscope (LSM700, Zeiss, Feldbach, Switzerland). Using BTC AM, fluorescent images were captured alternatively at excitation wavelength of 405 and 488 nm and the emission filtered at wavelength of 520 nm. Using Fluo-3 AM, cells were excited at 488nm and for Fura-2 at 405nm. Each analysis evaluated changes in fluorescence intensity of 8 representative whole cells (4 used as untreated control, 4 used for treatments). Images of each single cell were acquired every 3 min. Fluorescence intensity and the curve of time course were analyzed by the Zen 2008 software automatically.

## **4.5 Flow cytometry**

### **4.5.1 Quantification of differentiation capacity**

Preadipocytes were plated into 12-well plates and differentiated into adipocytes as described before. Three days after complete differentiation, cells were treated with different doses of LPS for 24 h, with 1 μM of ionomycin for 24 h or 3 h and with LPS and ionomycin in combination. After the accordant incubation times, the cells were washed two times with PBS at room temperature. Cells were incubated with Bodipy 493/503 (1:4000 in PBS) for 20min at room temperature and then washed again two times with PBS. Cells were detached with 0,4 ml/well of 0,5 g/l EDTA and transferred into FACS tubes containing 1,6 ml PBS + 0,5% BSA. The samples were mixed and analyzed by passing through a FACSCalibur flow cytometer.

#### **4.5.2 Assessment of cell viability**

Cells were handled as described in upper section. 8 µl of propidium iodide staining solution (PI solution) were added to each sample, the samples were mixed and analyzed by passing through a FACSCalibur flow cytometer.

#### **4.5.3 Transfection efficiency**

MSC-cells were seeded into 175 cm<sup>3</sup> culture flasks and differentiated into adipocytes as described before. After complete differentiation, the cells were infected with 15ml medium containing the lentiviral construct over night. On the following day, infected adipocytes were washed with pre-warmed PBS and maintained in adipogenic differentiation medium with 3% FBS for five days. The cells were then washed two times with PBS at room temperature, detached with 5ml trypsin, centrifuged, trypsin was removed, the cells were resuspended in 1,6 ml PBS + 0,5% BSA and transferred into FACS tubes. The samples were mixed and analyzed for green fluorescent protein (GFP) activity by passing through a FACSCalibur flow cytometer.

### **4.6 Cell transfections**

#### **4.6.1 Generation of recombinant lentiviruses**

Lentivirus production was carried in HEK293T cells and the transient transfection of the plasmid was achieved by the calcium chloride method. 20 µg of a plasmid containing GFP under the control of the phosphoglyceratekinase (PGK) promoter (53RPA-PGK-GFPas), 5 µg of the envelope vector pMD2.G and 15 µg of the packaging vector psPAX2 were mixed and the volume was adjusted to 250 µl with special water. 250 µl of 0.5 M CaCl<sub>2</sub> were added and the mixture was dropped slowly onto 500 µl HeBS2x while vortexing top speed. To allow optimal formation of the precipitate, the mixture was let still for 20 to 30 min. The precipitate was added slowly on the cell monolayer.

On the next day, cells were checked for visibility of a fine sandy precipitate and medium was changed. Virus containing supernatants were collected on day 2 and 3 post transfection, spun at 2500 rpm for 10 min at 4°C, filtered through 0.45 µm filter, pooled and kept on -80°C freezer until the start of the experiments.

#### **4.6.2 Infection of cells**

Infection of differentiated TT cells or MSC- derived adipocytes was carried out overnight with aliquots of the cell medium derived from the infected 293T cells containing the lentivirus (53RPK PGK GFP). On the following day, infected adipocytes were washed with pre-warmed PBS and maintained in adipogenic differentiation medium with 3% FBS until the experiments were performed.

#### **4.6.3 Microscopy**

Transduction efficiency was visualized by fluorescence microscopy (Olympus IX 50). The microscope was equipped with an Olympus U-TVO 5XC camera.

#### **4.6.4 Luciferase assays**

Luciferase activity in transfected cells was measured using Bright-Glo™ Luciferase Assay System (Promega Corp., Madison, WI, USA), according to the manufacturers protocol. Briefly, transfected cells growing in 12-well plates were removed from the incubator and the culture medium was aspirated. 100 µl of new cell culture medium and 100 µl of reagent were added to each well. Cells were incubated for at least 2 min to allow complete cell lysis and the supernatant was transferred into white 96-well plates (OptiPlate™-96, PerkinElmer). Luciferase activity was measured in a plate-reading luminometer.

### **4.7 Protein measurements**

Adipocytes were incubated for 24 h with different treatments. Supernatants were collected. For CT peptides, they were concentrated *in vacuo* at room temperature for 4 h and then kept on -20°C until analyzed. IL-6 supernatants were collected and diluted 1:20.

#### **4.7.1 Immunoluminometric Assay (ILMA)**

Procalcitonin concentrations were determined in supernatants by an ultrasensitive chemiluminometric assay (B·R·A·H·M·S PCT sensitive LIA assay) with a functional sensitivity of 6 pg/ml (Brahms, Hennigsdorf, Germany) following the manufacturers protocol.



#### **4.7.2 Radioimmuno Assay (RIA)**

ADM and CGRP concentrations were determined in supernatants by human-specific radioimmunoassay kits (Phoenix Europe GmbH, Karlsruhe, Germany) following the manufacturers protocol. The analytical sensitivity of the ADM assay was given at 4.3 pg/tube and that of the CGRP assay at 3.8 pg/tube.

#### **4.7.3 Enzyme-linked immunoassay (ELISA)**

IL-6 concentrations were determined in supernatants by a human IL-6 immunoassay (Quantikine, R&D Systems Europe, Ltd., Abingdon, UK) following the manufacturers instructions.

#### **4.8 cAMP concentration measurement**

cAMP concentration was measured using the cAMP-Glo™ Assay (Promega Corp., Madison, WI, USA) following the manufacturers instructions. Briefly, adipocytes growing in 24-well plates were exposed to appropriate stimuli for 1 h followed by washing them twice with PBS. 50 µl of lysis buffer were added to each well, cells were scraped and incubated for 15 min with shaking. 20 µl of the lysate were transferred to a white 96-well plate (OptiPlate™-96, PerkinElmer). 40 µl of the detection solution containing protein Kinase A were added, the plate mixed for 30-60 sec and incubated for 20 min. 80 µl of the Kinase Glo®-reagent were added, the plate mixed for 30-60 sec followed by incubation for 10 min. Luminescence was measured using a plate-reading luminometer.

#### **4.9 Adipocyte lysates**

Following stimulation, adipocytes were washed with PBS. Cells were harvested in a 10 mM Tris-HCl (pH 7.4) lysis buffer containing 1% Triton-100, 0.5% Nonidet P-40, protease inhibitors cocktail (Roche Diagnostics, Rotkreuz, Switzerland) and Halt™ phosphatase inhibitor cocktail (Thermo scientific, Wohlen, Switzerland) and incubated on ice for 10 min. Cell lysates were cleared by centrifugation (10,000 × g, 10 min).

#### **4.10 Western blot analysis**

Protein concentrations of lysates were determined with the DC protein assay kit from Bio-Rad (Biorad, Reinach, Switzerland). Reading of the protein concentrations was performed in 96-well plates using the SpectraMax 190 microplate reader (Molecular Devices, Inc.). Lysates containing equal amounts of proteins (20 µg/sample) were boiled for 5 min at 95°C in 1 x Lämmli sample buffer, subjected to 10 % SDS-PAGE minigel (both from Bio-Rad) and blotted on a nitrocellulose membrane. After blocking of the membrane (1 h, RT in blocking buffer), the membrane was incubated overnight at 4°C with primary antibody diluted 1:500, washed and incubated with horseradish peroxidase-conjugated goat anti-mouse or anti-rabbit antibodies (45 min, RT). Washing steps were carried out in tris-buffered saline containing 0.1% Tween 20 (Bio-Rad). The Western lightning enhanced chemiluminescence substrate (Perkin Elmer) was used for detection on a Medical X-Ray film (Kodak). Membranes were stripped in stripping buffer 2 times 5-10 min, washed 2 times for 10 min in PBS and for 5 min in TBST before blocking and then reprobed with anti-tubulin antibody as a control for equal loading.

#### **4.11 Statistical analysis**

Data represent means  $\pm$  standard error of the means (s.e.m.) from a minimum of three independent experiments, each done in triplicates or from one representative experiment out of three. For multigroup comparisons one-way analysis of variance was applied with the Bonferroni's posthoc multiple comparison test. P values < 0.05 were considered as significant. All analyses were performed using Prism 4.0 (GraphPad, San Diego, CA).

## 5. Results

Human preadipocyte-derived adipocytes were used as a model to study the regulation of extrathyroidal CALC gene expression. MSC-derived adipocytes were only used for lentiviral transfection experiments.

### 5.1 Differentiation efficiency of preadipocyte-derived adipocytes in our human cell culture model

Our preadipocyte-derived adipocyte model is a heterogeneous cell population whereby even under optimal conditions the differentiation efficiency from preadipocytes to adipocytes is incomplete. In order to evaluate the differentiation capacity of preadipocytes and to distinguish undifferentiated preadipocytes from fully differentiated adipocytes, our cells were stained with a bodipy dye specific for cellular lipid droplets and analysed by flow cytometry. The percentage of bodipy positive cells was compared to bodipy negative cells in three independent experiments with cells from the same donor but different cell passages.  $60.9 \pm 3.8$  % of the total cells in culture were identified as bodipy positive mature adipocytes,  $31.2 \pm 3.2$  % were identified as bodipy negative preadipocytes and the remaining  $7.8 \pm 2.7$  % of bodipy negative cells were identified as a third population and considered as debris from cells which died during the culture process (**Figure 8**).

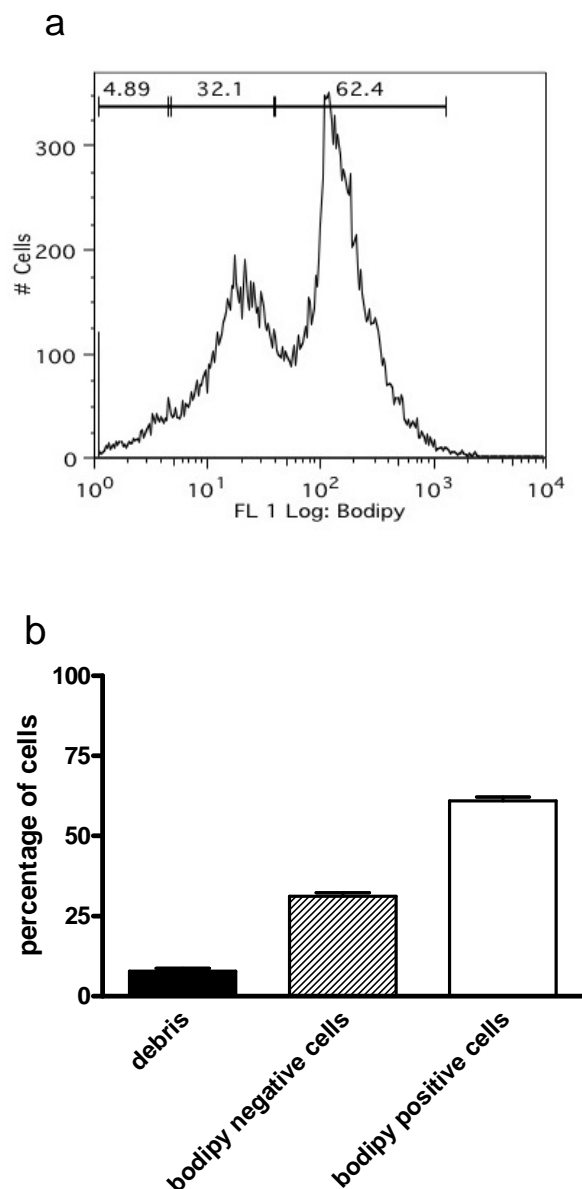


**Figure 8: Cell populations in our preadipocyte-derived adipocyte cell culture model after 14 days of differentiation.** (a) Three different cell populations determined by flow cytometry analysis after bodipy 493/503 staining from a total of 25000 cells. Section on the left hand side represents cell debris (4.89%), section in the middle the undifferentiated preadipocytes (32.1%) and section on the right hand side mature adipocytes (62.4%). Data obtained from one representative flow cytometry chart out of 9 analyses showing the number of cells according to the log of the bodipy concentration. (b) Percentage of cells per cell population represented by the mean  $\pm$  standard deviation of 9 samples from 3 independent experiments. The closed bar represents cell debris, the shaded bar the undifferentiated preadipocytes (bodipy negative cell population) and the open bar the mature adipocytes (bodipy positive cell population).

## **5.2 Effects of bacterial infection and inflammation on preadipocyte-derived adipocytes**

### **5.2.1 Different doses of LPS do not affect cell viability**

The term endotoxin came from the discovery that portions of gram-negative bacteria itself can cause toxicity, whereby the toxic effects of endotoxin have been shown to be due to LPS. To determine whether administration of LPS has an effect on the cell viability of preadipocytes and preadipocyte-derived adipocytes, cells were treated with 10ng/ml, 100ng/ml and 1µg/ml of LPS. After 24 hours of incubation, cells were stained with bodipy 493/503 and propidium iodide (PI) and analyzed by flow cytometry. The percentage of mature preadipocytes and preadipocyte-derived adipocytes was not affected compared to untreated cells in our cell cultures after exposure to LPS for 24 hours (**Figure 9 a**). Administration of different doses of LPS for 24 hours was only altering slightly the cell viability compared to control (p=n.s.) (**Figure 9 b**).

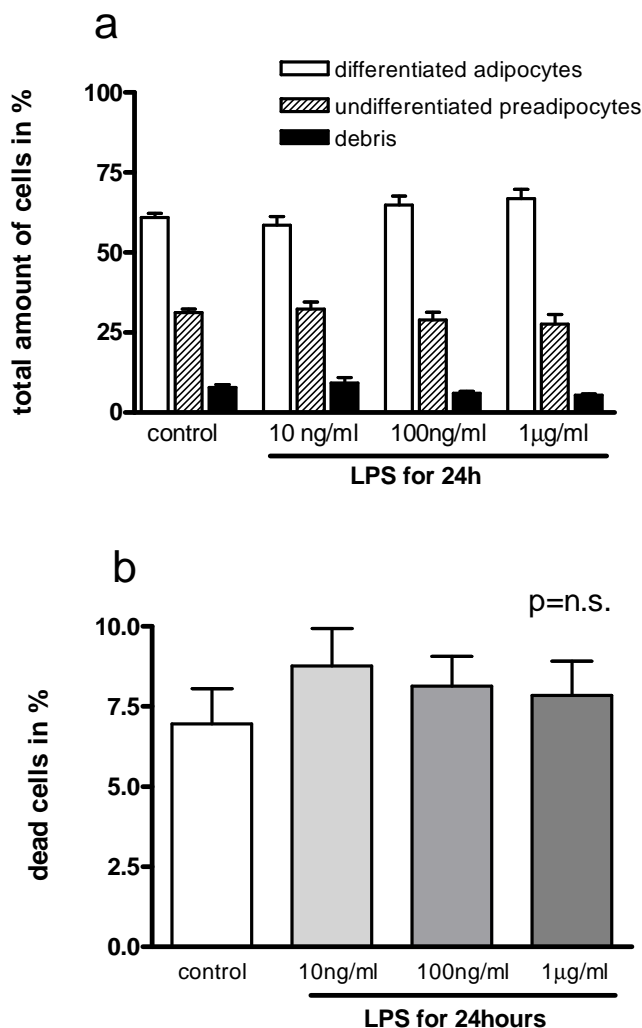


**Figure 9. Percentage of differentiated and dead cells after 24h incubation with different doses of LPS. (a)** Percentage of mature adipocytes (open bars), preadipocytes (shaded bars) and debris (closed bars) untreated (control) and after exposure to 10ng/ml, 100ng/ml and 1µg/ml LPS for 24 hours and staining with bodipy. **(b)** Percentage of dead cells after administration of 10ng/ml, 100ng/ml and 1µg/ml LPS ( $p=n.s.$  vs.control) and staining with PI followed by flow cytometry analysis.

### 5.2.2 Variations in LPS-induced CALC-I gene expression

The preadipocyte-derived adipocytes for our experiments were gained from subcutaneous fat tissue from different donors. To isolate the stromal vascular cell fraction containing preadipocytes, we used fat tissue samples from patients who differed in criteria such as sex, age, BMI, state of health and medication. The preadipocyte-derived adipocytes were differentiated *in vitro* into mature adipocytes and passaged several times for performing experiments. Additionally, stocks of cells

at different passages were kept frozen in liquid nitrogen for several months and then thawed for further passaging and performing experiments. As assessed by real-time PCR, the expression level of CALC-I gene mRNA induced by 100ng/ml LPS varied among the different experiments depending on the cell donor and cell passage used. In adipocytes derived from different donors a considerable variation in the fold of increase in LPS-induced CT or CGRP-I mRNA was measured which was in a range from 35 fold to no increase at all compared to control (**Figure 10**).

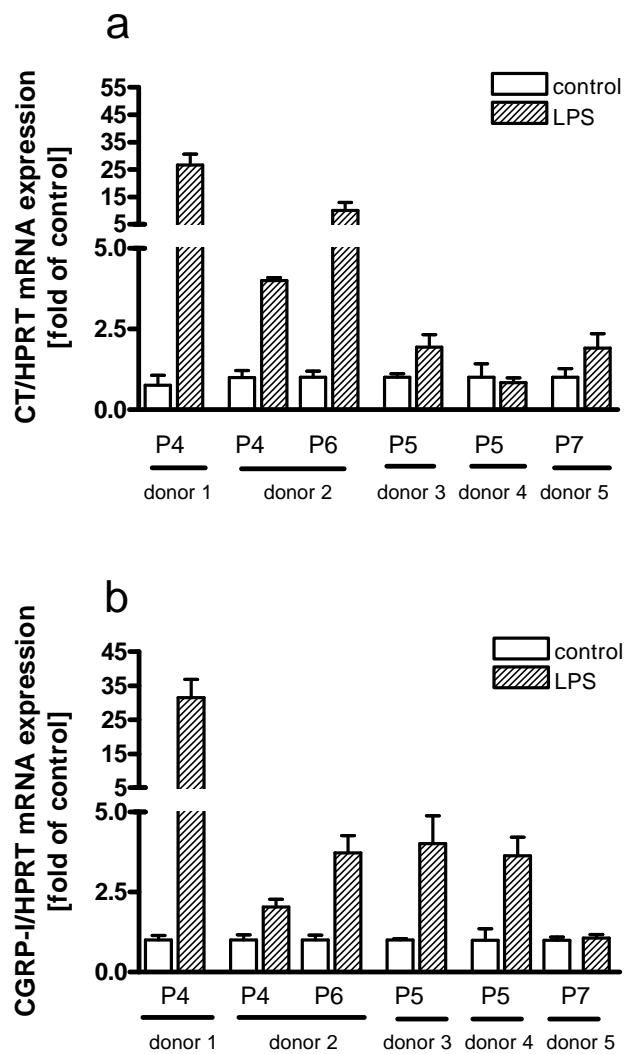


**Figure 10: CT and CGRP-I mRNA expression upon LPS stimulation in human adipocytes derived from different donors.** Preadipocyte-derived adipocytes from different donors and different passages (P) in cell cultures were treated with 100ng/ml LPS for 24 h (shaded bars) and compared to untreated cells (open bars) from the same donor or passage, respectively. mRNA expression of CT (**a**) and CGRP-I (**b**) was analysed by quantitative real-time PCR. Data are means  $\pm$  SEM given as ratio vs. housekeeping gene hypoxanthine phosphoribosyltransferase (HPRT).

### 5.2.3 LPS induces IL-6 and CALC-I gene mRNA expression in human adipocytes

LPS induced a dose-dependent increase in the mRNA expression level of the pro-inflammatory cytokine IL-6 (**Figure 11 a**), indicating that LPS provokes an inflammatory response in our adipocyte model. Administration of LPS was also leading to an increase in the mRNA level of CT and CGRP-I (**Figure 11 b and c**). As opposed to the case with IL-6, the increase in CALC-I gene mRNA was not dose-dependent in the chosen dose-range and peaked at a dose of 100ng/ml.

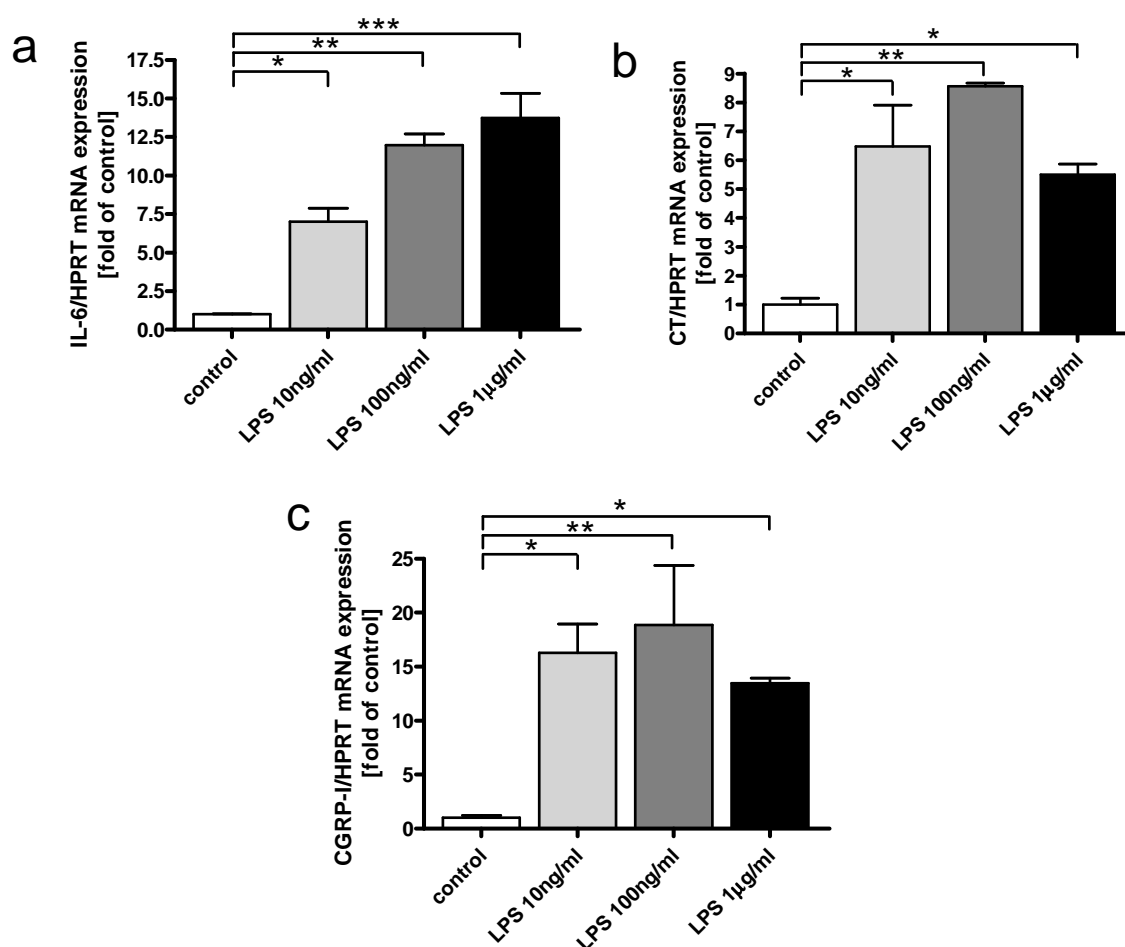


**Figure 11: IL-6, CALC-I and CALC-V gene expression upon LPS stimulation in human adipocytes.** Preadipocyte-derived adipocytes were treated with 10ng/ml, 100ng/ml and 1µg/ml LPS for 24 h. mRNA expression of IL-6, (a), CT (b) and CGRP-I (c) was analysed by quantitative real-time PCR. Data are means  $\pm$  SEM of one representative experiment out of at least three given as ratio vs. HPRT (\*,  $p < 0.05$  vs. control; \*\*,  $p < 0.01$  vs. control; \*\*\*,  $p < 0.001$  vs. control).



### 5.2.4 LPS-induced CALC-I gene expression is independent from NF $\kappa$ B pathway

The main target receptor for LPS is known to be TLR4 and human adipocytes have been shown to express this receptor (57). Since we find an increase in the mRNA expression of CT and CGRP-I conjointly with an increase in IL-6 mRNA, we investigated whether an inhibitor of the NF $\kappa$ B pathway might block the LPS-mediated CALC-I gene activity. As expected, attenuating the activity of NF $\kappa$ B by inhibiting the inhibitor of NF $\kappa$ B kinase subunit beta (IKK2) reduced the LPS-induced IL-6 mRNA expression. In contrast, the LPS-mediated CALC-I gene mRNA expression was increased by this inhibitor (**Figure 12**).

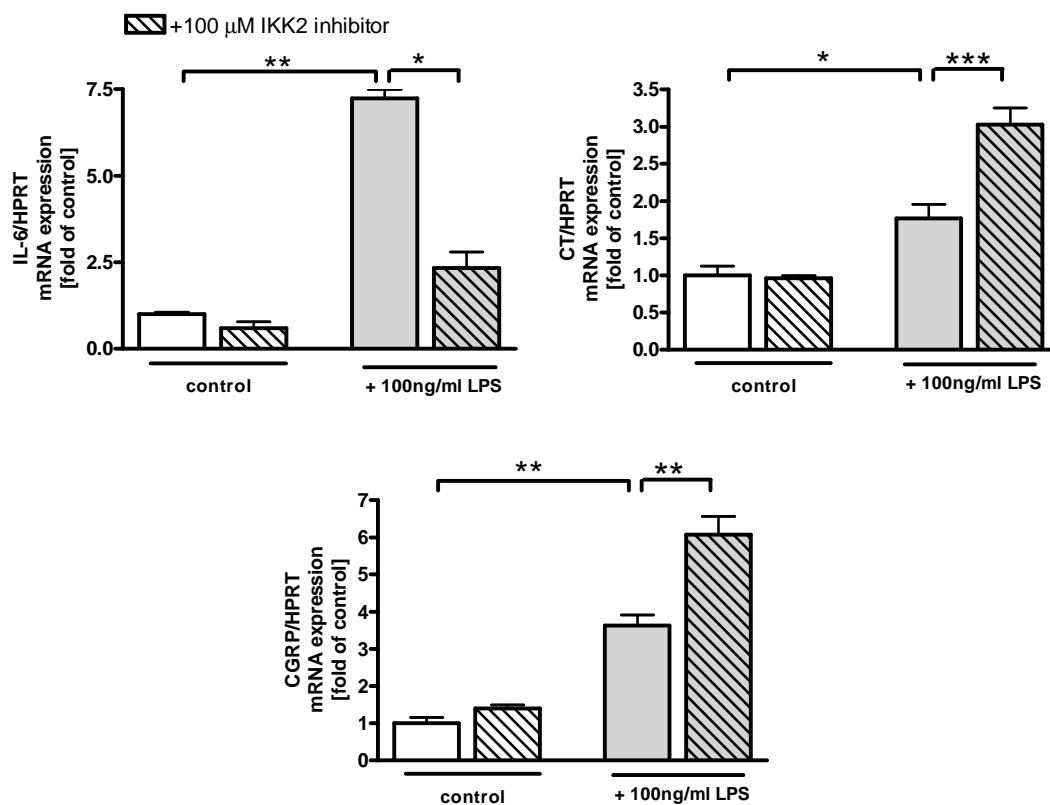


**Figure 12: Effect of IKK2 inhibitor on LPS-induced IL-6, CT and CGRP-I gene expression in human adipocytes.** Preadipocyte-derived adipocytes were untreated (control; white bars) or treated with 100ng/ml LPS for 24 h (grey bars) in the presence (shaded bars) or absence (open bars) of the IKK2 inhibitor SC-514 (100 $\mu$ M, 24 h). mRNA expression of IL-6 (upper panel left graph), CT (upper panel right graph) and CGRP-I (lower panel) was analysed by quantitative real-time PCR.

Whereas the IL-6 mRNA expression was reduced dose-dependently by the IKK2 inhibitor, CT and CGRP-I mRNA expression showed no dose-dependent increase (data not shown). Similarly, co-treatment of LPS-stimulated cells with pyrrodine dithiocarbamate (PDTC), a different inhibitor of NF $\kappa$ B, was leading to a decrease in IL-6 and to an increase in CALC-I mRNA expression (data not shown).

### 5.2.5 IL-1 $\beta$ and CALC-I gene expression

IL-1 $\beta$  is one of the prototypic early cytokines induced by LPS as inflammatory response to the bacterial infection. Exposure of preadipocyte-derived adipocytes to 100ng/ml of LPS for 24 hours induced an increase in IL-1 $\beta$  mRNA expression (**Figure 13**).

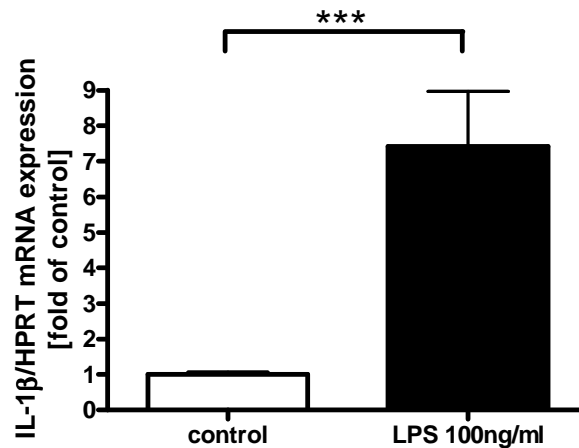


**Figure 13: IL-1 $\beta$  expression upon LPS stimulation in human adipocytes.** Preadipocyte-derived adipocytes were treated with 100ng/ml LPS for 24 h. mRNA expression of IL-1 $\beta$  was analysed by quantitative real-time PCR. (\*\*\*,  $p < 0.001$  vs. control).

When preadipocyte derived adipocytes were treated with different doses of IL-1 $\beta$  (20IU, 2IU and 0.2IU), only the highest dose of 20IU was sufficient to increase the expression level of CT (**Figure 14 a**) and CGRP-I gene mRNA (**Figure 14 b**).

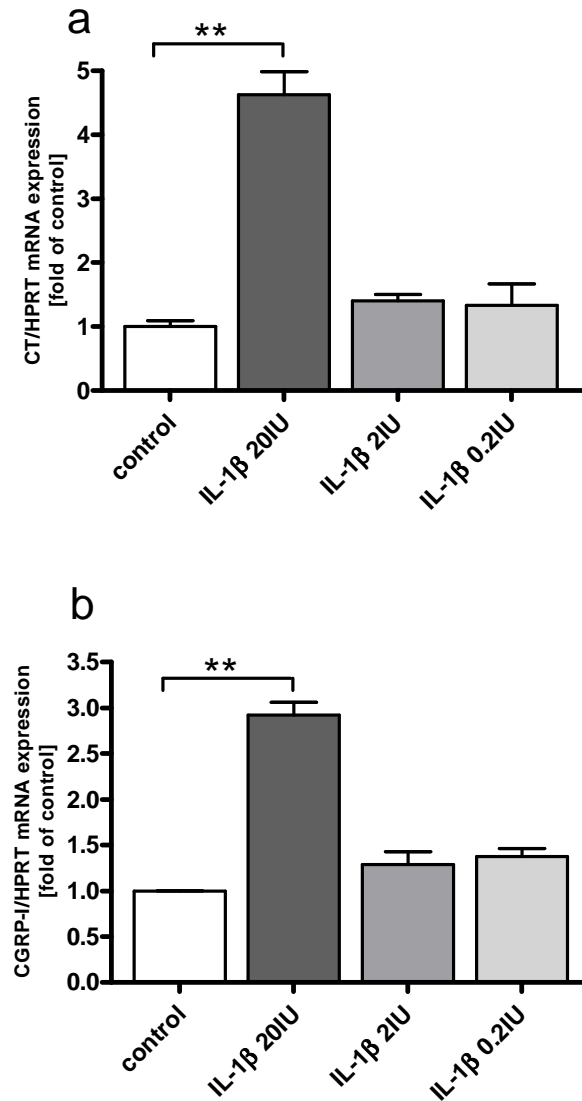


**Figure 14: CT and CGRP-I gene expression upon IL-1 $\beta$  stimulation in human adipocytes.** Preadipocyte-derived adipocytes were treated with 20IU, 2IU and 0.2IU IL-1 $\beta$  for 24 h. mRNA expression of CT (a) and CGRP-I (b) was analysed by quantitative real-time PCR (\*\*,  $p < 0.01$  vs. control).

### 5.2.6 Effect of IL-1RA on LPS-induced CALC-I gene expression

Next we aimed to clarify whether the effect of LPS on the increase in CALC-I gene expression is IL-1 $\beta$ -mediated as part of the inflammatory response. Therefore, adipocytes were treated with IL-1 $\beta$  and LPS in the presence or absence of the IL-1

receptor antagonist IL-1RA. IL-1RA is an agent that binds to the same receptor on the cell surface as IL-1, and thus prevents IL-1 binding and signaling.

Addition of IL-1RA blocked the IL-1 $\beta$ -induced CALC-I gene expression but this inhibitor did not prevent the increase in mRNA expression induced by LPS (**Figure 15**).

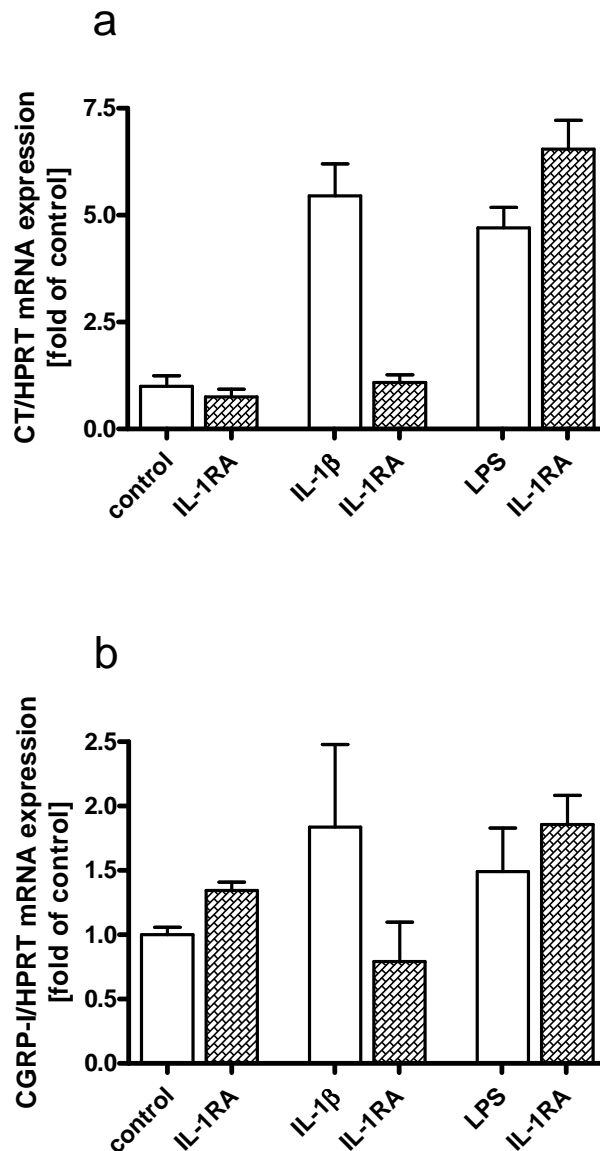


**Figure 15: Effect of IL-1RA on IL-1 $\beta$ - and LPS-induced CALC-I gene expression in human adipocytes.** Preadipocyte-derived adipocytes were treated with 20IU IL-1 $\beta$  and 100ng/ml LPS for 24 h in the presence (shaded bars) or absence (open bars) of IL-1RA (20ng/ml, 24 h) and mRNA expression of CT (**a**) and CGRP-I (**b**) was analysed by quantitative real-time PCR. Data are means  $\pm$  SEM of three independent experiments as ratio vs. HPRT.

## 5.3 Effects of ionomycin and LPS on intracellular calcium concentration in human preadipocyte-derived adipocytes

### 5.3.1 Effect of ionomycin on cell viability

Since  $\text{Ca}^{2+}$  has been shown to regulate the expression of the CALC gene in cells of thyroidal origin such as TT cells (83) it is tempting to speculate that the extrathyroidal CALC-I gene expression in human adipocytes is  $\text{Ca}^{2+}$  dependent. Methodologically, we used  $1\mu\text{M}$  ionomycin as positive control in order to establish the method of measuring  $[\text{Ca}^{2+}]_i$  changes in our adipocyte cell model. Ionomycin is an ionophore produced by the bacterium *Streptomyces globulatus* and is used to raise the intracellular level of calcium by facilitating the transport of  $\text{Ca}^{2+}$  ions through biological membranes. Potential cytotoxicity of ionomycin in adipocytes was examined. Cells were treated with  $1\mu\text{M}$  ionomycin for 3 or 24 hours in the presence or absence of LPS (100ng/ml for 24 hours) and with  $10\mu\text{M}$  ionomycin for 24 hours alone or in combination with LPS. After incubation, the cells were stained with bodipy 493/503 and PI and analyzed by flow cytometry.

Neither  $1\mu\text{M}$  ionomycin alone for 3 or 24 hours nor in combination with LPS was leading to an increased percentage of dead cells. Only in the cell population incubated with  $10\mu\text{M}$  ionomycin the amount of dead cells tended to increase (p=n.s.) (**Figure 16 a**). After bodipy staining we found that the cytotoxic effect of  $10\mu\text{M}$  ionomycin after 24 hours seems to be restricted to mature adipocytes. The percentage of undifferentiated adipocytes remained unaffected compared to the decreased percentage of differentiated cells and the increase in cell debris (**Figure 16 b**).

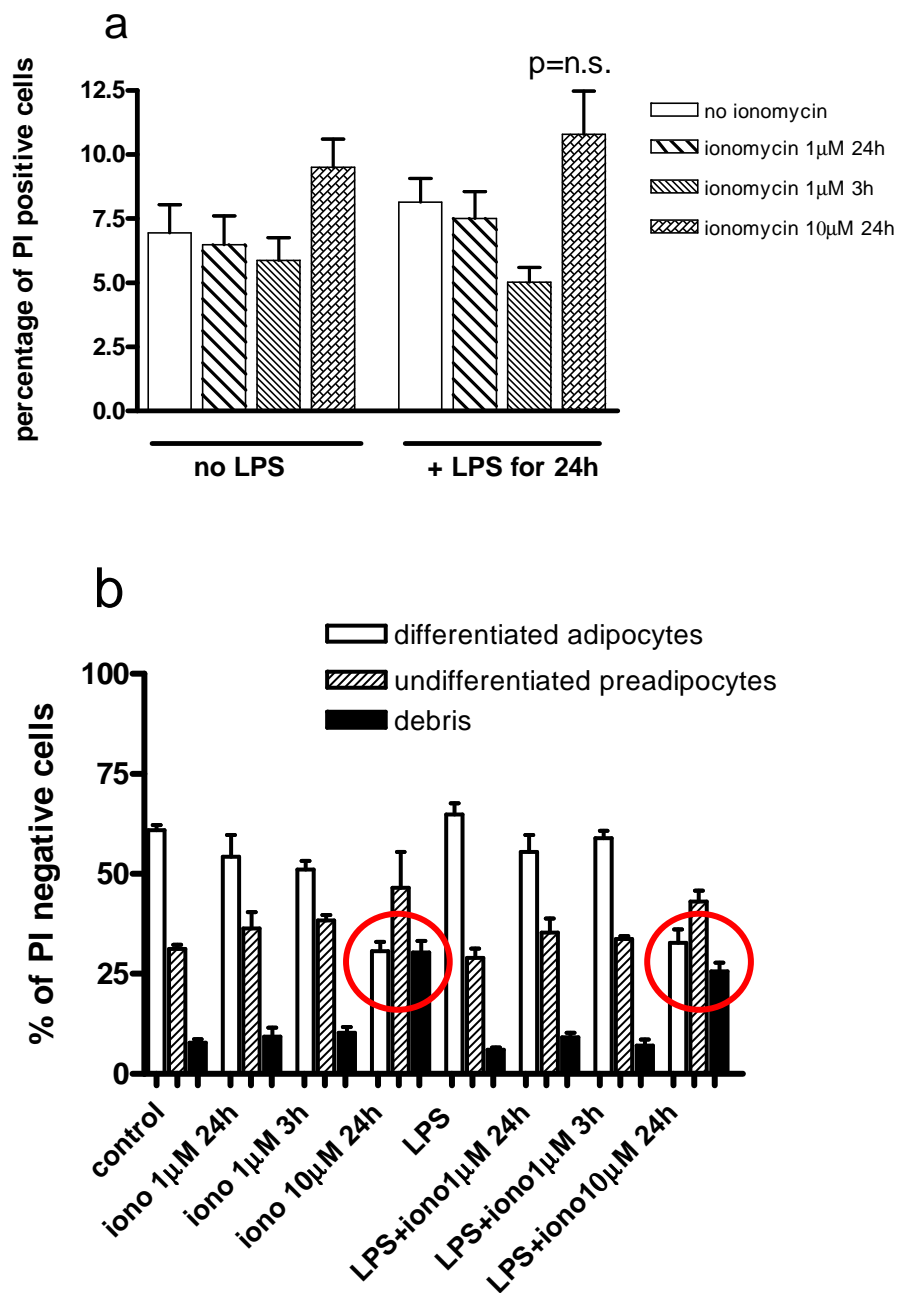


**Figure 16: Percentage of cells in our cultures after incubation with ionomycin alone or in combination with LPS.** (a) Administration of 1μM (for 3 or 24 hours) or 10μM ionomycin (iono) for 24 h in absence (no LPS) or presence of 100ng/ml LPS for 24 h (+LPS for 24h) led to a slight increase of dead cells ( $p=n.s.$ ), the most dead cells were detected when cells were incubated with 10μM ionomycin (b) Percentage of PI negative cells were classified into undifferentiated preadipocytes, mature adipocytes and cell debris. Red circles show the notable difference in percentage of cells after treatments. Results represent the mean  $\pm$  SEM from 3 independent experiments.

### 5.3.2 Effect of ionomycin on intracellular calcium concentration changes

Cells were loaded with Fluo-3 AM, which is a high affinity  $\text{Ca}^{2+}$  indicator, and changes in  $[\text{Ca}^{2+}]_i$  upon ionomycin were visualized by confocal microscopy. When  $\text{Ca}^{2+}$  is binding to Fluo-3, the fluorescence of the dye is increasing when excited at 488 nm. Exposure of adipocytes to  $1\mu\text{M}$  ionomycin led to a quick and transient increase in  $[\text{Ca}^{2+}]_i$  in the majority of preadipocyte-derived adipocytes (**Figure 17**). However, some adipocytes showed no increase in  $[\text{Ca}^{2+}]_i$  in response to the ionophor (i.e. yellow curve). The duration of elevated intracellular calcium varied among every cell. The increase in  $[\text{Ca}^{2+}]_i$  lasted from approximately 5 minutes (i.e. dark blue curve) until up to 15 minutes (i.e. pink curve).

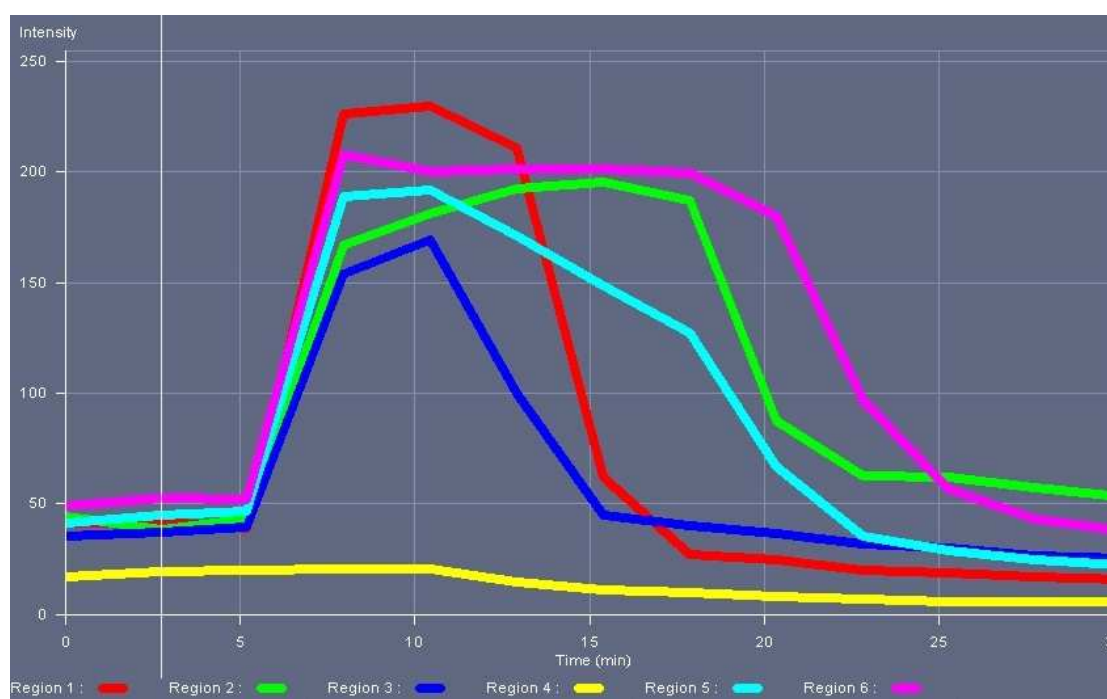


**Figure 17:**  $[\text{Ca}^{2+}]_i$  rises induced by ionomycin in preadipocyte-derived adipocytes loaded with Fluo-3. Fluo-3 loaded adipocytes were monitored for changes in  $[\text{Ca}^{2+}]_i$  by confocal microscopy for about 30 minutes after addition of  $1\mu\text{M}$  ionomycin. Each curve (red, pink, light blue, green, dark blue and yellow) represents the fluorescence intensity of  $\text{Ca}^{2+}$ -bound Fluo-3 from an individual cell.

Same as Fluo-3, Fura-2 is a fluorescent  $\text{Ca}^{2+}$  indicator but with a different excitation wavelength, namely 340 nm when bound to  $\text{Ca}^{2+}$  365 nm when not bound to  $\text{Ca}^{2+}$ .

With our available technical setup we used the excitation wavelength of 405 nm, which enabled us to follow changes in the fluorescence of  $\text{Ca}^{2+}$ -unbound dye, resulting in indirect measurement of increased  $[\text{Ca}^{2+}]_i$ . In cells loaded with Fura-2 we monitored a decrease in signal intensity in adipocytes upon administration of ionomycin. The rather stable signal in fluorescent intensity in cells without the characteristic adipocytes phenotype indicates that an ionomycin-induced increase in  $[\text{Ca}^{2+}]_i$  seems to occur more pronounced in mature adipocytes than in undifferentiated preadipocytes (**Figure 18**).

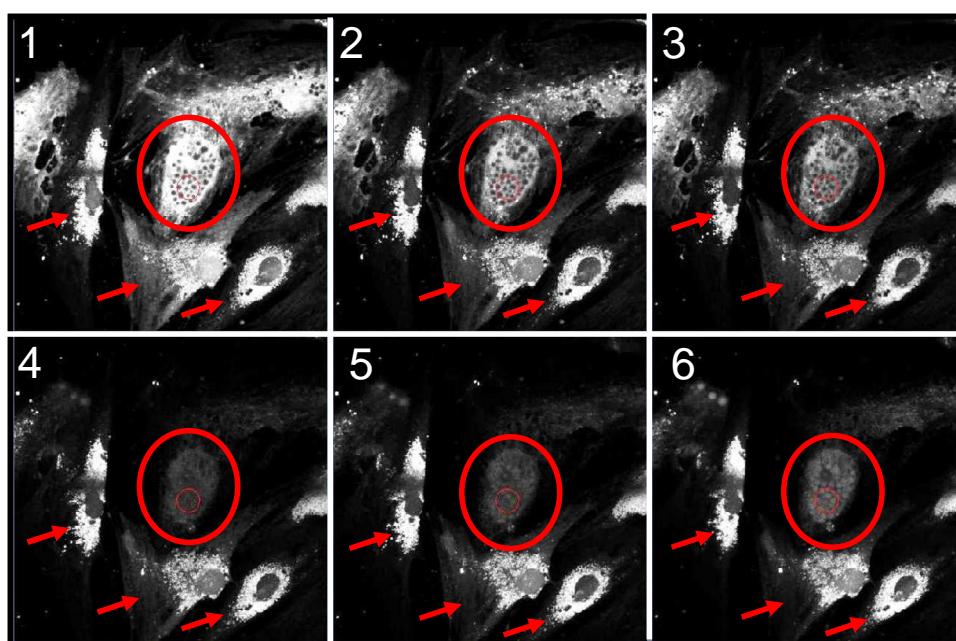


**Figure 18: Changes in signal intensity of  $\text{Ca}^{2+}$ -unbound Fura-2.** Time course showing signal intensity of  $\text{Ca}^{2+}$ -unbound dye in the cytoplasm of a mature adipocyte (marked with a circle) after administration of  $1\mu\text{M}$  ionomycin pictured with 6 images. Every 3 minutes after administration of ionomycin a picture was taken (images 1-6). Within the same time period of ionomycin exposure, the signal of  $\text{Ca}^{2+}$ -unbound dye remains much stronger in cells showing a non-adipose phenotype (marked with arrows).

### 5.3.3 Effect of LPS on intracellular calcium concentration

Preadipocyte-derived adipocytes have been examined for basal  $[\text{Ca}^{2+}]_i$  and variations upon LPS exposure. Cells were loaded with Fluo-3 AM and excited at 488 nm to



follow the fluorescent signal of  $\text{Ca}^{2+}$ -bound Fluo-3. The signal of  $\text{Ca}^{2+}$ -bound Fluo-3 increased slowly during the exposure time compared to the signal from untreated cells, which even declined (**Figure 19 a**). One disadvantage of staining the cells with fluorescent dyes for live imaging is that the fluorescence fades during the exposure time, irrespective of the treatment.

To validate the results obtained with Fluo-3, we performed experiments with BTC AM, an additional fluorescent  $\text{Ca}^{2+}$  indicator. Cells were loaded with BTC in the absence or presence of LPS and changes in fluorescence intensity were measured during 130 minutes after LPS administration. Excitation at 405 nm shows the fluorescence of BTC bound to  $\text{Ca}^{2+}$  and excitation at 488 shows the fluorescence of  $\text{Ca}^{2+}$ -unbound dye.

Some of the cells responded with an increase in  $[\text{Ca}^{2+}]_i$ , whereas for others, no response was evident or they only displayed small spontaneous and transient changes of  $[\text{Ca}^{2+}]_i$ . But the majority of the cells responding to LPS exhibited a slow and sustained increase in  $[\text{Ca}^{2+}]_i$ . In control cells, the fluorescence intensity of both,  $\text{Ca}^{2+}$ -unbound and  $\text{Ca}^{2+}$ -bound BTC declined slightly. In cells treated with LPS the decline in the signal intensity of  $\text{Ca}^{2+}$ -unbound BTC was significantly more pronounced than in untreated cells whereas the intensity of the  $\text{Ca}^{2+}$ -bound BTC declined less compared to control or even increased. These findings were considered as indirect evidence for increasing  $[\text{Ca}^{2+}]_i$ . Represented by the ratio of  $\text{Ca}^{2+}$ -bound BTC /  $\text{Ca}^{2+}$ -unbound BTC (405nm/488nm), an LPS-induced increase in  $[\text{Ca}^{2+}]_i$  could be observed after 90 min ( $p < 0.05$  vs. control) and this increase was enhanced thereafter ( $p < 0.001$  vs. control) (**Figure 19 b**).

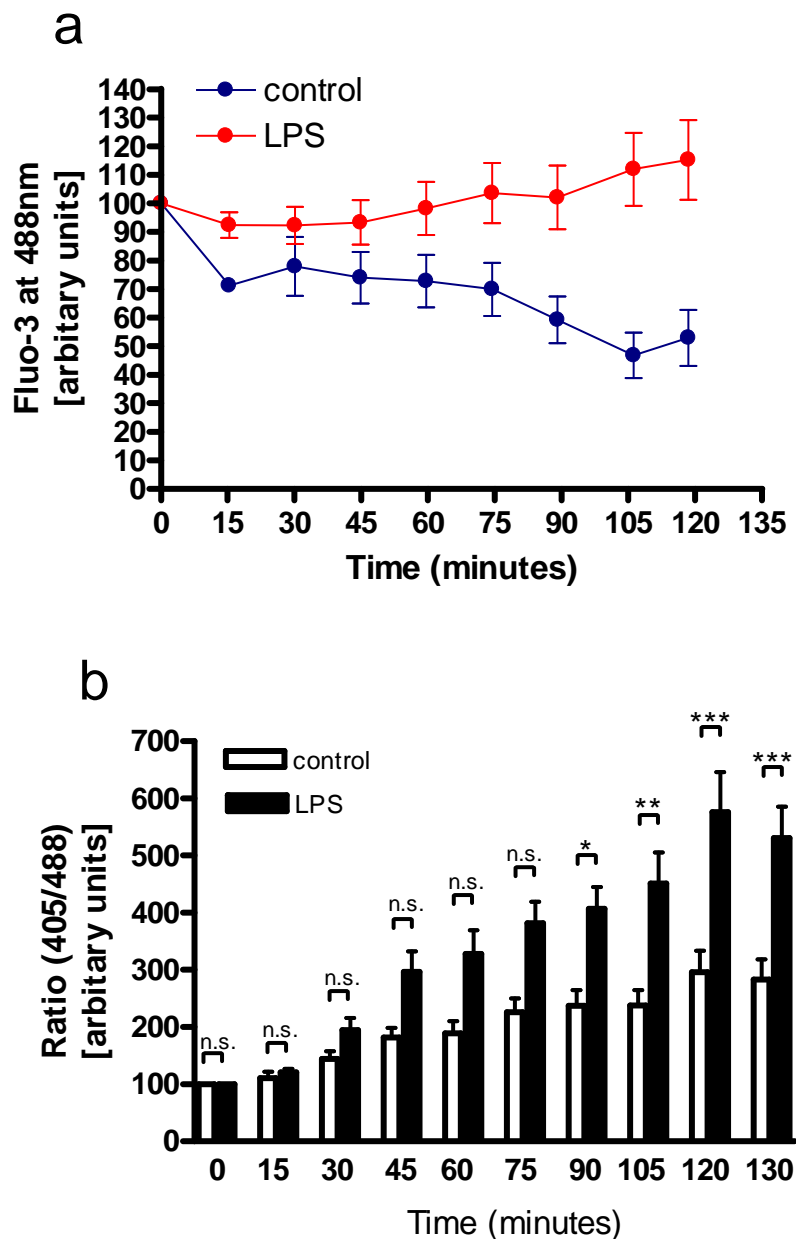


**Figure 19:  $[Ca^{2+}]_i$  increase induced by LPS in preadipocyte-derived adipocytes.**

(a) Representative tracing of  $[Ca^{2+}]_i$  with Fluo-3 AM in cells that responded to LPS with a slow sustained increase. Data are means  $\pm$  SEM from 5 single cells for control and 5 single cells treated with LPS. (b) Increase in intracellular calcium concentration in preadipocyte-derived adipocytes loaded with BTC AM given as ratio of 405/488 fluorescence from treated vs. untreated cells at certain time points after LPS addition. Data are expressed by means  $\pm$  SEM (n=22 single cells from three independent experiments; \*,  $p < 0.05$  vs. control; \*\*,  $p < 0.01$  vs. control; \*\*\*,  $p < 0.001$  vs. control; p = n.s., non significant vs. control).

Next, in order to clarify whether cells which did not respond with an increase in  $[Ca^{2+}]_i$  upon LPS treatment within 1 hour were not able to raise their  $[Ca^{2+}]_i$ ,  $1\mu M$  of ionomycin was added. Cells previously exposed to LPS responded with a single rapid and transient increase in  $[Ca^{2+}]_i$ , whereas the ionomycin-induced transient in cells not exposed to LPS was much smaller in amplitude and with a slower onset (**Figure 20**).

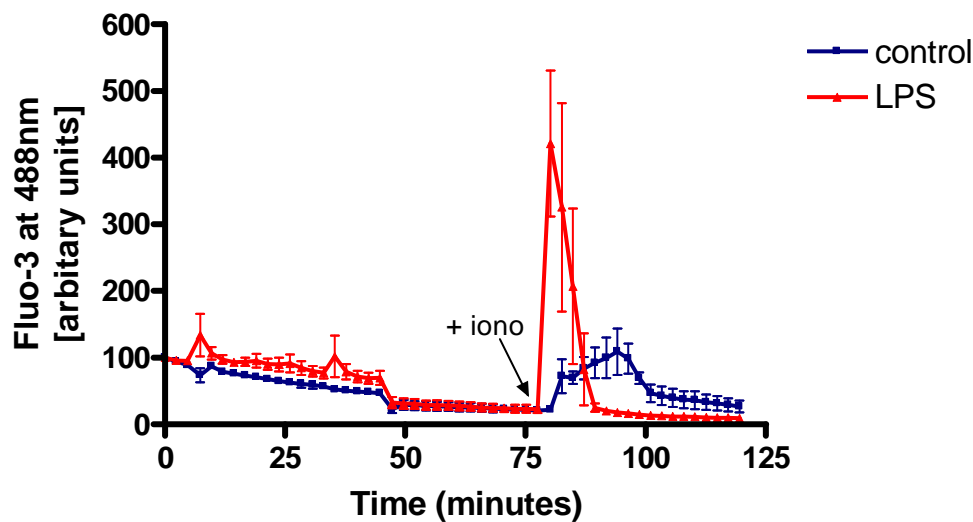


**Figure 20:**  $[Ca^{2+}]_i$  increase induced by ionomycin in preadipocyte-derived adipocytes exposed to LPS. Fluo-3 loaded adipocytes were monitored for  $[Ca^{2+}]_i$  as described in Materials and Methods. 7 minutes after measurement start,  $100ng/ml$  LPS were added to one chamber of the 2-well chamberslide. After 77 minutes,  $1\mu M$  ionomycin was added to both chambers. Data are means  $\pm$  SEM from 5 single cells for control and 5 single cells treated with LPS.

## **5.4 Role of calcium in lipopolysaccharide-induced CALC gene expression in human adipocytes**

### **5.4.1 Effect on LPS-induced CALC-I gene mRNA expression by inhibiting LPS-induced intracellular calcium increase**

To investigate whether augmented  $[Ca^{2+}]_i$  might be responsible for the LPS-induced increase in CT and CGRP-I mRNA, the cells were treated with different substances blocking an increase in  $[Ca^{2+}]_i$ . The increase in CT and CGRP-I mRNA expression after LPS administration ( $p < 0.001$  vs. control) (100 ng/ml for 24 hours) was lowered by simultaneous treatment with 20  $\mu$ M of verapamil, a  $Ca^{2+}$  ion flux inhibitor, preventing  $Ca^{2+}$  influx from the extracellular space ( $p < 0.05$  for CT and  $p < 0.01$  for CGRP-I vs. LPS). Addition of verapamil to cells treated with LPS also led to a reduced mRNA expression level of IL-6, but in a much lower extent than for CT and CGRP-I ( $p = n.s.$  vs. LPS) (**Fig. 21 a**).

When cells were co-treated with 20  $\mu$ M of 2-APB, an inositol triphosphate ( $IP_3$ ) receptor antagonist which inhibits store operated calcium release, the LPS induced CALC-I mRNA expression level was blocked almost down to control level ( $p < 0.001$  vs. LPS). Same as for verapamil, addition of 2-APB in cells exposed to LPS only led to a slight reduction of IL-6 mRNA expression in a much lower extent than for CT and CGRP-I ( $p = n.s.$  vs. LPS) (**Fig. 21 b**).

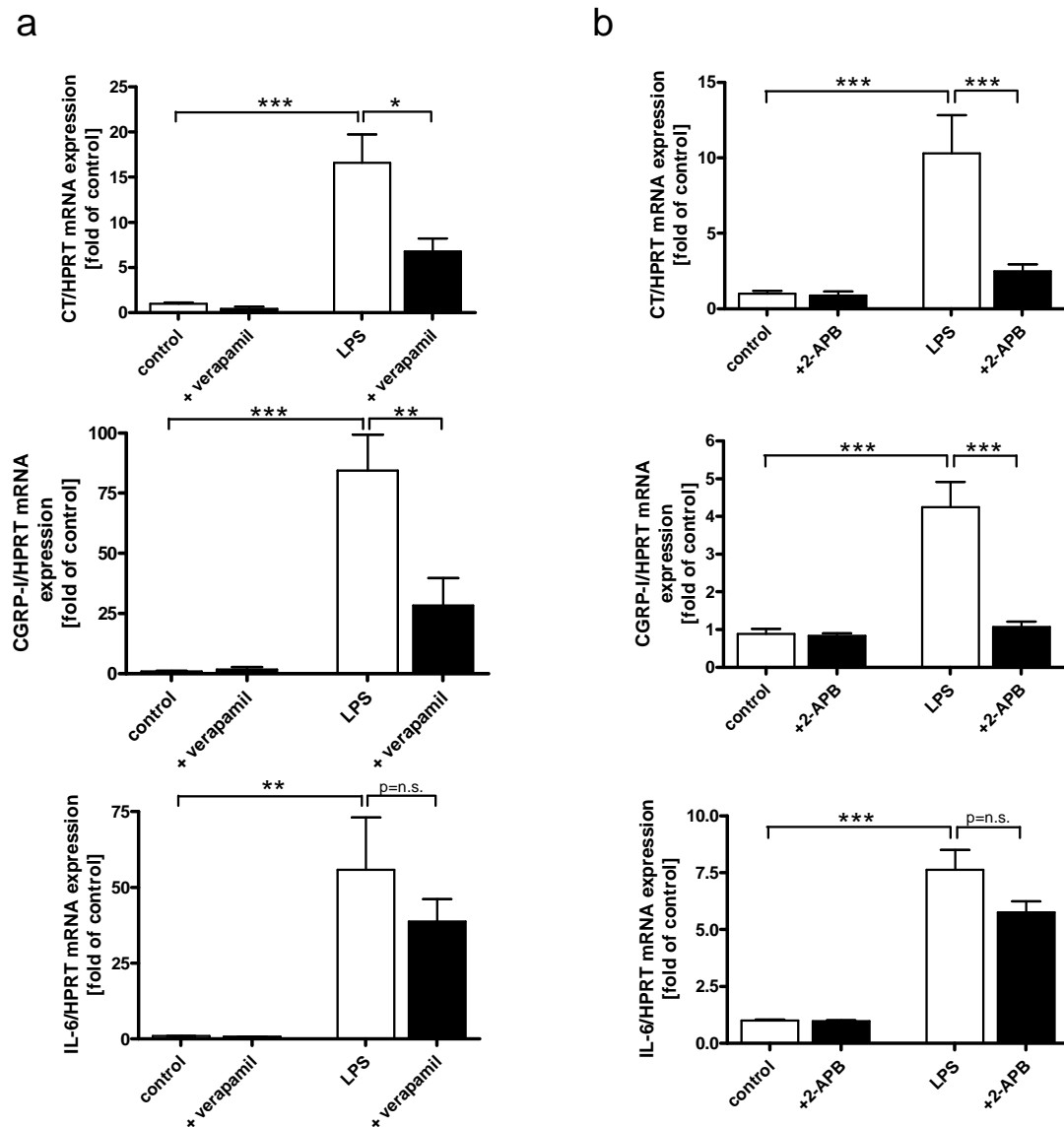


**Figure 21: Impact of reduced intracellular calcium concentration on LPS- induced CALC-I gene and IL-6 mRNA expression in human adipocytes.** (a) Preadipocyte-derived adipocytes were treated with 100ng/ml LPS for 24 h without (open bars) or with (closed bars) addition of 20 $\mu$ M of verapamil. mRNA expression for CT (upper panel), CGRP-I (middle panel) and IL-6 (lower panel) was analysed by quantitative real-time PCR. (b) Cells were treated with 100ng/ml LPS for 24 h without (open bars) or with (closed bars) addition of 20 $\mu$ M of 2-APB. mRNA expression of CT (upper panel), CGRP-I (middle panel) and IL-6 (lower panel) was analysed by quantitative real-time PCR. Data are means  $\pm$  SEM of three independent experiments given as ratio vs. HPRT (\*,  $p < 0.05$  vs. control; \*\*,  $p < 0.01$  vs. control;\*\*\*,  $p < 0.001$  vs. control;  $p = n.s.$ , non significant vs. control).

---

#### 5.4.2 Effects of intracellular calcium increase on LPS-induced CALC-I gene and IL-6 expression

We examined the effect of increased  $[Ca^{2+}]_i$  on LPS-induced CALC-I gene induction. Therefore cells were treated with 1 $\mu$ M ionomycin for different time spans from 3 to 24 hours. The duration of incubation with ionomycin did not influence its effects (data not shown). The CT and CGRP-I mRNA expression level upon ionomycin treatment was comparable with the increase after LPS treatment alone. IL-6 mRNA expression also increased with ionomycin administration. Addition of ionomycin in an inflammatory background, namely in cells co-treated with LPS for 24 hours, potentiated the increase in CT and CGRP-I mRNA expression ( $p < 0.001$  for CT and  $p < 0.01$  for CGRP-I vs. control, LPS and ionomycin alone). When LPS and ionomycin were combined, the IL-6 mRNA expression level also went up, but more in an additive manner and to a much lower extent than that of the mRNA of CT and CGRP-I ( $p < 0.001$  vs. control and  $p < 0.01$  vs. LPS alone) (**Fig. 22 a**). The increment of  $Ca^{2+}$  and LPS-induced CT, CGRP-I and IL-6 mRNA expression was reproduced when the cells were preincubated with thapsigargin (100nM, for 1 h). Thapsigargin acts as an endoplasmatic reticulum  $Ca^{2+}$  ATPase inhibitor, leading to  $[Ca^{2+}]_i$  elevation from an intracellular store source ( $p < 0.001$  vs. control, LPS and thapsigargin alone) (**Fig. 22 b**).

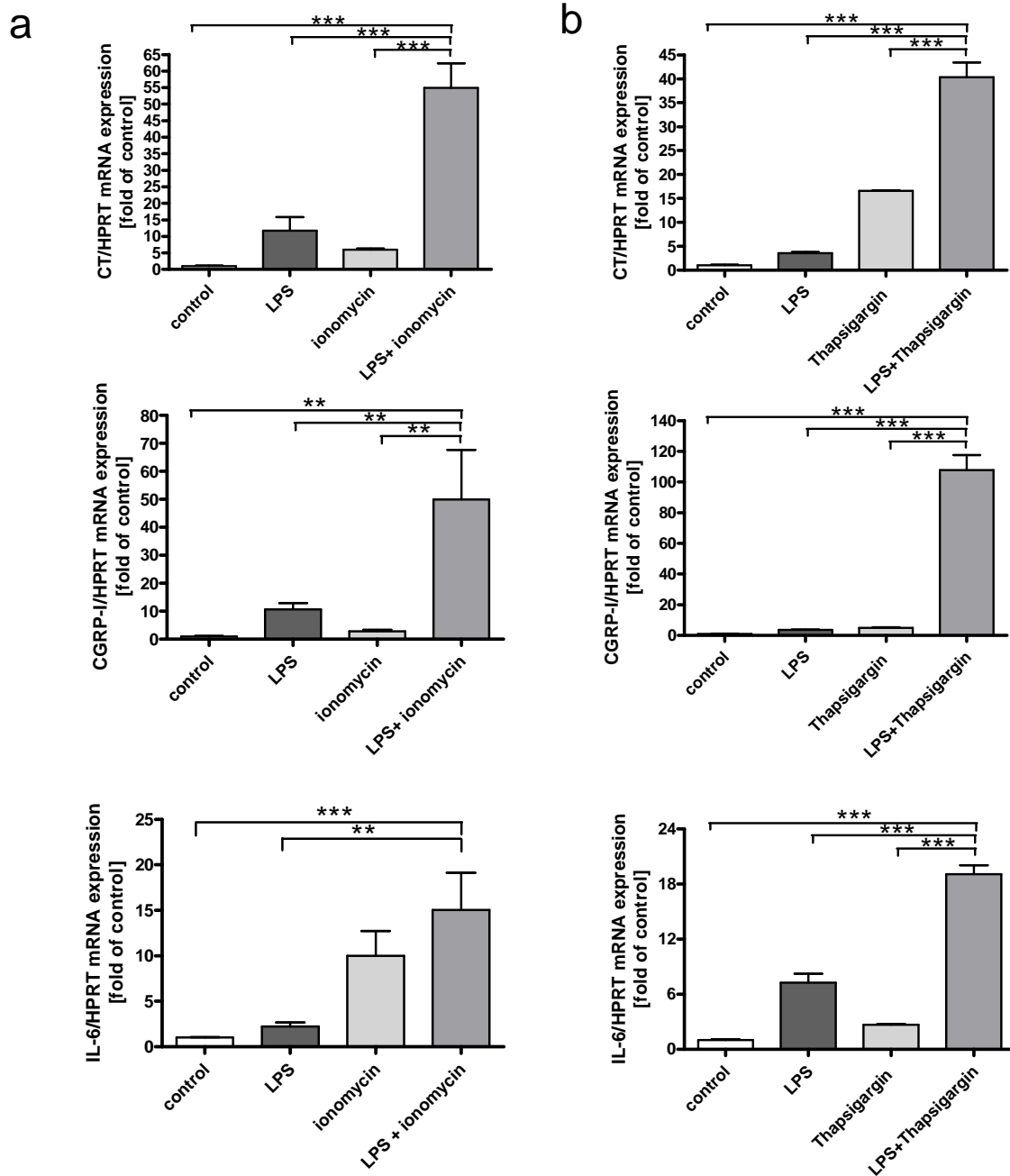


**Figure 22: Impact of increased intracellular calcium concentration on LPS- induced CALC-I gene and IL-6 mRNA expression in human adipocytes.** (a) Preadipocyte-derived adipocytes were treated with 100ng/ml LPS for 24 h, with 1 $\mu$ M of ionomycin for 3h or 24h or with LPS and ionomycin in combination. mRNA expression for CT (upper panel), CGRP-I (middle panel) and IL-6 (lower panel) was analysed by quantitative real-time PCR. (b) Adipocytes were treated with 100ng/ml LPS for 24 h, with 100nM of thapsigargin for 24h or with LPS and thapsigargin in combination after 1 h of pretreatment with thapsigargin. mRNA expression for CT (upper panel), CGRP-I (middle panel) and IL-6 (lower panel) was analysed by quantitative real-time PCR. Data are means  $\pm$  SEM of three independent experiments given as ratio vs. HPRT (\*\*,  $p < 0.01$  vs. control; \*\*\*,  $p < 0.001$  vs. control).

### 5.4.3 Effects of altering calcium concentration on CT peptide and IL-6 secretion

When  $[Ca^{2+}]_i$  was increased by ionomycin in conjunction with LPS, we measured the secretion of ProCT ( $p < 0.001$  vs. control), CGRP-I ( $p < 0.01$  vs. control) and IL-6 ( $p < 0.001$  vs. control) protein into the supernatant. Similar to the mRNA expression level, the amount of protein was reduced when  $Ca^{2+}$  influx from the extracellular space was prevented by addition of verapamil ( $p < 0.01$  for ProCT and  $p < 0.05$  for CGRP-I). In contrast, the LPS/ionomycin-induced IL-6 protein secretion was only slightly reduced in the presence of verapamil ( $p = n.s.$ ) (**Fig. 23**).

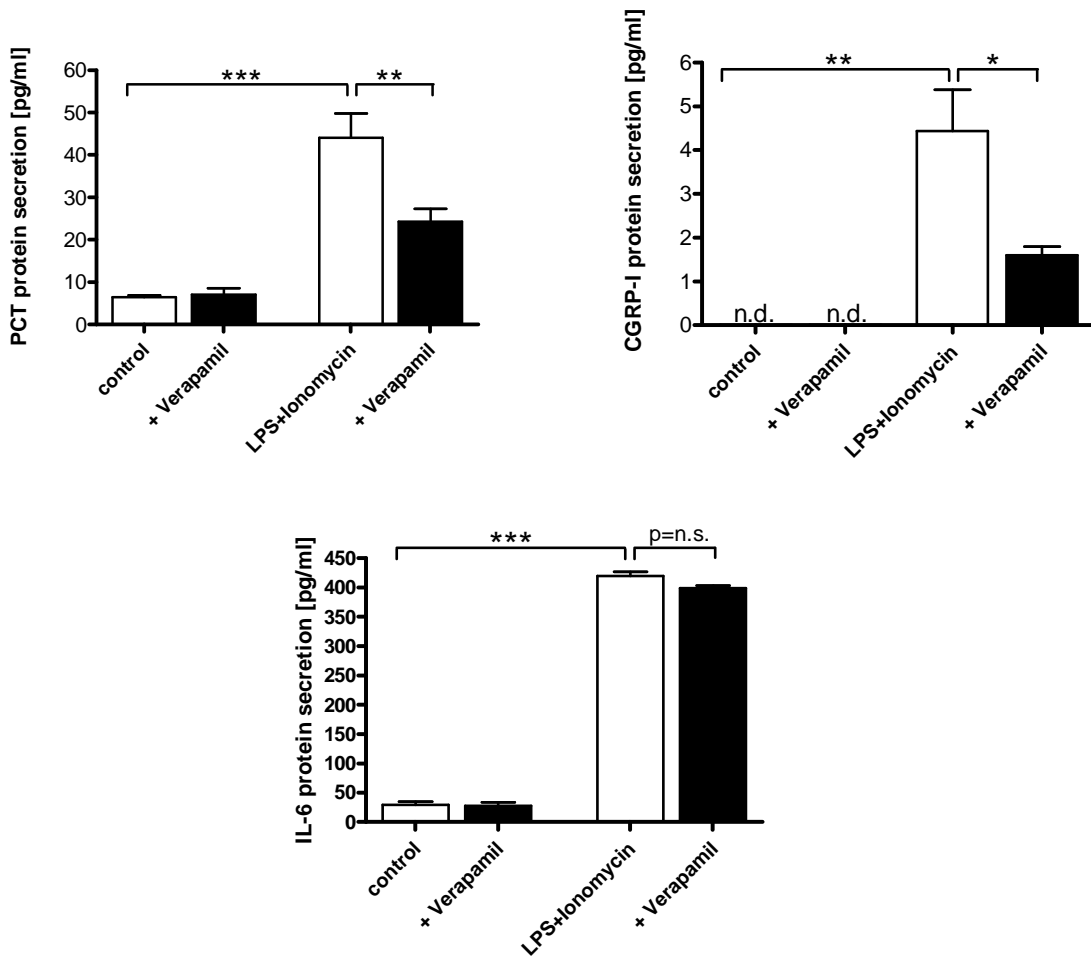


**Figure 23: Protein secretion of ProCT, CGRP and IL-6 after altering intracellular calcium concentrations.** After treatments for 24 hours with LPS and ionomycin without (open bar) or with (closed bar) the addition of verapamil, release of corresponding peptides into the supernatant was determined by supersensitive chemiluminometric assay (ProCT) (upper panel left), RIA (CGRP) (upper panel right) or ELISA (IL-6) (lower panel) (\*,  $p < 0.05$ ; \*\*,  $p < 0.01$ ; \*\*\*,  $p < 0.001$ ;  $p = n.s.$ , non significant).



#### 5.4.4 Effects of intracellular calcium concentration changes on LPS-induced CALC-V gene expression

Administration of 100 ng/ml LPS to the adipocytes for 24 hours tended to reduce CALC-V gene expression as assessed by ADM mRNA expression ( $p=n.s.$ ). 1 $\mu$ M ionomycin for 3 to 24 hours decreased ADM mRNA expression in both untreated and LPS treated cells ( $p<0.001$  vs. control). The decrease of ADM mRNA expression with elevated  $[Ca^{2+}]_i$  was reproduced when the cells were treated with 100nM of thapsigargin alone or in combination with LPS ( $p<0.001$  vs. control) (**Fig. 24 a**).

Addition of verapamil had no effect on mRNA expression of ADM on cells treated with LPS, ionomycin or their combination ( $p=n.s.$ ) (**Fig. 24 b**) and preventing the efflux from intracellular stores by addition of 2-APB did not affect mRNA expression of ADM ( $p=n.s.$ ) (**Fig. 24 c**). ADM protein secretion into the supernatant was not altered by treatment with LPS or verapamil and neither by their combination, whereby ionomycin alone or in combination with LPS lead to a profound decrease in ADM secretion ( $p<0.01$  and  $p<0.05$  vs. control) (**Fig.24 d**).

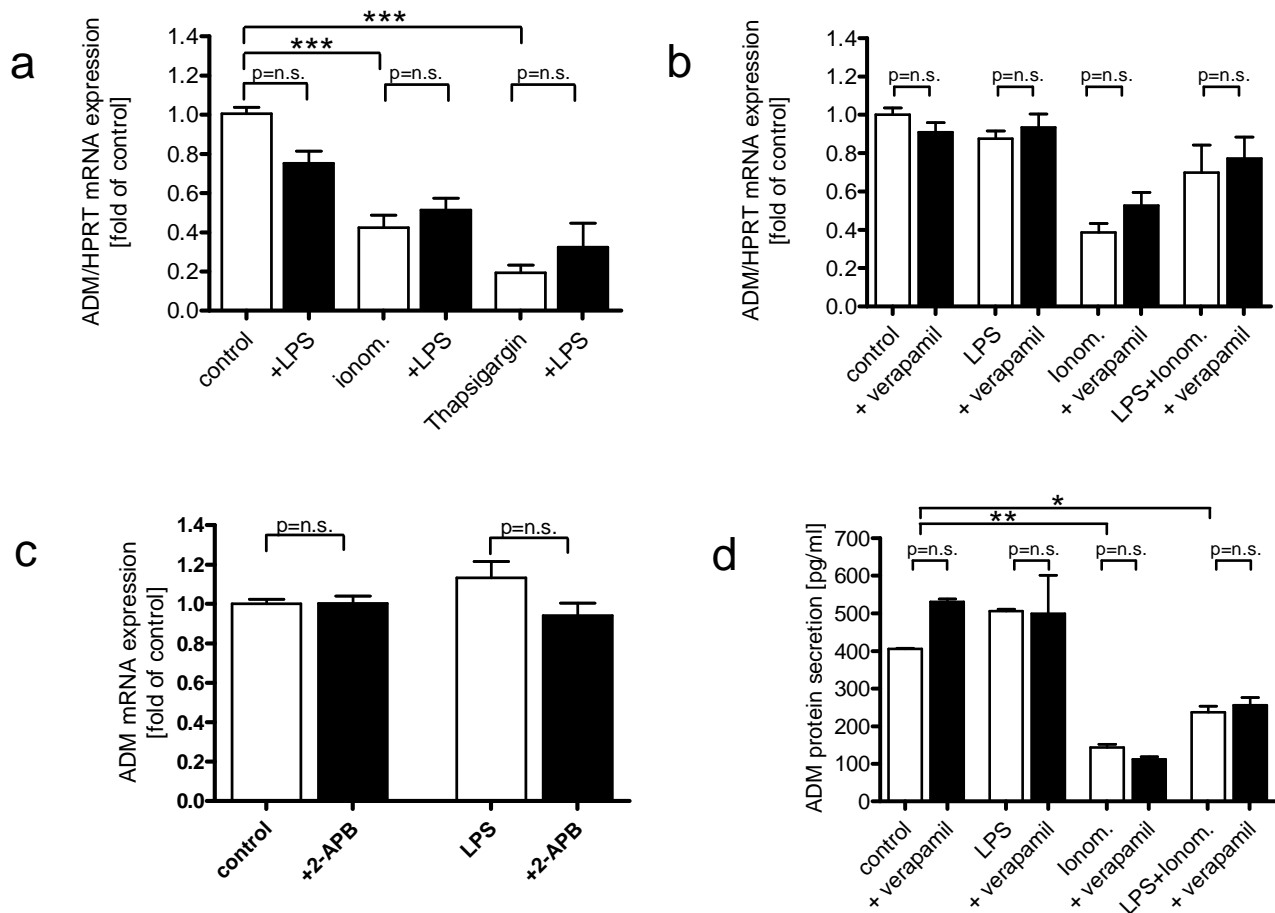


**Figure 24: Alterations in intracellular calcium concentration on LPS- induced CALC-V gene mRNA expression in human adipocytes.** (a) Preadipocyte-derived adipocytes were treated with 100ng/ml of LPS for 24 h, with 1 $\mu$ M of ionomycin for 3 h or 24 h or with 100nM thapsigargin for 24 h. mRNA expression for the CALC-V gene adrenomedullin (ADM) was analysed by quantitative real-time PCR. (b) Preadipocyte-derived adipocytes were treated with 100ng/ml of LPS, 1 $\mu$ M of ionomycin or their combination for 24 h without (open bars) or with (closed bars) addition of 20 $\mu$ M of verapamil. mRNA expression for ADM was analysed by quantitative real-time PCR. (c) Cells were treated with LPS for 24 h without (open bar) or with (closed bar) addition of 20  $\mu$ M of 2-APB. mRNA expression for ADM was analysed by quantitative real-time PCR. (d) After treatments with 100ng/ml of LPS, 1 $\mu$ M of ionomycin or their combination for 24 h without (open bar) or with (closed bar) 20 $\mu$ M verapamil addition, release of ADM peptide into the supernatant was determined by RIA.

## 5.5 CALC-I gene promoter activity upon increased $\text{Ca}^{2+}$

### 5.5.1 Stable transfection of CALC-I gene promoter deletion constructs

Bacterial induced CALC-I gene expression on the transcriptional level was examined by a lentiviral bidirectional vector system. This system is able to amplify simultaneously the expression of both, the target gene (CALC-I gene promoter connected to luciferase) and a reporter gene (GFP) using two independent promoters. The benefit of this vector is to ensure that every cell expressing GFP contains also a CALC-I gene promoter construct. To find the part on the promoter responsible for infection-induced CALC-I expression, five different CALC-I gene promoter deletion constructs were used for transfection (**Figure 25**).

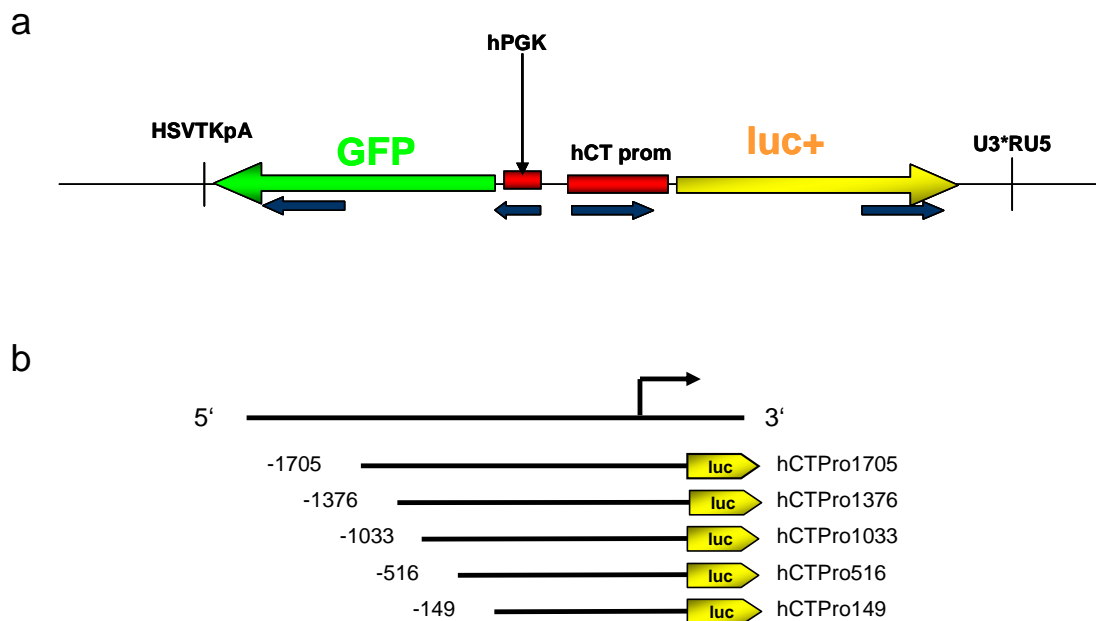
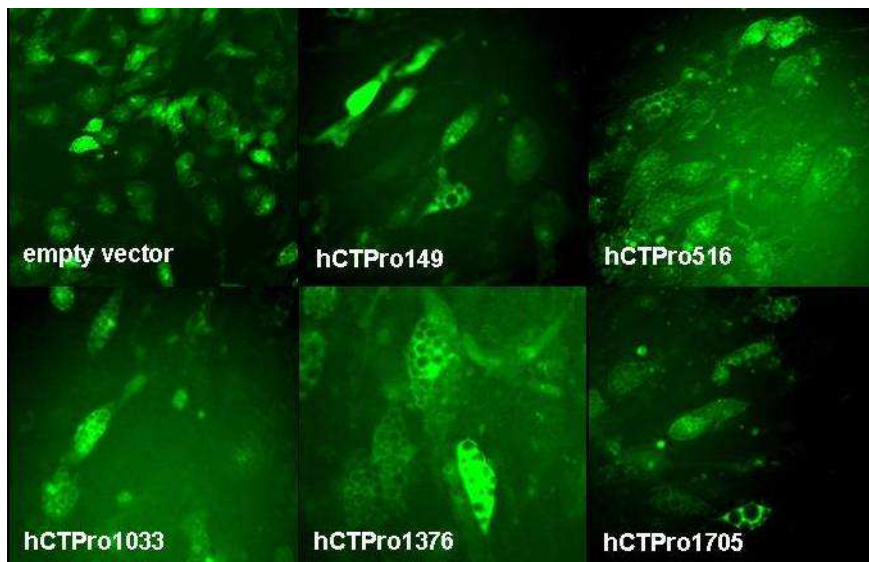


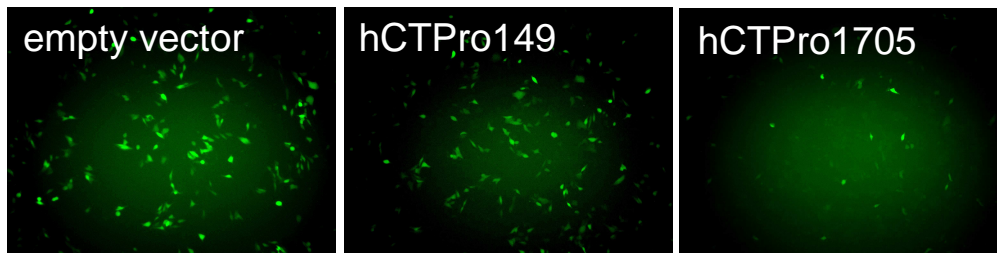
**Figure 25: CALC-I gene promoter deletion constructs.** (a) Bidirectional lentiviral system expressing the two genes green fluorescent protein (GFP) and Luciferase (luc+) at the same time under the control of two separate promoters. The bidirectional vector 53RPA-PGK-GFP expressed GFP under the PGK promoter for normalization of transduction efficacy (b) Schematic representation of the 5' deletions (hCTPro1705, hCTPro1376, hCTPro1033, hCTPro516, hCTPro149) in the promoter region of the human CT gene. 'hCTPro' indicates 'human CT promoter' and the number behind for the amount of base pairs from the transcriptional start site of the gene.

The lentiviral vectors containing the five different CALC-I gene promoter constructs were stably transfected into TT cells and into human MSC- derived adipocytes. The TT cells were used as positive control for successful virus generation and transfection. GFP activity in TT cells was observed 2 days and in adipocytes 5 days post transfection by fluorescence microscopy. **Figure 26 a** displays the mature adipocytes transiently transfected with the different promoter deletion constructs. As assessed by Flow cytometry analysis (data not shown), the transfection efficacy in adipocytes of the different constructs was only below 10%. The more base pairs the promoter construct contained, the lesser was the transfection efficiency. This phenomenon could be observed in TT cells, where less GFP positive cells were detected in cells transfected with hCTPro1705 than with hCTPro149 (**Figure 26 b**) and also in adipocytes. Accordingly, the activity of the hCTPro149 construct was about 5 times higher than that of the hCTPro516 and even around 100 times higher than that of the hCTPro1705 construct at basal conditions (**Figure 26 c**).

a



b



c

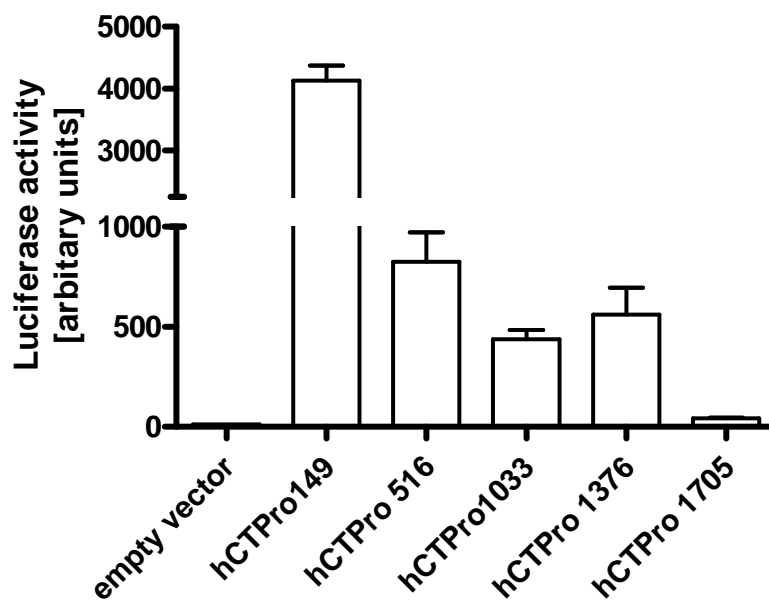


**Figure 26: Transduction of human MSC- derived adipocytes.** a) Mature human MSC-derived adipocytes were exposed to different lentiviral vectors containing the CALC-I gene promoter deletion constructs and GFP under a PGK promoter (53RPA PGK GFP). The pictures were taken with the Olympus IX 50 fluorescent microscope 5 days after transduction. b) TT cells transfected with the empty vector, the shortest CALC-I gene promoter deletion construct hCTPro149 and the largest construct hCTPro1705. The pictures were taken with the Olympus IX 50 fluorescent microscope 2 days after transduction. c) Basal luciferase activity of the different transfected hCTPro constructs shown in a).

### 5.5.2. Increased luciferase activity upon ionomycin

Stimulation of cells with ionomycin at 1 $\mu$ M for 1 hour, increased the activity of hCTPro516, hCTPro1033, hCTPro1376 and hCTPro1705. The ionophore effect was not observed with hCTPro149 and the empty control vector (**Figure 27**).

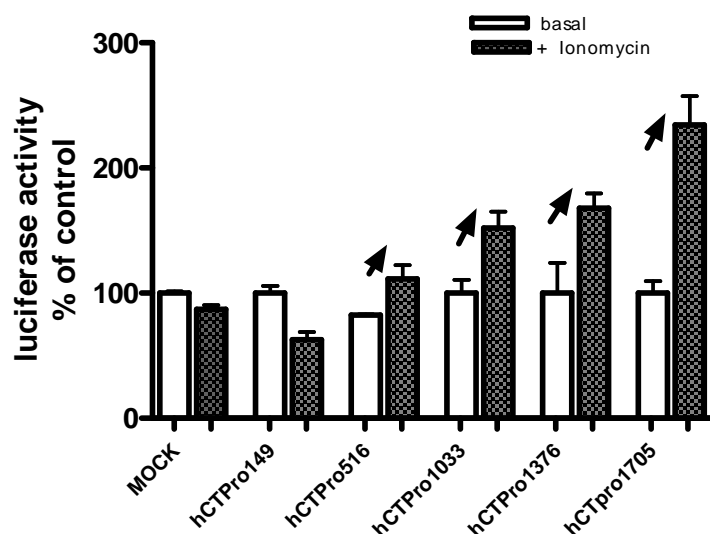


**Figure 27: Luciferase activity upon ionomycin in MSC-derived adipocytes transfected with lentiviral constructs containing different CALC-I gene promoter deletion constructs.** Cells were stimulated with none or 1 $\mu$ M ionomycin for 24 hours. The results are expressed as percentage of luciferase activity relative to that of the corresponding hCTPro construct under basal conditions.

When transfected adipocytes were stimulated with LPS for 24 hours, we could not observe any consistent results concerning differences in the luciferase activity as compared to basal.

## 5.6 Expression of DREAM in human preadipocytes and adipocytes

We examined whether the  $\text{Ca}^{2+}$ -dependent transcriptional regulator DREAM is expressed in the preadipocytes and adipocytes of our cell cultures. **Figure 28** shows the result of Western blotting using an anti-DREAM antibody, indicating the presence of endogenous DREAM in preadipocytes and in adipocytes after 7 days and 14 days of differentiation. TT cells, which are of thyroid origin and known to express DREAM (83) were used as positive control. From preadipocytes to mature adipocytes, the DREAM protein content increases with advancing differentiation state. In parallel, the tubulin protein content decreases in cells undergoing adipose differentiation as previously described by Spiegelman and Farmer (115) due to a change of cellular structure.

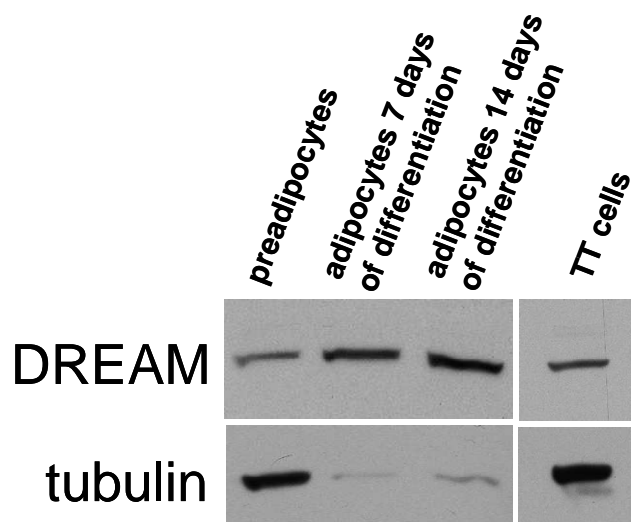


**Figure 28: Expression of DREAM.** Protein from whole lysate was extracted from preadipocytes and adipocytes after 7 days and after 14 days of differentiation. Western blotting (20  $\mu\text{g}$  of protein extract/sample) with anti-DREAM antibody shows the expression of DREAM in preadipocytes and adipocytes in both differentiation stages. TT cell protein extract was also analyzed as a positive control. For the loading control of protein the expression of tubulin is shown.

The results from section 5.5 and 5.6 are preliminary and need further investigation. However, the fact that hCTPro516 is responding to ionomycin and the fact that a DRE

sequence exists in the promoter region between basepair 149 and 516 provides a rationale to further investigate the impact of  $\text{Ca}^{2+}$  on CT expression via DREAM.

## **5.7 Effects of cAMP on LPS-induced CALC-gene expression in preadipocyte-derived adipocytes**

### **5.7.1 Increase in CALC-I gene mRNA expression with forskolin**

cAMP is an important second messengers activating numerous other enzymes involved in diverse cellular functions. In order to assess if increased cAMP levels also alter LPS-induced CALC gene expression, preadipocyte-derived adipocytes were exposed to forskolin in the presence or absence of LPS and changes in CALC gene and IL-6 mRNA levels were measured. Forskolin acts primarily as a direct activator of the adenylat cyclase, which results in increased cAMP in cells.

Forskolin strongly increased the mRNA expression of CT and CGRP-I and decreased the mRNA expression level of ADM. Basal mRNA expression of IL-6 was also increased slightly by foslolin. LPS in combination with forskolin did not alter the forskolin effect on CT and ADM mRNA expression ( $p=n.s.$ ) but led to an increased expression of forskolin-induced IL-6 and CGRP-I mRNA level ( $p<0.001$ ) (**Figure 29**).



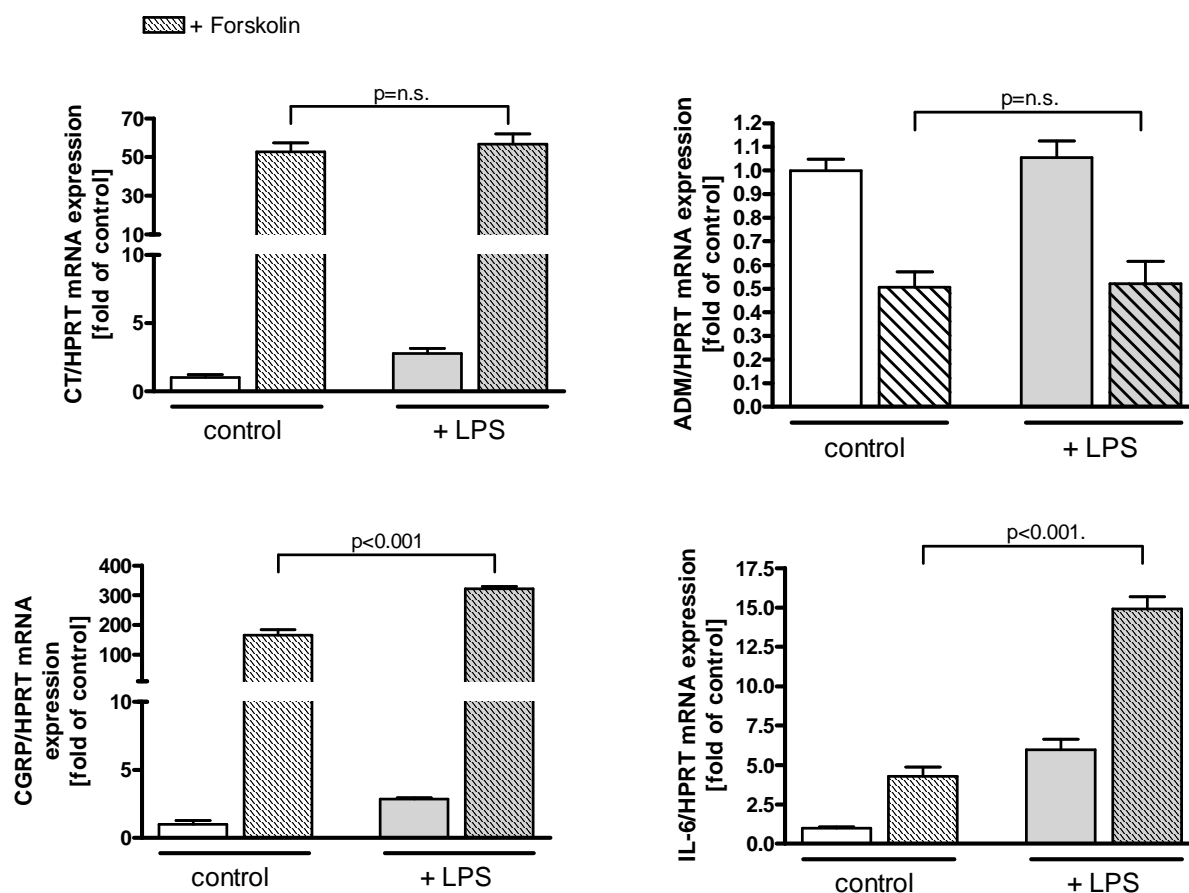


**Figure 29: Changes in mRNA expression level of CALC-I, CALC-V and IL-6 induced by forskolin in preadipocyte-derived adipocytes in presence or absence of LPS.** Adipocytes were exposed to 1 $\mu$ M forskolin (shaded bars) for 24 hours in the presence (grey bars) or absence (open bars) of LPS and assessed for changes in mRNA expression for CT, CGRP-I, ADM and IL-6 by real-time PCR. Data are means  $\pm$  SEM of three independent experiments given as ratio vs. HPRT (\*\*\*,  $p < 0.001$  vs. no LPS; p=n.s. or not statistically significant vs. no LPS).

### 5.7.2 Effects of LPS and IL-1 $\beta$ on cAMP levels in adipocytes

Since increased cAMP has been shown to have an impact on CALC gene expression, we determined the effect of LPS and IL-1 $\beta$  on cAMP levels within the cell. Preadipocyte-derived adipocytes were treated with 100ng/ml LPS, 20IU/ml IL-1 $\beta$  and their combination and the cAMP concentrations were measured after 1 hour of incubation. Exposure to LPS showed no effect on the cAMP level, but 1 hour after IL-

1 $\beta$  administration we measured an increased level in cAMP concentration, comparable to the increase caused by forskolin. In contrast, elevated  $[Ca^{2+}]_i$  caused by ionomycin did not lead to an increase of cAMP within 1 hour (**Figure 30**).

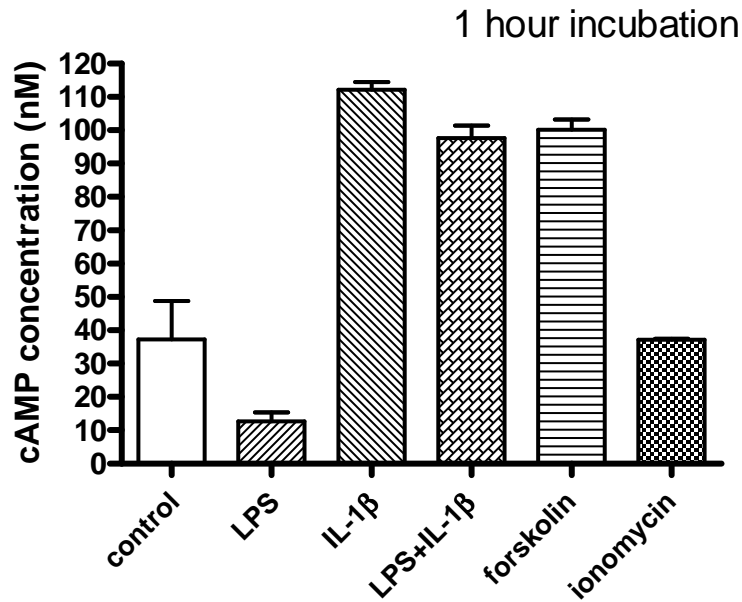


**Figure 30:** cAMP concentration level in preadipocyte-derived adipocytes. The concentration of cAMP are presented in adipocytes exposed to 100ng/ml LPS, 20IU/ml IL-1 $\beta$ , both together, 1 $\mu$ M forskolin and 1 $\mu$ M ionomycin for 1hour.

## 6. Discussion

Despite the substantial investment in critical care resources, bacterial infections and sepsis remain a major threat with a high morbidity and mortality. The host response to bacterial infection involves the activation of complex immune mechanisms and the release of a wide array of inflammatory mediators (116).

Expression levels of CT peptides, mainly of the CT precursor peptide ProCT increase ubiquitously, whereby the major source for CT peptide expression arises from parenchymal cells. As human adipose tissue and adipocytes themselves contribute to infection-and inflammation-induced CT peptide expression, we aimed to study the regulation of extrathyroidal CT peptide expression in a human preadipocyte-derived cell culture model. Fat tissue samples of different donors rather than neoplastic cell cultures were chosen, to bear more upon physiological conditions.

### *Human preadipocyte-derived adipocytes serve as a suitable model to study LPS-induced CALC gene expression*

First, we characterised and validated the suitability of our human preadipocyte-derived adipocytes model to study *in vitro* the effect of LPS on the expression of the CALC genes and thereby gain insight into potential regulatory mechanisms.

Adult human adipose tissue has been reported to be composed of 50–70% adipocytes, 20–40% stromal vascular cells such as preadipocytes, fibroblasts and non-differentiated mesenchymal cells and 1–30% infiltrated macrophages (117). Our cultures of *in vitro* differentiated adipocytes showed no or only negligible amounts of macrophage markers (i.e. CD68) and the medium provided to cell cultures favors preadipocyte expansion and adipogenesis. Especially, the expression of pro-inflammatory cytokines has been assigned to preadipocytes rather than to mature adipocytes (117, 118). Since our cell model consists of at least two different cell types (i.e. preadipocytes and adipocytes) we cannot exclude that preadipocytes do not contribute to some effects observed. However, it was demonstrated in previous work from our group (28) that the CALC-V gene is only weakly expressed and the CALC-I gene is not expressed at all in undifferentiated MSCs upon LPS or LPS in combination with inflammatory stimuli. Nevertheless, the definite source of mRNA expression and peptide secretion in our cell cultures does not preclude the validity of

the experimental evidence gathered, as both, the presence of preadipocytes goes along with mature adipocytes in human adipose tissue *in vivo*.

Using cells originating from different patients, we almost always observed an increase in CALC-I gene expression upon LPS stimulation independent of the donor, but the fold of increase varied considerably. While we do not have a final explanation for this variability, we suppose a context in inter-individual pheno- and genotypic differences of the diverse donors. There were no indications that the sex or the BMI might play a role. The latter finding concerning the BMI is so far surprising, as obesity is associated with chronic low grade inflammation, which in turn is associated with increased levels of ProCT (119). We found that in cells from one donor suffering from pancreatitis, LPS stimulation was leading to a slightly higher CALC-I gene expression level compared to others (see Figure 10, donor 2). This anecdotal observation indicates that an acute infection in the patient might either influence the sensitivity of the preadipocyte-derived adipocytes to LPS stimulation or increase the susceptibility of the cells to respond with enhanced CALC-I gene activity. In this context, it is mentionable that Ammori et al. described increased levels of calcitonin precursors in patients with acute pancreatitis (120).

In addition to the variability traced back to different donors, mRNA expression levels also varied depending on the batch of cells and the cell culture passages used for the single experiments. Most likely our cells experience alterations in their response to stimuli and their protein expression during passaging. In addition, the time to reach confluence and efficient differentiation varied; consequently the total ratio between undifferentiated preadipocytes and differentiated adipocytes varied from experiment to experiment, even within cells from the same donor and according to the passages. However, the tendency toward an increase in LPS- mediated CALC-I gene and IL-6 expression was consistent within the different experiments.

The expression of IL-6, CT and CGRP-I seem rather to result from a distinct response of intact cells to specific inflammatory pathways activated by LPS and not from a simple “toxic” effect. In contrast to previous results from our group shown in MSC-derived adipocytes, our preadipocyte-derived adipocytes did not react with elevated ADM mRNA expression levels or protein release upon LPS exposure for 24 hours. Additionally, the expression levels of CT and CGRP-I mRNA in preadipocyte-derived adipocytes was in a lower range compared to previous results from adipocytes derived from MSCs. These findings indicate that the preadipocyte-derived adipocyte cell

culture model cannot be equalled in all aspects with the MSC-derived adipocyte cell culture model.

### ***Distinct inflammatory signaling pathways are involved in LPS-induced IL-6 and CALC-I gene mRNA expression***

We confirmed that LPS increases the expression of IL-6 in human adipocytes via activation of the NF $\kappa$ B pathway (121). When inhibiting the activation of NF $\kappa$ B by blocking IKK2, we observed a reduction of IL-6 mRNA expression, contrasting the increased expression level of CALC-I gene mRNA. Since high amounts of ProCT and CGRP-I have been shown to be unfavorable prognostic findings, this might indicate a putative protective function of inflammatory signaling via NF $\kappa$ B in respect to CALC-I gene activation.

LPS uses different receptors and/or signaling pathways in different cell types and there are fundamental signaling differences between human and murine macrophages and between cells of myeloid and non-myeloid origins (122, 123), respectively. For instance IKK2 is not required for LPS-induced NF $\kappa$ B activation and cytokine production in human immature dendritic cells (122). LPS might signal via IKK2 in preadipocytes but not in adipocytes and, thus, explain the distinct mRNA expression pattern for IL-6 and CALC-I gene mRNA upon IKK2 inhibition. Indeed, our cell culture model consists of both, preadipocytes and mature adipocytes, whereby the expression of CT and CGRP-I is assigned to adipocytes (28, 117) and the pro-inflammatory response by IL-6 induction is more pronounced in preadipocytes (117).

### ***Role of IL-1 $\beta$ in extrathyroidal CALC-I gene expression***

Besides IL-6 and CALC-I genes, stimulation with LPS induces IL-1 $\beta$  expression in different cell types (124, 125). As principal function this cytokine is pro-inflammatory. In the current work, it was shown that the cells in our cell culture model are able to respond to LPS with increased IL-1 $\beta$  expression. Conversely, IL-1 $\beta$  itself induced CT gene expression and ProCT secretion in *ex-vivo* differentiated human adipocytes (47) and CGRP-I mRNA and protein secretion in MSC-derived adipocytes (28). These findings raised the question whether the increase in CALC-I gene expression mediated by LPS is occurring downstream of LPS via IL-1 $\beta$ . Importantly, inhibiting the IL-1 receptor was blocking the expression of IL-1 $\beta$ -induced CALC-I gene expression but not the expression induced by LPS.

***Role of calcium in LPS-induced CALC-I gene expression***

Little is known about the role of  $[Ca^{2+}]_i$  in LPS stimulation in human adipocytes whereas in macrophages it has been studied extensively. Even though the consensus has been that LPS does not cause an increase in  $[Ca^{2+}]_i$  but a baseline calcium concentration is required for proper cell activation in response to LPS (126), there are results with macrophages demonstrating that LPS stimulation increases phosphatidylinositol turnover (127) and increases in  $[Ca^{2+}]_i$  upon LPS in rat peritoneal macrophages have been described (128). In our experimental model, the adipocytes were stimulated with either LPS or, as a positive control, ionomycin. In the majority of adipocytes, but not in each single cell monitored for changes in  $[Ca^{2+}]_i$ , ionomycin was able to cause an increase in  $[Ca^{2+}]_i$ . LPS stimulation increased  $[Ca^{2+}]_i$ , only inconsistently. The fast, massive and transient response in  $[Ca^{2+}]_i$  increase elicited by ionomycin contrasted with the slow, modest but sustained increase induced by LPS. The onset and duration of the  $[Ca^{2+}]_i$  increase caused by either ionomycin or LPS was not correlated with a particular morphologic appearance of the adipocyte. Our findings on the effect of LPS on  $[Ca^{2+}]_i$  changes in adipocytes are in line with the findings made by Letari et al. where only 47% of individually observed rat peritoneal macrophages responded to LPS exposure with an increase in  $[Ca^{2+}]_i$ , and for their macrophages, same as for our adipocytes, a heterogeneous response was observed (128).

The  $Ca^{2+}$  mobilization observed after LPS exposure was dependent from an influx of  $Ca^{2+}$  from the extracellular space and probably a release from intracellular stores mediated by  $IP_3$ , followed by an influx through store-operated channels. Accordingly, LPS-induced CALC-I gene expression was reduced after diminishing  $[Ca^{2+}]_i$  by verapamil and 2-APB. On the other hand the LPS-induced CALC-I gene expression is potentiated with increasing  $[Ca^{2+}]_i$  through addition of ionomycin or depletion of intracellular  $Ca^{2+}$  stores with thapsigargin.

Interestingly, the number of adipocytes responding with increased  $[Ca^{2+}]_i$  upon LPS stimulation was markedly higher in cells deriving from donors where the LPS-induced CALC-I gene mRNA expression was more pronounced than in cells from donors with a low fold of mRNA increase. This observation might pull together a dependence of LPS-mediated CALC-I gene expression on increased  $[Ca^{2+}]_i$ . Moreover we found that upon ionomycin, changes in  $[Ca^{2+}]_i$  and changes in CALC-I gene expression were

more pronounced in mature adipocytes than in preadipocytes. The finding that adipocytes which did not react with increased  $[Ca^{2+}]_i$  upon LPS exposure answered much faster and with higher amplitude to ionomycin than control cells gives additional indication on a putative role of  $Ca^{2+}$  in LPS-induced infection and may serve as a link to our results showing how CALC-I gene expression is potentiated in the combination of LPS with agents increasing  $[Ca^{2+}]_i$ .

Varying intra- and extracellular  $Ca^{2+}$  with  $Ca^{2+}$  agonists and  $Ca^{2+}$  antagonists alters cellular production of numerous cytokines including TNF- $\alpha$ , IL-1 $\beta$ , IL-2, IL-8 and IL-6 (129-133). An increase in  $[Ca^{2+}]_i$  only triggers cytokine production in conjunction with LPS (129, 131). These findings are in accordance with our results showing increased expression of CT peptides and IL-6 when treating cells with  $Ca^{2+}$  liberators together with LPS. In our adipocyte model,  $Ca^{2+}$  acts at the transcriptional level of the LPS-induced CALC genes and IL-6, but presumably with a distinct molecular mechanism.  $Ca^{2+}$  seems to have a greater impact on LPS-induced CALC-I gene expression than on the one of IL-6. Further investigations are needed to unravel the mechanisms through which alterations in  $[Ca^{2+}]_i$  influence their gene expression. In thyroid C cells CT is secreted upon an increase in plasma  $Ca^{2+}$  to reduce the level of  $Ca^{2+}$ . The increase in  $Ca^{2+}$  probably triggers the activation of  $Ca^{2+}$ -sensing receptors on the surface membrane of thyroid cells (134), leading to an activation of G-coupled signaling pathway to increase intracellular  $Ca^{2+}$  (135).  $Ca^{2+}$  then binds to DNA via transcriptional cofactors (136) resulting in transcription of CT mRNA (137). Similar as for thyroid C-cells, the increased  $[Ca^{2+}]_i$  might result in activation of  $Ca^{2+}$ -regulated cofactors on the CALC-I gene promoter in adipocytes, leading to the high rates of ProCT and CGRP production in bacterial infection.

#### ***Distinct role of calcium in ADM expression***

An additional observation from our study was the distinct modulatory effect of increased  $[Ca^{2+}]_i$  on inflammatory CALC-gene expression. While LPS-mediated elevations of  $[Ca^{2+}]_i$  in an inflammatory background potentiated the activity of the CALC-I gene, CALC-V (ADM) gene expression was reduced, both at the mRNA and the protein level. Several studies exploring the effect of modulating  $[Ca^{2+}]_i$  in septic patients have been performed with mixed conclusions. In endotoxemia,  $Ca^{2+}$  antagonists improved survival in animal models of septic rats and mice (130, 138,

139). In contrast, inhibitors of  $\text{Ca}^{2+}$  release from intracellular store decreased survival in septic rats (140).

In our study, an increase in  $[\text{Ca}^{2+}]_i$  in human adipocytes led to a decrease in CALC-V mRNA expression and protein secretion which was not converted when reducing increased  $[\text{Ca}^{2+}]_i$ . Together this might indicate that at an early stage of sepsis an elevated  $[\text{Ca}^{2+}]_i$  might be responsible for the low amount of CALC-V compared to the high amount of CALC-I gene expression and that CALC-V gene expression is upregulated with progressing course of sepsis. Accordingly, Christ-Crain et al. (45, 46, 141) reported that proadrenomedullin (ProADM) is a prognostic factor in respiratory tract infection and sepsis with high levels indicating poor survival and serious adverse events. In contrast, the CALC-I gene product ProCT is more diagnostic than prognostic marker indicating the presence of bacterial infection and need for antibiotic therapy. The distinct effects of calcium on CALC-V and CALC-I transcription and translation could be interpreted as molecular basis for these clinically important and distinct characteristics.

#### ***Transcriptional regulation of CALC-I gene expression at its promoter level upon LPS and calcium***

With the use of lentiviral mediated reporter assays, we aimed to identify putative inflammation response elements within the CALC-I gene promoter. To determine changes in CALC-I gene promoter activity in adipocytes transfected with lentiviral constructs, luciferase reporter assays were carried out. This technique turned out not to be suitable for our adipocyte culture model due to the variability in transduction efficiency of the different lentiviral constructs in the cells. When adipocytes transfected with the different CALC-I promoter deletion constructs were treated with LPS, we had difficulties to obtain consistent results. We ascribed this inconsistency to some of the technical problems which might appear when working with cell cultures of human mature adipocyte. Adipocytes are spherical and vary in diameter from 10 to over 120  $\mu\text{m}$ . They are fragile and possess one unusual biophysical characteristic among mammalian cells: they have a specific gravity less than that of water. Consequently, they float in commonly used buffers, yielding an unstable output signal and making conventional analytical methods difficult (142). For the luciferase assay system we were using, the cells were lysed in the cell culture plates and then transferred into suitable 96-well plates. Homogenizing the suspension of lysed cells



by mixing before transferring them was probably producing severe mechanical damages. The transferred suspension was cloudy and sticky due to the lipid content from the fat droplets, which interfered with the assay. The fact that LPS only led to a slow and sustained increase in  $[Ca^{2+}]_i$  and this increase did not occur in all cells complicated the experimental settings even more, especially taking into account the low transfection efficiency. Nevertheless, in some pilot experiments we repeatedly managed to observe that treatment with ionomycin led to increased CALC-I gene promoter activity in adipocytes. Our results were in accordance with results from Matsuda et al. (83) where the ionomycin-induced increase in luciferase activity was starting with the first CALC-I gene promoter deletion construct containing the two DRE motifs. Additionally, the fact that preadipocytes and adipocytes were shown to express the  $Ca^{2+}$ -dependent transcriptional repressor DREAM will encourage us to further study  $Ca^{2+}$  as a potential key player in the LPS-induced extrathyroidal CALC gene expression.

#### ***Involvement of cAMP in extrathyroidal CALC-gene expression***

We found that elevated cAMP concentration levels caused by forskolin alter the mRNA expression of the CALC-I and CALC-V gene and of IL-6 in preadipocyte-derived adipocytes. Similar as observed for  $Ca^{2+}$ , increased cAMP levels led to increased expression levels of CT and CGRP-I mRNA but to reduced mRNA expression levels of ADM. The response in IL-6 mRNA expression to cAMP was comparable to the IL-6 mRNA expression response to  $Ca^{2+}$ , meaning that the mRNA increase triggered by forskolin and LPS alone seemed to increase additively when cells were co-treated with both substances. In contrast to  $Ca^{2+}$ , an inflammatory background caused by LPS did not alter the cAMP-induced expression of CT but treatment with forskolin increased CGRP-I mRNA expression in the presence of LPS. Albeit to a lesser extent as ProCT, circulating CGRP is elevated in sepsis, namely in the protracted and severe phases of septic shock (41, 143,144). The late state of sepsis is associated with elevations of intracellular cAMP in Kupffer cells (145). In the present work, we found that intracellular cAMP concentrations increase in preadipocyte-derived adipocytes within 1 hour after exposure to IL-1 $\beta$  but not after exposure to LPS or ionomycin. In contrast, LPS induced increasing levels of  $[Ca^{2+}]_i$  within a comparable time period. As both, LPS and IL-1 $\beta$  have been shown to induce expression of CT and CGRP, these findings indicate that  $Ca^{2+}$  and cAMP might both

be involved in extrathyroidal CALC gene expression. Both, increases in  $[Ca^{2+}]_i$  and cAMP levels lead to elevated CALC-I gene expression, even if the two CALC-I gene splicing products CT and CGRP-I seem not to respond to these two second messengers in exactly the same way. It appears that cAMP gets more important at later states of sepsis. However, this may not be the case for the CALC-V gene ADM which is downregulated with both,  $[Ca^{2+}]_i$  and cAMP levels but upregulated with progressing states of sepsis (141).

### ***Conclusions and outlook***

In conclusion, LPS and IL-1 $\beta$  induce an upregulation of the pro-inflammatory cytokine IL-6 and the CALC-I genes CT and CGRP-I in our cell cultures of preadipocyte-derived adipocytes. This is mediated by increased levels of  $[Ca^{2+}]_i$  and cAMP. The LPS-induced IL-6 and CALC-I gene expression seems not to be activated via the same signaling pathways. While IL-6 mRNA expression is regulated via the classical NF $\kappa$ B pathway, CALC-I gene expression is regulated otherwise. In contrast to the upregulation of the CALC-I gene, the CALC-V gene ADM is downregulated upon increased levels of  $[Ca^{2+}]_i$  and cAMP. The molecular mechanism of  $Ca^{2+}$  and cAMP mediating the extrathyroidal CALC-I gene expression in infection and inflammations remains unknown. However, in view of the presence of the transcriptional repressor DREAM in human adipocytes we suggest that  $Ca^{2+}$  and cAMP might act on transcriptional level of the CALC-I gene in coherence with DRE-DREAM and DREAM-CREM/CREB interaction. Further elucidation of the effect of LPS and IL-1 $\beta$  on CALC-I gene expression in respect to DRE-DREAM and DREAM-CREM/CREB interactions will help to unravel the mechanism of extrathyroidal CALC-I gene expression in bacterial infection and sepsis.

## 7. References

1. **Becker K.L., Müller B., Nylen E.S., Cohen R., R.H. S** 2001 Calcitonin gene family of peptides and its receptors. In: Principles and Practice of Endocrinology and Metabolism; JB Lippincott Co, Philadelphia, PA, USA. 3rd ed: Becker K.L. (ed). 520-534
2. **Born W., J.A. F** 1993 Calcitonin gene products:molecular biology, mechanism, and actions. In: Handb Exp Pharmacol; 569-616
3. **Muff R, Born W, Fischer J** 1995 Calcitonin, calcitonin gene-related peptide, adrenomedullin and amylin: homologous peptides, separate receptors and overlapping biological actions. *Eur J Endocrinol* 133:17-20
4. **Hutton J, Rhodes C** 1991 The enzymology of proinsulin conversion. *Cell Biophys* 19:57-62
5. **Schuetz P, Christ-Crain M, Thomann R, Falconnier C, Wolbers M, Widmer I, Neidert S, Fricker T, Blum C, Schild U, Regez K, Schoenenberger R, Henzen C, Bregenzer T, Hoess C, Krause M, Bucher H, Zimmerli W, Mueller B** 2009 Effect of procalcitonin-based guidelines vs standard guidelines on antibiotic use in lower respiratory tract infections: the ProHOSP randomized controlled trial. *JAMA* 302:1059-1066
6. **Müller B, Christ-Crain M, Schuetz P** 2007 Meta-analysis of procalcitonin for sepsis detection. *Lancet Infect Dis* 7:498-499; author reply 502-493
7. **Briel M, Schuetz P, Mueller B, Young J, Schild U, Nusbaumer C, Périat P, Bucher H, Christ-Crain M** 2008 Procalcitonin-guided antibiotic use vs a standard approach for acute respiratory tract infections in primary care. *Arch Intern Med* 168:2000-2007; discussion 2007-2008
8. **Stolz D, Christ-Crain M, Morgenthaler N, Miedinger D, Leuppi J, Müller C, Bingisser R, Struck J, Müller B, Tamm M** 2008 Plasma pro-adrenomedullin but not plasma pro-endothelin predicts survival in exacerbations of COPD. *Chest* 134:263-272
9. **COPP D, CHENEY B** 1962 Calcitonin-a hormone from the parathyroid which lowers the calcium-level of the blood. *Nature* 193:381-382
10. **HIRSCH P, GAUTHIER G, MUNSON P** 1963 THYROID HYPOCALCEMIC PRINCIPLE AND RECURRENT LARYNGEAL NERVE INJURY AS FACTORS AFFECTING THE RESPONSE TO PARATHYROIDECTOMY IN RATS. *Endocrinology* 73:244-252
11. **COPP D, CAMERON E, CHENEY B, DAVIDSON A, HENZE K** 1962 Evidence for calcitonin--a new hormone from the parathyroid that lowers blood calcium. *Endocrinology* 70:638-649
12. **Pellegriti G, Leboulleux S, Baudin E, Bellon N, Scollo C, Travagli J, Schlumberger M** 2003 Long-term outcome of medullary thyroid carcinoma in patients with normal postoperative medical imaging. *Br J Cancer* 88:1537-1542
13. **Müller B, Becker K** 2001 Procalcitonin: how a hormone became a marker and mediator of sepsis. *Swiss Med Wkly* 131:595-602
14. **Snider R.J, Nylen E, Becker K** 1997 Procalcitonin and its component peptides in systemic inflammation: immunochemical characterization. *J Investig Med* 45:552-560

15. **Rosenfeld M, Amara S, Roos B, Ong E, Evans R** 1981 Altered expression of the calcitonin gene associated with RNA polymorphism. *Nature* 290:63-65
16. **Beglinger C, Born W, Münch R, Kurtz A, Gutzwiller J, Jäger K, Fischer J** Distinct hemodynamic and gastric effects of human CGRP I and II in man. *Peptides* 12:1347-1351
17. **Wimalawansa S** 1997 Amylin, calcitonin gene-related peptide, calcitonin, and adrenomedullin: a peptide superfamily. *Crit Rev Neurobiol* 11:167-239
18. **Nuki C, Kawasaki H, Kitamura K, Takenaga M, Kangawa K, Eto T, Wada A** 1993 Vasodilator effect of adrenomedullin and calcitonin gene-related peptide receptors in rat mesenteric vascular beds. *Biochem Biophys Res Commun* 196:245-251
19. **Marutsuka K, Nawa Y, Asada Y, Hara S, Kitamura K, Eto T, Sumiyoshi A** 2001 Adrenomedullin and proadrenomedullin N-terminal 20 peptide (PAMP) are present in human colonic epithelia and exert an antimicrobial effect. *Exp Physiol* 86:543-545
20. **Pio R, Martinez A, Unsworth E, Kowalak J, Bengoechea J, Zipfel P, Elsasser T, Cuttitta F** 2001 Complement factor H is a serum-binding protein for adrenomedullin, and the resulting complex modulates the bioactivities of both partners. *J Biol Chem* 276:12292-12300
21. **Bone R, Balk R, Cerra F, Dellinger R, Fein A, Knaus W, Schein R, Sibbald W** 1992 Definitions for sepsis and organ failure and guidelines for the use of innovative therapies in sepsis. The ACCP/SCCM Consensus Conference Committee. American College of Chest Physicians/Society of Critical Care Medicine. *Chest* 101:1644-1655
22. **Bone R, Sibbald W, Sprung C** 1992 The ACCP-SCCM consensus conference on sepsis and organ failure. *Chest* 101:1481-1483
23. **Müller B, White J, Nylén E, Snider R, Becker K, Habener J** 2001 Ubiquitous expression of the calcitonin-i gene in multiple tissues in response to sepsis. *J Clin Endocrinol Metab* 86:396-404
24. **Domenech V, Nylén E, White J, Snider R, Becker K, Landmann R, Müller B** 2001 Calcitonin gene-related peptide expression in sepsis: postulation of microbial infection-specific response elements within the calcitonin I gene promoter. *J Investig Med* 49:514-521
25. **Becker K, Nylén E, Snider R, Müller B, White J** 2003 Immunoneutralization of procalcitonin as therapy of sepsis. *J Endotoxin Res* 9:367-374
26. **Morgenthaler N, Struck J, Chancerelle Y, Weglöhner W, Agay D, Bohuon C, Suarez-Domenech V, Bergmann A, Müller B** 2003 Production of procalcitonin (PCT) in non-thyroidal tissue after LPS injection. *Horm Metab Res* 35:290-295
27. **Linscheid P, Seboek D, Nylén ES, Langer I, Schlatter M, Becker KL, Keller U, Müller B** 2003 In vitro and in vivo calcitonin I gene expression in parenchymal cells: a novel product of human adipose tissue. *Endocrinology* 144:5578-5584
28. **Linscheid P, Seboek D, Zulewski H, Keller U, Müller B** 2005 Autocrine/paracrine role of inflammation-mediated calcitonin gene-related peptide and adrenomedullin expression in human adipose tissue. *Endocrinology* 146:2699-2708
29. **Linscheid P, Seboek D, Schaer D, Zulewski H, Keller U, Müller B** 2004 Expression and secretion of procalcitonin and calcitonin gene-related peptide

- by adherent monocytes and by macrophage-activated adipocytes. *Crit Care Med* 32:1715-1721
30. **Muller B, Becker KL, Schachinger H, Rickenbacher PR, Huber PR, Zimmerli W, Ritz R** 2000 Calcitonin precursors are reliable markers of sepsis in a medical intensive care unit. *Crit Care Med* 28:977-983
  31. **Dandona P, Nix D, Wilson M, Aljada A, Love J, Assicot M, Bohuon C** 1994 Procalcitonin increase after endotoxin injection in normal subjects. *J Clin Endocrinol Metab* 79:1605-1608
  32. **Simon L, Gauvin F, Amre D, Saint-Louis P, Lacroix J** 2004 Serum procalcitonin and C-reactive protein levels as markers of bacterial infection: a systematic review and meta-analysis. *Clin Infect Dis* 39:206-217
  33. **Harbarth S, Holeckova K, Froidevaux C, Pittet D, Ricou B, Grau G, Vadas L, Pugin J** 2001 Diagnostic value of procalcitonin, interleukin-6, and interleukin-8 in critically ill patients admitted with suspected sepsis. *Am J Respir Crit Care Med* 164:396-402
  34. **Schuetz P, Albrich W, Christ-Crain M, Chastre J, Mueller B** 2010 Procalcitonin for guidance of antibiotic therapy. *Expert Rev Anti Infect Ther* 8:575-587
  35. **Nylen E, Whang K, Snider RJ, Steinwald P, White J, Becker K** 1998 Mortality is increased by procalcitonin and decreased by an antiserum reactive to procalcitonin in experimental sepsis. *Crit Care Med* 26:1001-1006
  36. **Steinwald P, Whang K, Becker K, Snider R, Nylen E, White J** 1999 Elevated calcitonin precursor levels are related to mortality in an animal model of sepsis. *Crit Care* 3:11-16
  37. **Martinez J, Wagner K, Snider R, Nylen E, Muller B, Sarani B, Becker K, White J** 2001 Late immunoneutralization of procalcitonin arrests the progression of lethal porcine sepsis. *Surg Infect (Larchmt)* 2:193-202; discussion 202-193
  38. **Wagner K, Martinez J, Vath S, Snider R, Nylén E, Becker K, Müller B, White J** 2002 Early immunoneutralization of calcitonin precursors attenuates the adverse physiologic response to sepsis in pigs. *Crit Care Med* 30:2313-2321
  39. **Sexton P, Christopoulos G, Christopoulos A, Nylen E, Snider RJ, Becker K** 2008 Procalcitonin has bioactivity at calcitonin receptor family complexes: potential mediator implications in sepsis. *Crit Care Med* 36:1637-1640
  40. **Becker K, Nylén E, White J, Müller B, Snider RJ** 2004 Clinical review 167: Procalcitonin and the calcitonin gene family of peptides in inflammation, infection, and sepsis: a journey from calcitonin back to its precursors. *J Clin Endocrinol Metab* 89:1512-1525
  41. **Joyce C, Fiscus R, Wang X, Dries D, Morris R, Prinz R** 1990 Calcitonin gene-related peptide levels are elevated in patients with sepsis. *Surgery* 108:1097-1101
  42. **Hirata Y, Mitaka C, Sato K, Nagura T, Tsunoda Y, Amaha K, Marumo F** 1996 Increased circulating adrenomedullin, a novel vasodilatory peptide, in sepsis. *J Clin Endocrinol Metab* 81:1449-1453
  43. **Struck J, Tao C, Morgenthaler N, Bergmann A** 2004 Identification of an Adrenomedullin precursor fragment in plasma of sepsis patients. *Peptides* 25:1369-1372

44. **Eto T** 2001 A review of the biological properties and clinical implications of adrenomedullin and proadrenomedullin N-terminal 20 peptide (PAMP), hypotensive and vasodilating peptides. *Peptides* 22:1693-1711
45. **Christ-Crain M, Morgenthaler NG, Stolz D, Muller C, Bingisser R, Harbarth S, Tamm M, Struck J, Bergmann A, Muller B** 2006 Proadrenomedullin to predict severity and outcome in community-acquired pneumonia [ISRCTN04176397]. *Crit Care* 10:R96
46. **Christ-Crain M, Müller B** 2008 Calcitonin peptides--the mediators in sepsis or just another fairy tale? *Crit Care Med* 36:1684-1687
47. **Linscheid P, Seboek D, Nylen E, Langer I, Schlatter M, Becker K, Keller U, Müller B** 2003 In vitro and in vivo calcitonin I gene expression in parenchymal cells: a novel product of human adipose tissue. *Endocrinology* 144:5578-5584
48. **Berg A, Scherer P** 2005 Adipose tissue, inflammation, and cardiovascular disease. *Circ Res* 96:939-949
49. **Schäffler A, Schölmerich J, Salzberger B** 2007 Adipose tissue as an immunological organ: Toll-like receptors, C1q/TNFs and CTRPs. *Trends Immunol* 28:393-399
50. **Charrière G, Cousin B, Arnaud E, André M, Bacou F, Penicaud L, Casteilla L** 2003 Preadipocyte conversion to macrophage. Evidence of plasticity. *J Biol Chem* 278:9850-9855
51. **Kershaw E, Flier J** 2004 Adipose tissue as an endocrine organ. *J Clin Endocrinol Metab* 89:2548-2556
52. **Ronti T, Lupattelli G, Mannarino E** 2006 The endocrine function of adipose tissue: an update. *Clin Endocrinol (Oxf)* 64:355-365
53. **Takeda K, Akira S** 2001 Regulation of innate immune responses by Toll-like receptors. *Jpn J Infect Dis* 54:209-219
54. **Visintin A, Mazzone A, Spitzer J, Wyllie D, Dower S, Segal D** 2001 Regulation of Toll-like receptors in human monocytes and dendritic cells. *J Immunol* 166:249-255
55. **Dong Z, Yang Z, Wang C** 2005 Expression of TLR2 and TLR4 messenger RNA in the epithelial cells of the nasal airway. *Am J Rhinol* 19:236-239
56. **Pivarcsi A, Kemény L, Dobozy A** 2004 Innate immune functions of the keratinocytes. A review. *Acta Microbiol Immunol Hung* 51:303-310
57. **Bès-Houtmann S, Roche R, Hoareau L, Gonthier M, Festy F, Caillens H, Gasque P, Lefebvre d'Hellencourt C, Cesari M** 2007 Presence of functional TLR2 and TLR4 on human adipocytes. *Histochem Cell Biol* 127:131-137
58. **Armant M, Fenton M** 2002 Toll-like receptors: a family of pattern-recognition receptors in mammals. *Genome Biol* 3:REVIEWS3011
59. **Kern P, Saghizadeh M, Ong J, Bosch R, Deem R, Simsolo R** 1995 The expression of tumor necrosis factor in human adipose tissue. Regulation by obesity, weight loss, and relationship to lipoprotein lipase. *J Clin Invest* 95:2111-2119
60. **Montague C, Prins J, Sanders L, Zhang J, Sewter C, Digby J, Byrne C, O'Rahilly S** 1998 Depot-related gene expression in human subcutaneous and omental adipocytes. *Diabetes* 47:1384-1391
61. **Hoch M, Eberle A, Peterli R, Peters T, Seboek D, Keller U, Muller B, Linscheid P** 2008 LPS induces interleukin-6 and interleukin-8 but not tumor necrosis factor-alpha in human adipocytes. *Cytokine* 41:29-37

62. **Taylor B, Sibbald W, Edmonds M, Holliday R, Williams C** 1978 Ionized hypocalcemia in critically ill patients with sepsis. *Can J Surg* 21:429-433
63. **Zivin J, Gooley T, Zager R, Ryan M** 2001 Hypocalcemia: a pervasive metabolic abnormality in the critically ill. *Am J Kidney Dis* 37:689-698
64. **Müller B, Becker K, Kränzlin M, Schächinger H, Huber P, Nylén E, Snider R, White J, Schmidt-Gayk H, Zimmerli W, Ritz R** 2000 Disordered calcium homeostasis of sepsis: association with calcitonin precursors. *Eur J Clin Invest* 30:823-831
65. **Song S, Karl I, Ackerman J, Hotchkiss R** 1993 Increased intracellular Ca<sup>2+</sup>: a critical link in the pathophysiology of sepsis? *Proc Natl Acad Sci U S A* 90:3933-3937
66. **Bhattacharyya J, Thompson K, Sayeed M** 1991 Calcium-dependent and calcium-independent protease activities in skeletal muscle during sepsis. *Circ Shock* 35:117-122
67. **Liu M, Kang G** 1987 Liver glycogen metabolism in endotoxin shock. II. Endotoxin administration increases glycogen phosphorylase activities in dog livers. *Biochem Med Metab Biol* 37:73-80
68. **Zaloga G, Washburn D, Black K, Prielipp R** 1993 Human sepsis increases lymphocyte intracellular calcium. *Crit Care Med* 21:196-202
69. **Copp D** 1970 Calcitonin and calcium metabolism. *Can Med Assoc J* 103:821-824
70. **Syntichaki P, Tavernarakis N** 2003 The biochemistry of neuronal necrosis: rogue biology? *Nat Rev Neurosci* 4:672-684
71. **Friedman J, Raisz L** 1965 Thyrocalcitonin: inhibitor of bone resorption in tissue culture. *Science* 150:1465-1467
72. **Raisz L, Au W, Friedman J, Niemann I** 1967 Thyrocalcitonin and bone resorption. Studies employing a tissue culture bioassay. *Am J Med* 43:684-690
73. **Warshawsky H, Goltzman D, Rouleau M, Bergeron J** 1980 Direct in vivo demonstration by radioautography of specific binding sites for calcitonin in skeletal and renal tissues of the rat. *J Cell Biol* 85:682-694
74. **Canaff L, Zhou X, Hendy G** 2008 The proinflammatory cytokine, interleukin-6, up-regulates calcium-sensing receptor gene transcription via Stat1/3 and Sp1/3. *J Biol Chem* 283:13586-13600
75. **Hendy G, D'Souza-Li L, Yang B, Canaff L, Cole D** 2000 Mutations of the calcium-sensing receptor (CASR) in familial hypocalciuric hypercalcemia, neonatal severe hyperparathyroidism, and autosomal dominant hypocalcemia. *Hum Mutat* 16:281-296
76. **Coburn J, Elangovan L, Goodman W, Frazão J** 1999 Calcium-sensing receptor and calcimimetic agents. *Kidney Int Suppl* 73:S52-58
77. **Hirsch P, Lester G, Talmage R** 2001 Calcitonin, an enigmatic hormone: does it have a function? *J Musculoskelet Neuronal Interact* 1:299-305
78. **AM P** 1993 Calcium homeostasis. In: Mundy GR, Martin TJ (eds) *Physiology and Pharmacology of bone; Handbook Exp Pharm* 107: Springer-Verlag, Berlin; 1-65
79. **See A, Soo K** 1997 Hypocalcaemia following thyroidectomy for thyrotoxicosis. *Br J Surg* 84:95-97
80. **Bihan H, Becker K, Snider R, Nylén E, Vittaz L, Lauret C, Modigliani E, Moretti J, Cohen R** 2003 Calcitonin precursor levels in human medullary thyroid carcinoma. *Thyroid* 13:819-822

81. **Walter M, Meier C, Radimerski T, Iten F, Kränzlin M, Müller-Brand J, de Groot J, Kema I, Links T, Müller B** 2010 Procalcitonin levels predict clinical course and progression-free survival in patients with medullary thyroid cancer. *Cancer* 116:31-40
82. **Carrión A, Link W, Ledo F, Mellström B, Naranjo J** 1999 DREAM is a Ca<sup>2+</sup>-regulated transcriptional repressor. *Nature* 398:80-84
83. **Matsuda M, Yamamoto T, Hirata M** 2006 Ca<sup>2+</sup>-dependent regulation of calcitonin gene expression by the transcriptional repressor DREAM. *Endocrinology* 147:4608-4617
84. **Ledo F, Carrión A, Link W, Mellström B, Naranjo J** 2000 DREAM-alphaCREM interaction via leucine-charged domains derepresses downstream regulatory element-dependent transcription. *Mol Cell Biol* 20:9120-9126
85. **Fischer J, Born W** 1985 Novel peptides from the calcitonin gene: expression, receptors and biological function. *Peptides* 6 Suppl 3:265-271
86. **Poston G, Seitz P, Townsend CJ, Alexander R, Rajaraman S, Cooper C, Thompson J** 1987 Calcitonin gene-related peptide: possible tumor marker for medullary thyroid cancer. *Surgery* 102:1049-1054
87. **Hvarfner A, Bergström R, Mörlin C, Theodorsson E, Ljunghall S** 1988 The calcitonin gene-related peptide (CGRP) response to intravenous calcium is related to blood pressure. *Acta Physiol Scand* 132:439-440
88. **Cooper C, Borosky S, Peng T** 1985 Secretion of calcitonin gene-related peptide from baby rat thyroid glands in vitro. *Proc Soc Exp Biol Med* 180:562-566
89. **Grunditz T, Ekman R, Håkanson R, Rerup C, Sundler F, Uddman R** 1986 Calcitonin gene-related peptide in thyroid nerve fibers and C cells: effects on thyroid hormone secretion and response to hypercalcemia. *Endocrinology* 119:2313-2324
90. **Ahrén B, Ekman R, Laurberg P** 1989 Calcium stimulates the release of calcitonin gene-related peptide from the canine thyroid. *Am J Physiol* 256:E597-599
91. **Morara S, Wang L, Filippov V, Dickerson I, Grohovaz F, Provini L, Kettenmann H** 2008 Calcitonin gene-related peptide (CGRP) triggers Ca<sup>2+</sup> responses in cultured astrocytes and in Bergmann glial cells from cerebellar slices. *Eur J Neurosci* 28:2213-2220
92. **Houchi H, Yoshizumi M, Shono M, Ishimura Y, Ohuchi T, Oka M** 1996 Adrenomedullin stimulates calcium efflux from adrenal chromaffin cells in culture: possible involvement of an Na<sup>+</sup>/Ca<sup>2+</sup> exchange mechanism. *Life Sci* 58:PL 35-40
93. **Shimekake Y, Nagata K, Ohta S, Kambayashi Y, Teraoka H, Kitamura K, Eto T, Kangawa K, Matsuo H** 1995 Adrenomedullin stimulates two signal transduction pathways, cAMP accumulation and Ca<sup>2+</sup> mobilization, in bovine aortic endothelial cells. *J Biol Chem* 270:4412-4417
94. **Uezono Y, Shibuya I, Ueda Y, Tanaka K, Oishi Y, Yanagihara N, Ueno S, Toyohira Y, Nakamura T, Yamashita H, Izumi F** 1998 Adrenomedullin increases intracellular Ca<sup>2+</sup> and inositol 1,4,5-trisphosphate in human oligodendroglial cell line KG-1C. *Brain Res* 786:230-234
95. **Ji S, Xue J, Wang C, Su S, He R** 2005 Adrenomedullin reduces intracellular calcium concentration in cultured hippocampal neurons. *Sheng Li Xue Bao* 57:340-345



96. **Huang W, Wang L, Yuan M, Ma J, Hui Y** 2004 Adrenomedullin affects two signal transduction pathways and the migration in retinal pigment epithelial cells. *Invest Ophthalmol Vis Sci* 45:1507-1513
97. **Willoughby D, Cooper D** 2007 Organization and Ca<sup>2+</sup> regulation of adenylyl cyclases in cAMP microdomains. *Physiol Rev* 87:965-1010
98. **Serazin-Leroy V, Morot M, de Mazancourt P, Giudicelli Y** 2001 Differences in type II, IV, V and VI adenylyl cyclase isoform expression between rat preadipocytes and adipocytes. *Biochim Biophys Acta* 1550:37-51
99. **Nemecek G** 1978 Stimulation of hamster adipocyte cyclic 3':5'-nucleotide phosphodiesterase activity by ionophore A23187 and calcium. *J Cyclic Nucleotide Res* 4:299-309
100. **de Bustros A, Ball D, Peters R, Compton D, Nelkin B** 1992 Regulation of human calcitonin gene transcription by cyclic AMP. *Biochem Biophys Res Commun* 189:1157-1164
101. **Sassone-Corsi P** 1995 Transcription factors responsive to cAMP. *Annu Rev Cell Dev Biol* 11:355-377
102. **Carrión A, Mellström B, Naranjo J** 1998 Protein kinase A-dependent derepression of the human prodynorphin gene via differential binding to an intragenic silencer element. *Mol Cell Biol* 18:6921-6929
103. **Ledo F, Kremer L, Mellström B, Naranjo J** 2002 Ca<sup>2+</sup>-dependent block of CREB-CBP transcription by repressor DREAM. *EMBO J* 21:4583-4592
104. **Ardailou R** 1975 Kidney and calcitonin. *Nephron* 15:250-260
105. **Marx S, Woodward C, Aurbach G** 1972 Calcitonin receptors of kidney and bone. *Science* 178:999-1001
106. **Moran J, Hunziker W, Fischer J** 1978 Calcitonin and calcium ionophores: cyclic AMP responses in cells of a human lymphoid line. *Proc Natl Acad Sci U S A* 75:3984-3988
107. **Poyner D, Andrew D, Brown D, Bose C, Hanley M** 1992 Pharmacological characterization of a receptor for calcitonin gene-related peptide on rat, L6 myocytes. *Br J Pharmacol* 105:441-447
108. **Van Valen F, Piechot G, Jürgens H** 1990 Calcitonin gene-related peptide (CGRP) receptors are linked to cyclic adenosine monophosphate production in SK-N-MC human neuroblastoma cells. *Neurosci Lett* 119:195-198
109. **Zaidi M, Datta H, Bevis P** 1990 Kidney: a target organ for calcitonin gene-related peptide. *Exp Physiol* 75:27-32
110. **Uezono Y, Nakamura E, Ueda Y, Shibuya I, Ueta Y, Yokoo H, Yanagita T, Toyohira Y, Kobayashi H, Yanagihara N, Wada A** 2001 Production of cAMP by adrenomedullin in human oligodendroglial cell line KG1C: comparison with calcitonin gene-related peptide and amylin. *Brain Res Mol Brain Res* 97:59-69
111. **Ishizaka Y, Tanaka M, Kitamura K, Kangawa K, Minamino N, Matsuo H, Eto T** 1994 Adrenomedullin stimulates cyclic AMP formation in rat vascular smooth muscle cells. *Biochem Biophys Res Commun* 200:642-646
112. **Yousufzai S, Ali N, Abdel-Latif A** 1999 Effects of adrenomedullin on cyclic AMP formation and on relaxation in iris sphincter smooth muscle. *Invest Ophthalmol Vis Sci* 40:3245-3253
113. **Eguchi S, Hirata Y, Kano H, Sato K, Watanabe Y, Watanabe T, Nakajima K, Sakakibara S, Marumo F** 1994 Specific receptors for adrenomedullin in cultured rat vascular smooth muscle cells. *FEBS Lett* 340:226-230

114. **deBustros A, Baylin S, Levine M, Nelkin B** 1986 Cyclic AMP and phorbol esters separately induce growth inhibition, calcitonin secretion, and calcitonin gene transcription in cultured human medullary thyroid carcinoma. *J Biol Chem* 261:8036-8041
115. **Spiegelman B, Farmer S** 1982 Decreases in tubulin and actin gene expression prior to morphological differentiation of 3T3 adipocytes. *Cell* 29:53-60
116. **Galley H, Webster N** 1996 The immuno-inflammatory cascade. *Br J Anaesth* 77:11-16
117. **Chung S, Lapoint K, Martinez K, Kennedy A, Boysen Sandberg M, McIntosh M** 2006 Preadipocytes mediate lipopolysaccharide-induced inflammation and insulin resistance in primary cultures of newly differentiated human adipocytes. *Endocrinology* 147:5340-5351
118. **Fain J, Madan A, Hiler M, Cheema P, Bahouth S** 2004 Comparison of the release of adipokines by adipose tissue, adipose tissue matrix, and adipocytes from visceral and subcutaneous abdominal adipose tissues of obese humans. *Endocrinology* 145:2273-2282
119. **Wellen K, Hotamisligil G** 2005 Inflammation, stress, and diabetes. *J Clin Invest* 115:1111-1119
120. **Ammori B, Becker K, Kite P, Snider R, Nylén E, White J, Larvin M, McMahon M** 2003 Calcitonin precursors in the prediction of severity of acute pancreatitis on the day of admission. *Br J Surg* 90:197-204
121. **Vitseva O, Tanriverdi K, Tchkonja T, Kirkland J, McDonnell M, Apovian C, Freedman J, Gokce N** 2008 Inducible Toll-like receptor and NF-kappaB regulatory pathway expression in human adipose tissue. *Obesity (Silver Spring)* 16:932-937
122. **Andreakos E, Sacre S, Smith C, Lundberg A, Kiriakidis S, Stonehouse T, Monaco C, Feldmann M, Foxwell B** 2004 Distinct pathways of LPS-induced NF-kappa B activation and cytokine production in human myeloid and nonmyeloid cells defined by selective utilization of MyD88 and Mal/TIRAP. *Blood* 103:2229-2237
123. **Sacre S, Andreakos E, Feldmann M, Foxwell B** 2004 Endotoxin signaling in human macrophages: signaling via an alternate mechanism. *J Endotoxin Res* 10:445-452
124. **Zhong W, Burke P, Hand A, Walsh M, Hughes L, Forse R** 1993 Regulation of cytokine mRNA expression in lipopolysaccharide-stimulated human macrophages. *Arch Surg* 128:158-163; discussion 163-154
125. **Xia Y, Feng L, Yoshimura T, Wilson C** 1993 LPS-induced MCP-1, IL-1 beta, and TNF-alpha mRNA expression in isolated erythrocyte-perfused rat kidney. *Am J Physiol* 264:F774-780
126. **Rodeberg D, Babcock G** 1996 Role of calcium during lipopolysaccharide stimulation of neutrophils. *Infect Immun* 64:2812-2816
127. **Prpic V, Weiel J, Somers S, DiGuseppi J, Gonias S, Pizzo S, Hamilton T, Herman B, Adams D** 1987 Effects of bacterial lipopolysaccharide on the hydrolysis of phosphatidylinositol-4,5-bisphosphate in murine peritoneal macrophages. *J Immunol* 139:526-533
128. **Letari O, Nicosia S, Chiavaroli C, Vacher P, Schlegel W** 1991 Activation by bacterial lipopolysaccharide causes changes in the cytosolic free calcium concentration in single peritoneal macrophages. *J Immunol* 147:980-983

129. **Ohmori Y, Hamilton T** 1992 Ca<sup>2+</sup> and calmodulin selectively regulate lipopolysaccharide-inducible cytokine mRNA expression in murine peritoneal macrophages. *J Immunol* 148:538-545
130. **Hotchkiss R, Osborne D, Lappas G, Karl I** 1995 Calcium antagonists decrease plasma and tissue concentrations of tumor necrosis factor-alpha, interleukin-1 beta, and interleukin-1 alpha in a mouse model of endotoxin. *Shock* 3:337-342
131. **Lo C, Garcia I, Cryer H, Maier R** 1996 Calcium and calmodulin regulate lipopolysaccharide-induced alveolar macrophage production of tumor necrosis factor and procoagulant activity. *Arch Surg* 131:44-50
132. **West M, Clair L, Bellingham J** 1996 Role of calcium in lipopolysaccharide-stimulated tumor necrosis factor and interleukin-1 signal transduction in naive and endotoxin-tolerant murine macrophages. *J Trauma* 41:647-652
133. **Weigert C, Düfer M, Simon P, Debre E, Runge H, Brodbeck K, Häring H, Schleicher E** 2007 Upregulation of IL-6 mRNA by IL-6 in skeletal muscle cells: role of IL-6 mRNA stabilization and Ca<sup>2+</sup>-dependent mechanisms. *Am J Physiol Cell Physiol* 293:C1139-1147
134. **Freichel M, Zink-Lorenz A, Holloschi A, Hafner M, Flockerzi V, Raue F** 1996 Expression of a calcium-sensing receptor in a human medullary thyroid carcinoma cell line and its contribution to calcitonin secretion. *Endocrinology* 137:3842-3848
135. **Bouschet T, Henley J** 2005 Calcium as an extracellular signalling molecule: perspectives on the Calcium Sensing Receptor in the brain. *C R Biol* 328:691-700
136. **Ikura M, Osawa M, Ames J** 2002 The role of calcium-binding proteins in the control of transcription: structure to function. *Bioessays* 24:625-636
137. **Matsuda M, Yamamoto TA, Hirata M** 2006 Ca<sup>2+</sup>-dependent regulation of calcitonin gene expression by the transcriptional repressor DREAM. *Endocrinology* 147:4608-4617
138. **Hotchkiss R, Karl I** 1994 Dantrolene ameliorates the metabolic hallmarks of sepsis in rats and improves survival in a mouse model of endotoxemia. *Proc Natl Acad Sci U S A* 91:3039-3043
139. **Sirmagul B, Kilic F, Tunc O, Yildirim E, Erol K** 2006 Effects of verapamil and nifedipine on different parameters in lipopolysaccharide-induced septic shock. *Heart Vessels* 21:162-168
140. **Cameron E, Zhuang J, Menconi M, Phipps R, Fink M** 1996 Dantrolene, an inhibitor of intracellular calcium release, fails to increase survival in a rat model of intra-abdominal sepsis. *Crit Care Med* 24:1537-1542
141. **Christ-Crain M, Morgenthaler N, Stolz D, Müller C, Bingisser R, Harbarth S, Tamm M, Struck J, Bergmann A, Müller B** 2006 Pro-adrenomedullin to predict severity and outcome in community-acquired pneumonia [ISRCTN04176397]. *Crit Care* 10:R96
142. **Bernstein R, Hyun W, Davis J, Fulwyler M, Pershadsingh H** 1989 Flow cytometric analysis of mature adipocytes. *Cytometry* 10:469-474
143. **Beer S, Weighardt H, Emmanuilidis K, Harzenetter M, Matevossian E, Heidecke C, Bartels H, Siewert J, Holzmann B** 2002 Systemic neuropeptide levels as predictive indicators for lethal outcome in patients with postoperative sepsis. *Crit Care Med* 30:1794-1798

144. **Arnalich F, Sánchez J, Martínez M, Jiménez M, López J, Vázquez J, Hernanz A** 1995 Changes in plasma concentrations of vasoactive neuropeptides in patients with sepsis and septic shock. *Life Sci* 56:75-81
145. **Hahn P, Yoo P, Ba Z, Chaudry I, Wang P** 1998 Upregulation of Kupffer cell beta-adrenoceptors and cAMP levels during the late stage of sepsis. *Biochim Biophys Acta* 1404:377-384

## 8. Acknowledgments

First of all, I want to thank my supervisor Prof. Beat Müller for the opportunity to perform my PhD thesis in his lab. I feel deeply grateful for all the freedom and reliance he gave me during my years as a PhD student and especially for supporting my work-life balance after the birth of my child.

Furthermore, I want to thank Prof. Alex Eberle and Prof. Karl Hofbauer for refereeing my PhD thesis and Prof. Jean Pieters for leading the oral exam.

I also thank PD Henryk Zulewski, Prof. Mirjam Christ-Crain and Prof. Ulrich Keller for all their kind support, helpful inputs and interesting discussions.

I am grateful to Dr. Martin Walter for letting me participate in his interesting and successful studies on MTC.

I would like to address my thankfulness to Kaethi Dembinski for invaluable technical support and advices. Without her help this work could not have been realized.

Additionally her jolly nature and all the nice and funny discussions during lunch and coffee breaks even made the hard working days pleasant.

I deeply appreciated to have Dr. Jean Grisouard as a colleague and want to thank him for supporting me with priceless advises and critical scientific inputs to my project. I could always benefit of his experience in the scientific field. Additionally his positive attitude and happiness always cheered me up.

Many thanks go to Dr. Katharina Timper. It was a great and enjoyable experience to work together with her in a lab. Her very kind and inspiring characteristics helped me to motivate myself in busy times even when everything seemed to go wrong.

Thanks as well to the former members of the lab Jürg Lerch, Marco Fischer, Elisa Bouillet, Constanze Baranek, Dr. Philippe Linscheid, to our nice lab neighbors

Stephanie Häuselmann, Vera Lorenz and Berit Rosc and to all the other friendly and kind people from the DBM. Especially I would like to thank Dr. Dalma Seboek Kinter for her invaluable friendship and for all her help and support concerning my thesis.

I am grateful to Dr. Daniel Frey and Dr. Ralph Peterli for providing us with fat tissue samples.

I appreciated a lot the great help from Beat Erne with the calcium measurements and confocal microscopy. Many thanks also to Vreni Jäggin and Emmanuel Traunecker for their help with flow cytometry.

During my graduate studies I enjoyed the priceless support of my dear friends and my beloved family, making them the ones that should be appreciated most. Especially I would like to thank my father Dr. Paul Radimerski for helping with linguistic issues and Fredy Herzog for often taking care of Ivan enabling me to write on my thesis. The largest part of my affection goes to my future husband Christoph Herzog whom I want to thank for all his love and support and to my son Ivan whom I want to thank for all the joy and pleasure he is giving to my live.

## 9. Curriculum vitae

**name :** Tanja Marianna Radimerski  
**birth place/date:** Basel, 18<sup>th</sup> of December 1976  
**nationality :** Swiss and Czech  
**Family status :** unmarried  
1 child



### Education:

2006 - 2010      **PhD studies in medical-biological research**  
University Hospital Basel, Switzerland  
Department of Biomedicine  
  
Supervision: Prof. Dr. Beat Müller  
  
Title: The regulation of calcitonin genes upon bacterial infection  
and sepsis in human adipocytes

2002-2003      **Diploma thesis in neurobiology**  
University of Basel, Switzerland  
Neurobiology  
  
Supervision: Prof. Dr. Heinrich Reichert  
  
Title: Genetic rescue of the *ems* mutant brain  
phenotype in *Drosophila* by Coral *emx* transgene expression

1997-2003      University of Basel, Switzerland  
Faculty of science  
Biology

### Working experience:

2003 - 2006      **Novartis Pharma AG**  
Supply Chain  
Global Material Master Management  
Key Account Manager

1997 - 2003      **Novartis International AG**  
supervision of the Novartis Communication Shop

- May 2003            **Sekundarschule Reinach:** Substitute teacher for biology, geographics and mathematics
- 2002                **Hilfsassistenz Uni Basel**  
**Orientierungs- Schule Basel:** Substitute teacher for biology, geographic and mathematics  
**Sekundarschule Reinach:** Substitute teacher for biology and geographic

**Languages :**            German (mother language)  
                              English (orally and written)  
                              French and Czech (basic understanding)

**Computer skills :**        MS-Office (Outlook, Word, Excel, PowerPoint)  
                              EndNote, GraphPad Prism

**Further education :**    Höheres Lehramt Mittelschulen, Zürich, Switzerland  
                              (2 Semester 2005/2006)

**Publications :**

**T.Radimerski**, J. Grisouard, K. Timper, H. Zulewski, M. Christ-Crain, U. Keller, B. Müller (2010)

Role of calcium in lipopolysaccharide-induced calcitonin gene expression in human adipocytes. *Innate Immunity (in press)*

M. Fischer, K. Timper, **T.Radimerski**, K. Dembinski, D.M. Frey, H. Zulewski, U. Keller, B. Müller, M. Christ-Crain, J. Grisouard (2010)

Metformin induces glucose uptake in human preadipocyte-derived adipocytes from various fat depots. *Diabetes, Obesity and Metabolism 12: 356–359*

Walter MA, Meier C, **Radimerski T**, Iten F, Kränzlin M, Müller-Brand J, de Groot JW, Kema IP, Links TP, Müller B (2010)

Procalcitonin levels predict clinical course and progression-free survival in patients with medullary thyroid cancer. *Cancer Jan 1;116(1):31-40.*

Egger B, Leemans R, Loop T, Kammermeier L, Fan Y, **Radimerski T**, Strahm MC, Certa U, Reichert H (2002)

Gliogenesis in Drosophila: Genome-wide analysis of downstream genes of *glial cells missing* in the embryonic nervous system. *Development 129:3295-3309*



## **10. Appendix**

### **Declaration**

I declare that I wrote this thesis '*The regulation of calcitonin genes upon bacterial infection and sepsis in human adipocytes*' with the help indicated and only handed it in to the faculty of science of the University of Basel and to no other faculty and no other university.

Basel, 2010

## Publication

Accepted for publication in *Innate Immunity*

### **Role of calcium in lipopolysaccharide-induced calcitonin gene expression in human adipocytes**

Running Title: LPS induced Ca<sup>2+</sup> increase and CALC-gene expression

Tanja M. Radimerski\* <sup>1</sup>, Jean Grisouard <sup>1</sup>, Katharina Timper <sup>1,2</sup>, Henryk Zulewski <sup>1,2</sup>,  
Mirjam Christ-Crain <sup>1,2</sup>, Ulrich Keller <sup>1,2</sup> and Beat Müller <sup>1,3</sup>

<sup>1</sup> Department of Biomedicine, University Hospital Basel, CH-4031 Basel, Switzerland

<sup>2</sup> Division of Endocrinology, Diabetes and Clinical Nutrition, University Hospital Basel, CH-4031 Basel, Switzerland

<sup>3</sup> Department of Internal Medicine, Kantonsspital Aarau, CH-5001 Aarau, Switzerland

**Key words:** bacterial infection, CALC genes, calcium, human adipocytes, lipopolysaccharide,

\*Corresponding author:

Mailing address: University Hospital Basel, Department of Biomedicine,  
Hebelstrasse, 20, 4031 Basel, Switzerland

Phone.: +41 61 265 23 81

Fax: +41 61 265 23 50

e-mail: tanja.radimerski@unibas.ch